University of London
Imperial College of Science, Technology and Medicine
Department of Computing

Some directed graph algorithms and their application to pointer analysis

David J. Pearce

February 2005

Submitted in partial fulfilment of the requirements for the degree of
Doctor of Philosophy in Engineering of the University of London

Abstract

This thesis is focused on improving execution time and precision of scalable pointer analysis. Such an analysis statically determines the targets of all pointer variables in a program. We formulate the analysis as a directed graph problem, where the solution can be obtained by a computation similar, in many ways, to transitive closure. As with transitive closure, identifying strongly connected components and transitive edges offers significant gains. However, our problem differs as the computation can result in new edges being added to the graph and, hence, online algorithms are needed to efficiently identify these structures. Thus, pointer analysis has often been likened to the dynamic transitive closure problem.

Two new algorithms for maintaining the topological order of a directed graph online are presented. The first is a unit change algorithm, meaning the solution must be recomputed immediately following an edge insertion. While this has a marginally inferior worse-case time bound, compared with a previous solution, it is far simpler to implement, has smaller storage requirements and fewer restrictions. For these reasons, we find it to be faster in practice and provide an experimental study over random graphs to support this. Our second is a batch algorithm, meaning the solution can be updated after several insertions, and it is the first truly online solution to obtain an optimal time bound of $O(v+e+b)$ over a batch b of edge insertions. Again, we provide an experimental study over random graphs comparing this against the standard approach to topological sort. Furthermore, we demonstrate how both algorithms can be extended to the problem of dynamically detecting strongly connected components (i.e. cycles), thus achieving the first solutions which do not need to traverse the entire graph for half of all edge insertions.

Several other new techniques for improving pointer analysis are also presented. These include difference propagation, which avoids redundant work by tracking changes in the points-to sets, and a novel approach to field-sensitive analysis of C. Finally, a detailed study of numerous solving algorithms, evaluating our techniques and algorithms against previous work, is contained herein. Our benchmark suite consists of many common C programs ranging in size from 15,000-200,000 lines of code.

Acknowledgements

I am grateful to my supervisor Paul Kelly for his guidance throughout this work and for having the courage to let me develop my own directions. He has always supported my work through helpful advice, astute criticism and stimulating conversation. He also encouraged me to undertake internships at Bell Labs and IBM Hursley. For these things, I thank him.

Many other people have been helpful to me throughout my time at Imperial College. My second supervisor, Chris Hankin, has provided many excellent comments and suggestions on my work. His depth of knowledge on program analysis has also been invaluable. I would also like to thank Oskar Mencer, who has always given an interesting and alternate viewpoint on life, and those members of the Software Performance Group, in particular Olav Beckmann and Kwok Cheung Yeung, for many interesting and delightful discussions.

To my parents I am, of course, indebted for giving me such an excellent start in life. They encouraged my interest in computers from an early age and have provided both moral and financial support throughout the years.

I must also thank the Engineering and Physical Sciences Research Council (EPSRC), without whose financial support I could not have done this work.

Lastly, but my no means least, I must thank my partner Melika King for her love and patience throughout the final and most testing years of my work.

Contents

List of Figures

List of Tables

Chapter 1

Introduction

Pointer analysis is the problem of determining statically what the pointer variables in a program may target. Consider the following C program:

```
void foo() {
 int *p,*q,a,b;
 p = &a;
 if(...) q = p;
 else q = &b;
 /* point P1 */
 ...
}
```

Here a pointer analysis concludes that, during any execution of the program, the following will hold at P1: `p` *points-to* `a` and `q` *points-to* `a` or `b`. We write $p \mapsto \{a\} \wedge q \mapsto \{a, b\}$ to state this formally, where $\{a\}$ and $\{a, b\}$ are the *target sets* of p and q respectively. A solution is *sound* if the target set obtained for each variable contains all its actual runtime targets. Thus, $q \mapsto \{a\}$ is an unsound solution for the above because q can also point to b. A solution is *imprecise* if an inferred target set is larger than necessary and the superfluous targets are called *spurious*. So, for the above example, an imprecise (but sound) solution for p is $p \mapsto \{a, b\}$. In general, obtaining a perfectly precise and sound solution is undecidable [Lan92b, Ram94] and, in practice, even relatively imprecise information is expensive. Nevertheless, efficient algorithms do exist which can analyse large programs in seconds and this work is about improving the runtime of such analyses further. In particular, by developing increasingly efficient techniques, we aim ultimately to obtain greater precision.

Of course, analysing the flow of data through a program is not a new idea and there is an extensive body of literature on this subject of *data flow analysis* (e.g. [HU75, KU76, Hec77, KU77, Ken81, RP86, HDT87, RP88, Bur90]). The most important contribution in this field was almost certainly *Abstract Interpretation*, which is a general framework for describing and reasoning about program analyses. This was developed initially by Cousot and Cousot [CC77, Cou78, CC79] and has since received considerable attention (e.g. [Myc81, BHA85, MJ86, JS87, BJCD87, Mel87,

MH87, Wad87, WH87, Bru91, CC91, CC92a, CC92b, HM94]). Furthermore, numerous pointer analyses have been developed which follow the traditional approaches of Abstract Interpretation (e.g. [HBCC99, WL95, EGH94, Lan92a]). In light of this, the reader may wonder what contributions can be made in this field. The reality, however, is that pointer analyses formulated under the Abstract Interpretation framework have proved highly inefficient in both time and space. For this reason, an alternative approach to program analysis known as *set constraints* or sometimes *inclusion constraints* has become popular. While this method has found success in many areas, it was Andersen who first used it for pointer analysis [And94]. Since then, a number of set constraint-based pointer analyses have been developed and there are examples showing the technique scales to programs with several hundred-thousand lines of code or more (e.g. [HT01, LH03]).

Although set constraints are not new (they can be traced back to [Rey69, JM81]), their application to such large problems appears to be. In particular, the study of efficient algorithms for solving set constraints has only recently become serious (e.g. [Hei94, MR97, HM97b]). Indeed, much of the motivation for this stems from program analysis problems similar to pointer analysis. Thus, we find that there remains much scope for new algorithmic developments and this thesis explores some of them. For example, set constraint-based pointer analysis is efficient because it reduces to an algorithmic problem similar in nature to that of *dynamic transitive closure* [HM97b]. Here, the idea is to maintain the transitive closure of a directed graph as edges are inserted or deleted. A well known optimisation, which offers significant performance gains in practice, is to identify and collapse *strongly connected components* (i.e. cycles) in the graph [FFSA98]. However, while efficient solutions for detecting cycles in *static* graphs were known (e.g. [Tar72, NSS94]), those for *dynamic* graphs were not. A key contribution of this thesis is the development of such algorithms. Part of this contribution is the observation that dynamic cycle detection is closely related to *dynamic topological sort* — the problem of maintaining a topological sort under edge insertions and/or deletions. As a result, the majority of our effort has focused on developing efficient new algorithms for this problem (as few previously existed) and their extension to dynamic cycle detection, it turns out, is all but trivial.

Another area explored in this thesis is the use of more advanced set constraint systems. As mentioned already, solving pointer analysis with (traditional) set constraints can be reduced to something analogous to dynamic transitive closure. This allows for efficient solving, but it also reduces the level of precision obtainable. To achieve greater precision necessitates more complex set-constraint systems. Generally speaking, these represent fundamentally harder problems which take much longer to solve. However, by extending the traditional set-constraint system to permit *weights* on the constraints, we obtain something offering significantly greater precision, but remaining comparable (in terms of difficulty) with dynamic transitive closure. In particular, our extension corresponds roughly to the introduction of *edge weights* into the dynamic graph. Furthermore, we find that strongly connected components can still be collapsed in many cases and, hence, this remains a significant optimisation.

1.1 Applications

The applications of pointer analysis are many, but perhaps the most important uses today are in Compilers and Software Engineering.

Compilers. Modern superscalar and VLIW processors require sufficient Instruction Level Parallelism (ILP) to reach peak utilisation. For this reason, exposing ILP through instruction scheduling and register allocation is a crucial role of the compiler. This task is complicated by the presence of instructions which indirectly reference memory, since their data dependencies are not known. For languages such as C/C++, this problem is particularly acute because pointer variables (the main source of indirect memory references) can target practically every memory location without restriction. Therefore, to achieve maximum pipeline throughput, the compiler must rely on pointer analysis to disambiguate indirect memory references.

Automatic parallelisation is another example of how the compiler can achieve a speedup by exposing parallelism within the program. This type of transformation is performed at a higher level than those for ILP and, hence, more significant gains are possible. Indeed, much success has been achieved through automatic parallelisation of numerical FORTRAN programs (e.g. [PKL80, AK87, Wol82, PW86, CDL88, Wol89, GKT91, McK94, HAM+95, SMH98]). However, similar results have yet to be seen on programs written in C/C++ or Java. The main reason for this is simply that, without precise information about pointer targets, compilers for these languages cannot perform automatic parallelisation safely.

Finally, pointer analysis finds many other important uses within the compiler. In particular, it often enables traditional optimisations (e.g. common sub-expression elimination) to be applied at places which would otherwise be deemed unsafe.

Software Engineering. Reliability of large software systems is a difficult problem facing software engineering. Subtle programming errors, which go undetected during testing, can have disastrous consequences. An historic example is the 1988 worm which caused havoc by infecting large parts of the internet [ER89]. The worm replicated by exploiting a *buffer overrun* vulnerability in the `fingerd` daemon, which existed through programming error. This type of mistake is usually associated with the misuse of pointers and accounts for the majority of security holes in modern software [WFBA00]. One approach to tackling these problems is to construct tools which either aid program understanding or, in some way, check for programming error. Examples of the former include program slicers (e.g. [RY89, RT96, HRB88, BH93, HBD03, Bin98, Luc01, DFHH00]), static debuggers (e.g. [Bou93a, Fla97]) and software visualisers (e.g. [JHS02, SYM00, Mye86, Rei97]). Examples of the latter can usually be divided into two camps: static analysis tools (e.g. [DRS03, FLL+02, BCC+02, BCC+03, WFBA00]) and model checkers (e.g. [Hol97, HJMS03, HHWT97, AHM+98, God97, The96]). The former generally operate on programs directly, whilst the latter operate on abstract models of programs. In languages such as C/C++ and Java, pointer analysis is invariably found in all these tools where it forms a foundation for other analyses.

1.2 Contributions

The main contributions of this work are as follows:

- A fully dynamic, unit change algorithm for maintaining the topological order of a directed acyclic graph. While this has marginally inferior time complexity, compared with a previous algorithm, it is far simpler to implement. For this reason, we find it to be faster in practice and provide an experimental study on random graphs to support this claim.

- The first batch algorithm for maintaining the topological order of a DAG. For a batch b of edge insertions, this has an optimal $O(v + e + b)$ bound on its runtime, which improves upon the best previous bound of $O(b(v + e))$ obtained by any unit change algorithm. We also provide an experimental comparison of this algorithm against the alternatives.

- Extensions to the above algorithms for dynamically identifying strongly connected components (cycles) in digraphs. Thus, we obtain the first solutions which do not traverse the entire graph for half of all edge insertions in the worst case. Furthermore, these algorithms are important for the pointer analysis problem, where dynamically identifying cycles can lead to significant improvements in analysis time.

- A theoretical and practical investigation into a technique called *difference propagation*. We show how this permits practical, cubic time solving algorithms.

- A small extension to the language of set constraints which elegantly formalises a field-sensitive pointer analysis for the C language. As a byproduct, function pointers are supported for free with this mechanism.

- A large experimental study looking at numerous set-constraint solvers and techniques, including online cycle detection, iteration order, difference propagation and field-sensitivity. Our benchmark suite contains 11 common C programs, ranging in size from 15,000 to 200,000 lines of code.

Much of the work contained in this thesis has been previously published (see [PKH03, PKH04a, PKH04b, PK04]). However, while the other authors of these papers provided suggestions, advice and feedback, the work itself as well as the actual paper writing was performed solely by the author of this thesis.

1.3 Thesis Organisation

This thesis is organised as follows. In Chapter 2, we examine our chosen method of pointer analysis, known as set constraints, and consider how it can be used efficiently. This is followed by an in-depth examination of the trade-offs in terms of precision and efficiency, which must be balanced with care to achieve scalable pointer analysis. Included here is a survey of previous work relating to the use of set constraints in pointer analysis. However, it is important to realise that

the available literature on pointer analysis is vast and, inevitably, we cannot cover everything in this field. Instead, we restrict our attention to that which relates directly, while providing a brief introduction to the alternatives.

In Chapter 3, we divert our attention from pointer analysis to consider some more general problems relating to directed graphs. It is here that we present two novel algorithms for the dynamic topological sort problem, as well as providing an extensive experimental study into their practical behaviour. Of particular import to this thesis, however, is that we show in Chapter 3 how these algorithms can be used to dynamically detect cycles in digraphs.

Chapter 4 returns to consider how pointer analysis can be solved efficiently using set constraints. Here, we introduce difference propagation and demonstrate how it can be used to give a solver with optimal worst-case time complexity. Furthermore, we provide an extensive experimental study which examines the techniques developed in Chapters 3 and 4. In Chapter 5, we take this further by extending our analysis with a novel approach for field-sensitive analysis of C, which is about modelling aggregate variables more accurately. Finally, we consider future work and draw conclusions in Chapter 6.

Chapter 2

Constraint-Based Pointer Analysis

This chapter begins with an introduction to *set constraints*, which is the mechanism we use to formulate our pointer analysis. Having covered this in detail, we look at what is known about the trade-offs between cost and precision for pointer analysis in general. Finally, we briefly examine some of the alternative approaches to pointer analysis found in the literature and discuss their relative strengths and weaknesses.

Systems of *set constraints* (or sometimes *inclusion constraints*) are not new and can be traced back to [Rey69, JM81]. Through the work of Heintze, Aiken and others, they have recently become a well established approach to program analysis (e.g. [Hei94, Aik99, Aik94, AW93, AW92]). Applications in this field include control-flow analysis (e.g. [HM97b, HM97a]), debugging (e.g. [WFBA00, Fla97]) and more. The first example of a pointer analysis formulated using set constraints was that of Andersen [And94] and, since then, many have followed in his footsteps (e.g. [FFSA98, FFA97, HT01, LH03, GLS01, RMR01, PKH03, PKH04a]). Of course, set constraints are not the only way of performing pointer analysis and, as well as *abstract interpretation*, a technique called *unification* is popular. Understanding the differences between these different approaches is not easy, although a common view holds that abstract interpretation is precise but slow, while unification is fast but imprecise. Set constraints lie somewhere in the middle — they are more precise than unification, but still capable of analysing programs with a hundred thousand lines of code or more (e.g. [PKH04a, HT01, LH03, FFSA98]).

We now present our set-constraint formulation of the pointer analysis problem, which is based upon the following language:

$$p \supseteq q \mid p \supseteq \{q\} \mid p \supseteq *q \mid \ *p \supseteq q \mid \ *p \supseteq \{q\}$$

Where p and q are constraint variables and $*$ is the usual dereference operator. We can think of each variable as containing the set of variables it points to. Thus, $p \supseteq \{x\}$ states *p may point to x*. Those involving "$*$" are referred to as *complex constraints*. Essentially, we have obtained something simpler by specialising to our problem domain. The exact differences are covered in Appendix A and, for those knowledgeable about set constraints, the main points are a lack of general constructors and projection.

To perform the analysis we first translate the source program into the set-constraint language, by mapping each source variable to a unique constraint variable and converting assignments to constraints. Then, we solve the constraints to find a least solution, which can be formalised as deriving all possible facts under the inference system of Figure 2.1. For example, consider the following program, its translation and derived solution (shown below the line):

```
int *f(int *p) { return p; }          (1)  f_* ⊇ f_p

void g() {
 int x,y,*p,*q,**r,**s,**t;
 s=&p;                                (2)  g_s ⊇ {g_p}

 if(...) {
  p=&x;                               (3)  g_p ⊇ {g_x}
  r=s;                                (4)  g_r ⊇ g_s
  t=r;                                (5)  g_t ⊇ g_r
 } else {
  p=&y;                               (6)  g_p ⊇ {g_y}
  t=s;                                (7)  g_t ⊇ g_s
 }
 q=f(*t);                             (8)  f_p ⊇ *g_t
                                      (9)  g_q ⊇ f_*
 f(q);                               (10)  f_p ⊇ g_q
}
```

---

(12)	$g_r \supseteq \{g_p\}$	$(\mathit{trans}, 2+4)$
(13)	$g_t \supseteq \{g_p\}$	$(\mathit{trans}, 5+12)$
(14)	$f_p \supseteq g_p$	$(\mathit{deref}_1, 8+13)$
(15)	$f_p \supseteq \{g_x\}$	$(\mathit{trans}, 3+14)$
(16)	$f_p \supseteq \{g_y\}$	$(\mathit{trans}, 6+14)$
(17)	$f_* \supseteq \{g_x\}$	$(\mathit{trans}, 1+15)$
(18)	$f_* \supseteq \{g_y\}$	$(\mathit{trans}, 1+16)$
(19)	$g_q \supseteq \{g_x\}$	$(\mathit{trans}, 9+17)$
(20)	$g_q \supseteq \{g_y\}$	$(\mathit{trans}, 9+18)$

Notice that variable names are augmented with scope information to ensure uniqueness. Also, f_* represents the return value of f. The final solution for a variable is the smallest set satisfying the fully derived constraint system. Thus, in the example, constraints $19 + 20$ imply the smallest solution for q is $\{g_x, g_y\}$. Therefore, our analysis concludes $q \mapsto \{g_x, g_y\}$ holds at all points in the program. The key point here is that *we must derive all facts in order to make a sound conclusion.*

$$[\textit{trans}]\quad \frac{\tau_1 \supseteq \{\tau_2\} \quad \tau_3 \supseteq \tau_1}{\tau_3 \supseteq \{\tau_2\}} \qquad [\textit{deref}_1]\quad \frac{\tau_1 \supseteq *\tau_2 \quad \tau_2 \supseteq \{\tau_3\}}{\tau_1 \supseteq \tau_3}$$

$$[\textit{deref}_2]\quad \frac{*\tau_1 \supseteq \tau_2 \quad \tau_1 \supseteq \{\tau_3\}}{\tau_3 \supseteq \tau_2} \qquad [\textit{deref}_3]\quad \frac{*\tau_1 \supseteq \{\tau_2\} \quad \tau_1 \supseteq \{\tau_3\}}{\tau_3 \supseteq \{\tau_2\}}$$

Figure 2.1: An inference system for pointer analysis

Regarding the hardness of this problem, it is known that at least $O(t^3)$ time is needed to solve a set of t constraints [MR97, Hei94]. For completeness, we provide a similar proof of this here:

Lemma 1. *Solving t constraints under the inference system of Figure 2.1 requires $O(t^3)$ time.*

Proof. This result stems from two facts: firstly, the total number of trivial constraints generated (i.e. those of the form $p \supseteq \{q\}$) is bounded by $O(tv)$, where v is the number of variables; secondly, at most $O(v^2)$ simple constraints (i.e. those of the form $p \supseteq q$) are possible. From these it follows that, in the worse case, the *trans* rule must be applied at least $O(tv^2)$ times. This is because, for each variable, there are at most t trivial constraints which must be propagated across $O(v)$ simple constraints. Note, the *deref* rules need only be applied $O(tv)$ times, since each dereferenced variable has $O(v)$ targets. To arrive at the cubic result on the time needed for this problem, we need only consider that the number of variables is bounded by the number of constraints and, thus, in the worse case $t \approx v$. □

2.1 Solving the Analysis

Thus far, we have said the aim is to derive all possible facts using the inference system of Figure 2.1. The main focus of this thesis is in exploring techniques for doing this more efficiently. Therefore, we now examine some of the basic ideas to motivate the remaining chapters.

To solve a set of our constraints efficiently we formulate them into a directed graph, where each variable is represented by a unique node and each constraint $p \supseteq q$ by an edge $p \leftarrow q$. In addition, we associate with each variable n a set $Sol(n)$, into which the *points-to* solution for n is accumulated. Thus, for the example of the previous section we obtain the following graph:

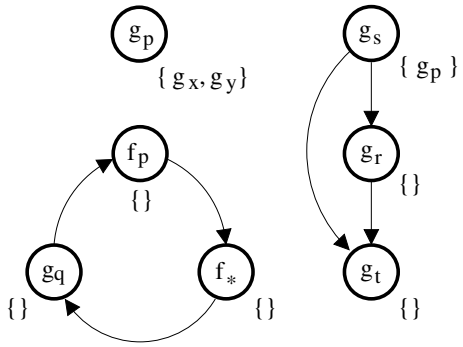

In the above, we have placed $Sol(n)$ for each variable n below its corresponding node. Note, this initially contains x iff $n \supseteq \{x\}$ is in the constraint set. At this point, the constraints can be

solved by repeatedly selecting an edge $x \rightarrow y$ and merging $Sol(x)$ into $Sol(y)$ until no change is observed. This is often referred to as *converging* or *reaching a fixpoint*. During this process, new edges arising from the complex constraints must be added to the graph. To see why, recall that our example contained the complex constraint $f_p \supseteq *g_t$. We know that, initially $Sol(g_t) = \emptyset$, but at some point during the analysis $Sol(g_t) = \{g_p\}$. Clearly then, there is a dependence from g_p to f_p and this could not have been known at graph construction time. Therefore, the edge $g_p \rightarrow f_p$ must be added as the solution for g_t becomes available. Thus, solving the above constraint graph gives:

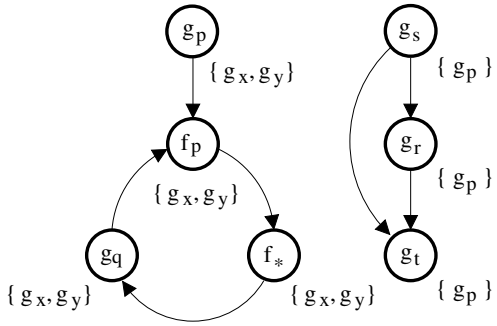

Thus, we see that a new edge has been added because of the constraint $f_p \supseteq *g_r$. A useful observation is that nodes in the same cycle always end up with the same solution [FFSA98, HT01]. So, in our example, nodes f_p, f_* and g_q have the same final solution. Therefore, we can simplify the graph by collapsing them into a single representative, giving:

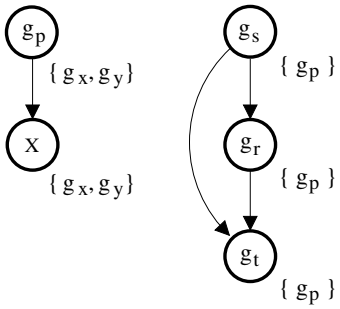

The gain from this simplification comes from time saved by not propagating targets between internal nodes. However, identifying these cycles is complicated by the dynamic nature of the graph as edges added during solving may introduce new cycles. Therefore, to exploit all such simplification opportunities we must be able to determine when a newly added edge introduces a cycle. One way of achieving this would be to run the standard algorithm due to Tarjan for detecting *strongly connected components* (cycles) in digraphs (see Appendix B). However, this visits each node and edge every time it is run and, hence, would be expensive. Therefore, what we really want is an *online algorithm*, which performs a minimal amount of work after an edge has been added. In Chapter 3 we cover this topic and its related work in detail.

In a similar vein to the above, a technique we refer to as *subsumed node compaction* can also help simplify the constraint graph. The idea, originally suggested by Rountev and Chandra [RC00], is illustrated by the following:

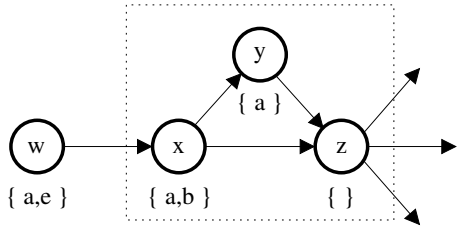

Here, x, y, z must have the same solution and, hence, can be collapsed into one. Note, we assume here that y and z have not had their address taken and are not targeted by a constraint such as $y \supseteq *p$. Rountev and Chandra also provided a linear time algorithm for detecting such opportunities in the constraint graph. Note, unlike with cycle detection, there is nothing to be gained from using an online algorithm here since new opportunities cannot arise during the analysis.

The approach to solving set constraints we have presented is sometimes called *Standard Form (SF)* [AW93]. An alternative to this, known as *Inductive Form (IF)*, is often described in the literature as a sparser and more efficient representation [SFA00, RMR01]. In general, we find there is little evidence to support this claim: the only experimental study is [FFSA98]. The conclusions from this appear to show that inductive form has an advantage. Unfortunately, we must discount this result due to an artifact of the cycle detection algorithm used which, for efficiency reasons, does not identify and collapse all cycles. Thus, it happens that under inductive form the algorithm consistently collapses more cycles, giving it an apparent advantage. However, in this thesis, we develop cycle detectors efficient enough to collapse all cycles under standard form, thereby eliminating this distinction between them. Therefore, we cannot draw concrete conclusions about the relative efficiency of either approach and, in general, equal success has been achieved (e.g. [HT01, LH03] versus [RMR01, FFSA98]). For the purposes of this thesis, we are concerned only with Standard Form and, in the remainder, it is assumed. The reader can find a detailed discussion of inductive form in Appendix A.

2.1.1 Set Implementation

An important detail affecting any algorithm for solving a constraint-based pointer analysis is the implementation of the solution sets themselves. In particular, the cost of performing a set union directly impacts upon solving time. Commonly used data structures include Bit Vector, Sorted Array and Balanced Binary Trees:

1. Bit Vector - an array of booleans, where each represents a unique element in D, the set of all possible pointer targets. Thus, the storage needed by a Bit Vector, even with one element is $O(D)$. Likewise, the set union operation is not linear in set size, but $|D|$. Finally, inserting an element takes $O(1)$ time and iterating all elements of a set takes $O(D)$ time.

2. Sorted Array - an array of elements from D, sorted according to some total ordering of D. In this case, storage is linear in set size, as is the time for set union, insertion and iteration.

3. Balanced Binary Tree - Similar to the sorted array, except set union has a marginally lower bound of $O(min(m \log n, m + n))$, when inserting m elements into n. This arises since, when $|n| > |m|$, we can insert each element of m in $\log n$ time without iterating all of n. Otherwise, we just iterate all of m and n to avoid the $\log$ factor. Memory usage is higher than for sorted array as each element is a node containing two subtree links. Finally, it takes $O(\log n)$ to insert an element.

In general, we find that the tree representation performs badly compared with sorted array. Furthermore, existing work suggests a hybrid of bit vector and sorted array provides the best choice [HT01, LH03].

One issue is that many variables may share the same solution during some or all of the analysis. Thus, memory could be saved by eliminating this duplication through sharing. Of course, the amount of duplication available depends upon the nature of programs, but Heintze and Tardieu suggest useful benefit can be obtained. They employed a simple compaction scheme, with solution sets stored in a hash table using set size as the key. Thus, at the cost of extra computation (i.e. table lookup), any duplicate sets are now shared. Unfortunately, they did not evaluate the effectiveness of this idea and the amount of compaction obtainable remains unclear. Having said that, we find this technique so essential for analysing large programs that it is used in all experiments contained in this thesis.

The importance of reducing the memory requirements needed to solve large systems of set constraints is so great that, in an effort to do better, recent work has begun exploiting *Binary Decision Diagrams (BDD)* [WL04, ZC04, Zhu02, LH04, BLQ$^+$03]. These were originally developed to cope with the incredibly large number of states involved in hardware verification [Bry86], but have also found success in related areas such as model checking (e.g. [JEKL90, Kwi03]) and program analysis (e.g. [BR01, MRF$^+$02]). Without going into too much detail, the essence of BDDs is that they can represent a large set very compactly by aggressively exploiting regularity within it. This is achieved by storing the set as a directed acyclic graph, which can have far fewer nodes than elements in the set. This means, firstly, that space requirements can be significantly reduced and, secondly, that the cost of a set union is proportional to the number of nodes, *not the number of elements*. Unfortunately, the Achilles heel of BDDs is that they require a variable ordering which greatly affects their performance and, furthermore, it is well known that finding an optimal ordering is an NP-complete problem [BW96]. Nevertheless, it appears that even simple orderings generally offer good performance and ongoing work is investigating which do well within the context of pointer analysis. The reader is referred to [BLQ$^+$03] for a good introduction to BDDs and pointer analysis.

2.2 Extending the Basic Model

Having laid out the basic formulation of our pointer analysis, we now examine how it might be extended to improve precision. However, with the exception of *field-sensitivity*, we do not consider these extensions in the remainder of this thesis. Our purpose with what follows then, is to facilitate an understanding of the limitations of our system, and to provide some indication of the difficulty in going beyond it.

2.2.1 Context-Sensitivity

The analysis we have described is commonly categorised as being context-insensitive — meaning information about the *calling context* of a function is discarded. In contrast, context-sensitive analyses consider a function separately for each calling context. This is equivalent to fully inlining each function before performing the analysis, which is known to be exponential in program size and, hence, generally impractical for large programs [WL04, NKH04a]. Context-insensitivity overcomes this limitation by generalising a function's calling contexts into one. Unfortunately, this introduces the *unrealisable paths problem* — a further source of imprecision. For example:

	(context-insensitive)	(context-sensitive)
`void f(int **q, int *p) {`		
`int a, b, *r = &a;`	$f_r \supseteq \{f_a\}$	$f_{r,1} \supseteq \{f_{a,1}\}$
		$f_{r,2} \supseteq \{f_{a,2}\}$
`*q = p;`	$*f_q \supseteq f_p$	$*f_{q,1} \supseteq f_{p,1}$
		$*f_{q,2} \supseteq f_{p,2}$
`r = p;`	$f_r \supseteq f_p$	$f_{r,1} \supseteq f_{p,1}$
		$f_{r,2} \supseteq f_{p,2}$
`}`		
`int a,b,*p,*q;`		
`f(&p,&a);`	$f_q \supseteq \{p\}$	$f_{q,1} \supseteq \{p\}$
	$f_p \supseteq \{a\}$	$f_{p,1} \supseteq \{a\}$
`f(&q,&b);`	$f_q \supseteq \{q\}$	$f_{q,2} \supseteq \{q\}$
	$f_p \supseteq \{b\}$	$f_{p,2} \supseteq \{b\}$

Here, the insensitive analysis connects both calls to the same constraint variables, concluding that $q, p \mapsto \{a, b\}$. In contrast, the sensitive analysis duplicates the constraints of `f` for each calling context and obtains a more accurate solution. This approach is sometimes referred to as *cloning* [WL04] and, while they are similar, it is distinct from *procedure cloning* because the source code itself is not actually modified. An interesting artifact of this approach is that we can distinguish between the solution of a variable under different contexts. For example, in the above, the analysis will conclude that $f_{p,1} \mapsto \{a\} \wedge f_{q,1} \mapsto \{p\}$, while $f_{p,2} \mapsto \{b\} \wedge f_{q,2} \mapsto \{q\}$. This is useful, since it tells us that $f_p \mapsto \{a\} \wedge f_q \mapsto \{q\}$ does not hold in any context. However, this type of information is only useful to a certain class of clients, termed the *context-sensitive* clients. The rest are *context-insensitive* clients and, for them, the individual contexts under which a pointer targets

a particular location is not important. For example, virtual call resolution is a context-insensitive client, since it can only reduce a virtual call to a static call when it has a single target *across all contexts*. Thus, it must combine the different contextual solutions of a pointer, referred to as *projecting away context*, before it can determine whether a virtual call can be reduced or not. Of course, context-insensitive clients can benefit from context-sensitivity, since it can still improve the combined solution for a pointer (e.g. p or q above).

An apparent inefficiency with cloning is that many constraints are needlessly duplicated, such as $f_r \supseteq \{f_a\}$ above. In an effort to address this, an alternative approach to context-sensitive analysis has arisen, known as the *summary method* [CRL99, CH00, NKH04a]. This begins with a *bottom-up* phase which, starting from the leaves of the call-graph, generates a summary for each function and inlines it at all call sites. A summary captures those aspects of the function which can affect its caller (e.g. $*f_q \supseteq f_p$ above). Thus, as each function call is replaced with the summary of its target(s), we are left with *disjoint* constraint sets — one for each function in the program. Once this is completed, a top-down phase then solves each of these, starting at the root of the call graph and proceeding downwards. The following demonstrates this on our previous example:

`void f(int **q, int *p) {`	(Initial Constraints)	(Disjoint Constraints)
		$f_p \supseteq \{a\}$
		$f_p \supseteq \{b\}$
		$f_q \supseteq \{p\}$
		$f_q \supseteq \{q\}$
`int a, b, *r = &a;`	$f_r \supseteq \{f_a\}$	$f_r \supseteq \{f_a\}$
`*q = p;`	$*f_q \supseteq f_p$	$*f_q \supseteq f_p$
`r = p;`	$f_r \supseteq f_p$	$f_r \supseteq f_p$
`}`		
`int a,b,*p,*q;`		
`f(&p,&a);`	$f_q \supseteq \{p\}$	$f_{q,1} \supseteq \{p\}$
	$f_p \supseteq \{a\}$	$f_{p,1} \supseteq \{a\}$
		$*f_{q,1} \supseteq f_{p,1}$
`f(&q,&b);`	$f_q \supseteq \{q\}$	$f_{q,2} \supseteq \{q\}$
	$f_p \supseteq p$	$f_{p,2} \supseteq \{b\}$
		$*f_{q,2} \supseteq f_{p,2}$

Here, we see the initial constraint set on the left and the disjoint sets produced by the bottom-up phase on the right. The key point to realise is that the summary for function `f` consists of one constraint: $*f_q \supseteq f_p$. Thus, we have cloned just this constraint — not all three — for the two calling contexts, which represents a saving over the full cloning method. However, we must also retain the original constraints of `f`, in order to compute a solution for its local variables. Notice that the calling contexts for `f` have been inlined into this to ensure disjointness. An interesting difference between this approach and cloning is that contextual information is not available. For example, the summary based analysis concludes for the above that $f_p \mapsto \{a, b\} \wedge f_q \mapsto \{q, p\}$, but we cannot tell from this under which context each value holds.

In the literature, there have been several attempts to implement the summary method as described (e.g. [CRL99, FFA00, CH00]). One of the first was by Chatterjee *et al.* who named their approach *Relevant Context Inference*. However, their system was rather cumbersome (perhaps as it was *flow-sensitive* — see Section 2.2.2) and performed poorly even on small programs ($\leq$ 6000LOC). Since then, several works have shown the technique capable of analysing large programs ($\leq$ 200KLOC) [CH00, FFA00, NKH04a]. The most interesting of these is by Nystrom *et al.* who found a way to improve the basic system. Their approach uses *cut-and-paste*, instead of *copy-and-paste*, when inlining summaries. This means constraints in the summary are removed from those of the function itself (i.e. $*f_q \supseteq f_p$ would be deleted in the above). While some care is needed to do this properly, it does reduce the amount of work involved during the top-down phase and, surprisingly, improves overall precision as well. In contrast, cloning has received little attention, perhaps due to a perception that it could not possibly scale beyond small programs. However, Whaley and Lam have recently showed this assumption may be incorrect [WL04]. With the aid of Binary Decision Diagrams, they were able to analyse programs with $\approx$ 100KLOC and more than 10^{14} contexts in their expanded call graph in under 20 minutes.

One issue, which has been the subject of much debate, is whether or not a context-sensitive analysis provides a sufficient increase in precision to justify its cost. One of the first to study this was Ruf [Ruf95], who directly compared a context-sensitive algorithm with an insensitive one and observed only small differences in precision. To account for this, he speculated that the use of the (imprecise) *static heap model* (see Section 2.2.4) and the small size of his benchmarks ($\leq$ 6000LOC) might be to blame. In particular, most functions used by his benchmarks had just one caller and, thus, could not benefit from context-sensitivity.

Another important work here is that of Foster *et al.* [FFA00] who compared a summary-based context-sensitive analysis with a context-insensitive, set-constraint analysis. Again, their experimental results showed only minor improvements in precision for the sensitive analysis. To explain this, they argued that C functions typically side-effect heap structures and global variables. This implies that, to see the full benefits of context-sensitivity, an accurate heap model is needed. However, like Ruf, they used the imprecise *static heap model*, which could explain their results.

In fact, Nystrom *et al.* have since shown that the *copy-and-paste* approach to inlining summaries (used by Foster *et al.* above) also suffers a further and inherent imprecision [NKH04a]. Thus, in their work, they perform a similar study using the improved *cut-and-paste* technique and reach somewhat different conclusions. They observed that, while most benchmarks showed little or no gain in precision, a few obtained significant benefit. Furthermore, upon manual inspection of the benchmarks, it was found the majority fell into one of three classes: either they were too trivial to benefit; or they were almost entirely recursive in nature (hence unsuited to context-sensitive analysis); or the static heap model (which they also used) was the primary cause of imprecision[1]. Thus, their findings add weight to the hypothesis that an accurate heap model is needed to obtain the full benefits of context-sensitivity.

[1]The findings of this manual inspection are not mentioned directly in [NKH04a]. However, they were presented in the accompanying SAS04 presentation and also through private correspondence.

The final piece of work relating to our discussion is that of Whaley and Lam who (as mentioned already) employed the cloning approach [WL04]. Their findings differ from the others in that they appear to show useful gains in precision, even though a static heap model was used. However, they also noted that projecting away the context, as a context-insensitive client does, loses most of the benefit. Thus, it seems that their results do concur with previous findings, since these all assume context is projected away.

In the literature, there are a number of other works on context-sensitive pointer analysis which warrant some discussion here (e.g. [DLFR01, FRD00, FFA00, LPH01]). These all employ an alternative approach to pointer analysis called *unification* (discussed later in Section 2.3.2), which is less accurate, but more efficient than set constraints. While several studies of these algorithms report benefits from context-sensitivity (e.g. [DLFR01, FRD00, FFA00]), we caution against reading too much into them. This is because it is likely that these gains do not arise from context-sensitivity itself, but from the effect that implementing it has on unification. For example, in [FRD00], the authors do not use unification to model flow across function boundaries. Instead, they use something similar to set constraints, and this simple refinement of the unification system could well account for the increases in precision they observed.

2.2.2 Flow-Sensitivity

A flow-insensitive analysis (as ours is) ignores all control-flow information, including statement order. In contrast, a flow-sensitive analysis retains this. The following highlights this difference:

`int **p,**q,*a,*b,c;`	(flow-insensitive)	(flow-sensitive)
`1. p=&a;`	$p \supseteq \{a\}$	$p_1 \supseteq \{a\}$
`2. q=p;`	$q \supseteq p$	$q_2 \supseteq p_1$
`3. p=&b;`	$p \supseteq \{b\}$	$p_3 \supseteq \{b\}$

Here, the insensitive conclusion is that $p = q \mapsto \{a, b\}$, while the sensitive one gives the more precise $p_1 \mapsto \{a\}, q_2 \mapsto \{a\}, p_3 \mapsto \{b\}$. The difference arises because the insensitive analysis uses a single constraint variable to represent the entire life of a program variable. The sensitive analysis, on the other hand, breaks each program variable into separate constraint variables, each having a single definition point. This transformation is more commonly known as *Static Single Assignment (SSA)* form [CFR$^+$89, CFR$^+$91, HH98]. One might conclude from this that our constraint language, along with the SSA transformation, is sufficient for flow-sensitive pointer analysis. However, SSA form cannot be constructed without pointer information [LH98, CCL$^+$96, CG93, HH98]. To see why, consider this continuation of our example:

`4. a=&c;`	$a \supseteq \{c\}$	$a_4 \supseteq \{c\}$
`5. *p=...;`	$*p \supseteq \{\ldots\}$	$*p_3 \supseteq \{\ldots\}$
`6. b=a;`	$b \supseteq a$	$b_6 \supseteq a_?$

The problem is that we cannot determine which label to give a in the last statement without knowing what p points to (since it may target a). One workaround is to transform only those

variables which cannot be assigned through a pointer (i.e. their address has not been taken). To go beyond this requires some form of *incremental static single assignment form*, where we begin with a rough transformation and update it as the analysis proceeds. There are only a few works which attempt something along these lines [CSS96, Guy03, HH98]. The work of Guyer *et al.* [Guy03, GL03] is perhaps the most interesting here, as it provides the only study of flow-sensitive, set constraint-based pointer analysis. The data from this appears to show a flow-sensitive analysis running roughly ten times slower that its insensitive variant, while offering some useful improvements in precision. Unfortunately, the work does not examine in detail the effect on precision of using flow-sensitivity. In particular, standard metrics (e.g. average set size) are not provided. This, coupled with the limited size of benchmarks, means much is left unclear about why this is happening and whether these observations can be expected to apply to larger benchmarks.

The work of Hind, Burke, Pioli *et al.* [HP97, HP98, HBCC99, Pio99, HP00] provides us with some additional insight into the effects of flow-sensitivity. These works are all essentially the same, with the same benchmarks and approach to pointer analysis being used (i.e. *abstract interpretation* — see Section 2.3.1). Again, while their method of performing pointer analysis differs from ours, their results regarding precision remain relevant. The overall conclusion of this work is that flow-sensitivity offers only small gains in precision, and two explanations are offered: firstly, the authors claim most pointer variables are usually assigned only once per function; secondly, they state that imprecision arising from context-insensitivity is swamping the data, making the gains from flow-sensitivity appear insignificant.

An interesting twist on this debate is that, for many clients, the standard way of evaluating flow-sensitive analyses may be misleading. This is especially true for error-checking tools, which are concerned only with specific values which give rise to errors. One goal of such tools is to reduce the number of *false-positives* (i.e. errors which do not exist) being reported. For example, consider a tool which checks for NULL pointer dereferences. This will not benefit from reductions in average set size at dereference sites, unless these reductions always eliminate NULL from the *points-to* sets. Thus, an analysis which made little impact on average set size, but eliminated most NULL values would be more useful. Most previous studies on flow-sensitivity (in particular that of Hind, Burke, Pioli *et al.*) would consider such an analysis to be unbeneficial, since they focus only on average set size. However, consider the following:

```
void bar(int *q) { q[0] = ...; }
void foo(int *p) { if(p != NULL) bar(p); }

int x = ...;
foo(NULL);
foo(&x);
```

The point about this example is that flow-sensitivity is *necessary* for an analysis to determine no error exists. This is because the life of `p` must be broken up to distinguish its value inside the `if` body. In truth, all previous flow-sensitive analyses we are aware of would still be unable to

catch this, because they do not model conditional statements (see Section 2.2.5). Nevertheless, we argue that flow-sensitivity is a necessary precursor to this type of error checking.

Flow-sensitivity also has important implications for the time complexity of the pointer analysis problem. For example, Landi showed that the flow-sensitive pointer analysis problem is undecidable if dynamic memory is allowed [Lan92b]. A simpler proof was later given by Ramalingam [Ram94]. One restriction was that the source language must permit aggregate variables, although this has since been shown unnecessary [Cha03]. Another point is that precise flow-insensitive pointer analysis is NP-Hard, even when dynamic storage is not permitted [Hor97]. An implication of this is that the analysis we have described does not achieve precise flow-insensitivity, since it has a polynomial time solution. This may seem strange, but can be understood if we consider the precise definition of a flow-insensitive solution. That is, the smallest solution which holds for all possible interleavings of statements. For example:

```
void *a,*b,*c,*p;
```

`b=&a;`	(1)	$b \supseteq \{a\}$	
`c=&b;`	(2)	$c \supseteq \{b\}$	
`p=&c;`	(3)	$p \supseteq \{c\}$	
`p=*p;`	(4)	$p \supseteq *p$	
	(5)	$p \supseteq c$	$(\mathit{deref}_1, 3{+}4)$
	(6)	$p \supseteq \{b\}$	$(\mathit{trans}, 2{+}5)$
	(7)	$p \supseteq b$	$(\mathit{deref}_1, 4{+}6)$
	(8)	$p \supseteq \{a\}$	$(\mathit{trans}, 1{+}7)$
Conclude		$p \mapsto \{a, b, c\}$	

Here, we have shown the conclusion our analysis would reach. In fact, the precise flow-insensitive solution is actually $p \mapsto \{a, b\}$. This is because, no matter what ordering of statements is used, p is only dereferenced once and, thus, cannot point to a. However, our system applies the deref_1 rule more than once — effectively allowing p to be dereferenced many times.

2.2.3 Field-Sensitivity

So far, we have not indicated how `struct` variables should be handled by our analysis and there are three approaches: *field-insensitive*, where field information is discarded by modelling each aggregate with a single constraint variable; *field-based*, where one constraint variable models all *instances* of a field; and finally, *field-sensitive*, where a unique variable models each field of an aggregate. The following example aims to clarify this:

```
typedef struct  int *f1; int *f2;  aggr;
```

`aggr a,b;`	(field-insensitive)	(field-based)	(field-sensitive)
`int *c,d,e,f;`			
`a.f1 = &d;`	$a \supseteq \{d\}$	$f1 \supseteq \{d\}$	$a_{f1} \supseteq \{d\}$
`a.f2 = &f;`	$a \supseteq \{f\}$	$f2 \supseteq \{f\}$	$a_{f2} \supseteq \{f\}$
`b.f1 = &e;`	$b \supseteq \{e\}$	$f1 \supseteq \{e\}$	$b_{f1} \supseteq \{e\}$
`c = a.f1;`	$c \supseteq a$	$c \supseteq f1$	$c \supseteq a_{f1}$
Conclude	$c \mapsto \{d, f\}$	$c \mapsto \{d, e\}$	$c \mapsto \{d\}$

Here, the field-insensitive and field-based solutions are imprecise in different ways. In general, their relative precision depends on the program in question. For example, analysing a program with many aggregates of the same type would likely be best done with a field-insensitive analysis. This is because the field-based analysis will combine the solution for each instance of a given field into one, thereby losing a lot of information. In contrast, if the program has a small number of aggregates with a large number of fields then the opposite will be true.

Most previous set constraint-based pointer analyses are either field-insensitive (e.g. [FFA00, HH98, HP00, FFSA98]) or field-based (e.g. [And94, HT01, GLS01]). Algorithms for field-sensitive analysis are harder to develop and implement, which may explain why they have received less attention. In particular, there are only two previous works looking at field-sensitive analysis of C [YHR99, CR99a]. In fact, more has been done on field-sensitive analysis of Java [RMR01, LH03, WL02, LPH01], again possibly because it is a slightly simpler problem than for C. In Chapter 5, we examine this further, whilst also presenting a novel approach to field-sensitive analysis of C. Several studies have looked at the relative merits of the three approaches to modelling aggregates, with the conclusion that field-sensitive analyses are considerably more precise [YHR99, DMM98, LH03, LPH01, RMR01]. However, it is important to realise that, since the problem differs between Java and C, it does not necessarily make sense to compare studies of Java with those for C. For example, previous results show that of the three, field-sensitive analyses are generally fastest when analysing Java [LH03, RMR01, WL02], but slowest when analysing C [YHR99, PKH04a]. The main reason for this is that in C we can take the address of a field, where as in Java we cannot. This means that using a field-sensitive analysis in C increases the number of potential pointer targets (often dramatically), leading to an increase in average set size [YHR99, PKH04a]. For Java, on the other hand, the number of potential targets cannot go up with field-sensitivity — thus, average set size *can only go down*.

For the analysis of C programs, there is little data available on the relative precision of the three methods. In [YHR99], a field-sensitive analysis is shown to offer twice the precision of an insensitive analysis, although their benchmarks are too small to draw any firm conclusions. In Chapter 5, we perform an identical experimental study using much larger benchmarks and find a similar increase in precision. However, as we will see, our results also indicate the pay off decreases with benchmark size. For field-based analyses, Heintze and Tardieu [HT01] present data which appears to show a field-based analysis gives more precise results compared with an

insensitive one. However, their data is described as "preliminary" and, in particular, we find their metric for comparison unsatisfactory because it has not been properly normalised. Thus, the only real conclusion we draw from this work is that field-based analyses are faster than their insensitive counterparts. Unfortunately, we must also caution that, in our opinion, field-based analysis of C is not safe. The interested reader is referred to Section 5.4.1 for a more technical discussion of this.

For Java, several studies show field-sensitive analyses are faster and more precise than the alternatives [RMR01, LH03, WL02]. As mentioned already, average set size might be one explanation for this. Another might be the proliferation of indirect function calls (due to virtual functions). This is relevant because a less precise analysis will identify more targets for an indirect call, thus introducing more constraints. Furthermore, these constraints are considerably more expensive than those for dereferencing a data pointer, since they cause non-trivial value flow. Unfortunately, the overall picture is complicated by a study showing little difference in precision between a field-based and field-sensitive analysis, with the latter also running slower [LPH01]. They argue that this should be expected from the strong encapsulation supported by Java. Indeed, this has some merit, if we consider that most fields in Java programs are read/written through get/set methods. Thus, context-insensitivity combines all distinct accesses to a particular field, yielding the same effect as the field-based approach. An example is given in Figure 2.2 and it seems that some simple strategies (such as inlining these get/set methods) would be very beneficial here. In fact, at least one analysis attempts something along these lines [MRR02], with promising results. Still, it seems unclear why other studies (e.g. [LH03]) of field-sensitivity have not encountered this problem and we can only speculate that they use some hidden technique to overcome it.

2.2.4 The Heap

Another important aspect affecting the precision of pointer analysis is the approach taken to modelling the heap. We consider there to be two useful techniques for this: the *static model*, where a distinct variable models every heap object allocated at a particular program point; and the *dynamic model*, where calling context is used to distinguish heap variables allocated at the same program point but on different execution paths. Clearly, the latter should produce more precise results although it is also likely to be more expensive to compute. Indeed, extending our constraint language to support a dynamic heap model is not an easy undertaking. One approach is to adopt the so called *call-strings* method used widely in control-flow analysis. This is done by introducing the following rule which specialises heap objects as they flow *upwards in the call graph*:

$$[trans_H]\ \frac{f_p \supseteq g_q \qquad g_q \supseteq \{HEAP_{s||g}\} \qquad f\ calls\ g}{f_p \supseteq \{HEAP_{s||g||f}\} \qquad HEAP_{s||g||f} \supseteq HEAP_{s||g}}$$

Here, the $||$ operator is simple string concatenation. Thus, we see that as a heap object flows upwards in the call graph, it will be split into separate variables — one specialised for each calling context. Figure 2.3 demonstrates how this can improve the precision of a pointer analysis.

One particular problem with using a static heap model is the pervasive use of `malloc` wrappers. These are functions which the application uses in place of `malloc` to allocate heap memory.

`class myclass {`	
`  private:`	
`   int *f1;`	
`   int *f2;`	
`  public:`	
`   int *get(myclass *this) {`	
`     return this->f1;`	$get_* \supseteq get_{this} \rightarrow f1$
`   }`	
`   void set(int *v, myclass *this) {`	
`    this->f1=v;`	$set_{this} \rightarrow f1 \supseteq set_v$
`   }`	
`};`	
`myclass a,b;`	
`int *c,d,e;`	
`a.set(&d);`	$set_v \supseteq \{d\}$
	$set_{this} \supseteq \{a\}$
`b.set(&e);`	$set_v \supseteq \{e\}$
	$set_{this} \supseteq \{b\}$
`c = a.get();`	$c \supseteq get_{this}$
Conclude	$c \mapsto \{d, e\}$

Figure 2.2: Illustrating how get/set methods affect field-sensitivity. For now, we can just assume the $\rightarrow$ operator does the right thing, and in Chapter 5 we consider it further. Notice that the `this` variable is passed explicitly to each member function, reflecting what actually happens in practice. The point is that by combining information at function boundaries we are losing the advantage from being field-sensitive.

	Static model	Dynamic model
`int a,b;` `int **f() { return malloc(...); }`		
	(1) $f_* \supseteq \{HEAP\}$	(1) $f_* \supseteq \{HEAP_f\}$

`void g()`
`{`
`int *q;`
`int **p;`
`p = f();`
	(2) $g_p \supseteq f_*$	(2) $g_p \supseteq f_*$
		(3) $g\ calls\ f$

`*p = &a;`	(3) $*g_p \supseteq \{a\}$	(4) $*g_p \supseteq \{a\}$
`q = *p;` `}`	(4) $g_q \supseteq *g_p$	(5) $g_q \supseteq *g_p$

`void h()`
`{`
`int **q;`
`q = f();`
	(5) $h_q \supseteq f_*$	(6) $h_q \supseteq f_*$
		(7) $h\ calls\ f$

`*q = &b;` `}`	(6) $*h_q \supseteq \{b\}$	(8) $*h_q \supseteq \{b\}$
	(7) $g_p \supseteq \{HEAP\}$ $(trans, 1+2)$	(9) $g_p \supseteq \{HEAP_{fg}\}$ $(trans_H, 1+2+3)$
		(10) $HEAP_{fg} \supseteq HEAP_f$
	(8) $HEAP \supseteq \{a\}$ $(deref_2, 3+7)$	(11) $HEAP_{fg} \supseteq \{a\}$ $(deref_2, 4+9)$
	(9) $g_q \supseteq HEAP$ $(deref_1, 4+7)$	(12) $g_q \supseteq HEAP_{fg}$ $(deref_1, 5+9)$
	(10) $g_q \supseteq \{a\}$ $(trans, 8+9)$	(13) $g_q \supseteq \{a\}$ $(trans, 11+12)$
	(11) $h_q \supseteq \{HEAP\}$ $(trans, 1+5)$	(14) $h_q \supseteq \{HEAP_{fh}\}$ $(trans_H, 1+6+7)$
		(15) $HEAP_{fh} \supseteq HEAP_f$
	(12) $HEAP \supseteq \{b\}$ $(deref_2, 6+11)$	(16) $HEAP_{fh} \supseteq \{b\}$ $(deref_2, 8+14)$
	(13) $g_q \supseteq \{b\}$ $(trans, 9+12)$	
Conclude	$g_q \mapsto \{a, b\}$	$g_q \mapsto \{a\}$

Figure 2.3: Illustrating how a dynamic heap model can improve the precision of a pointer analysis. Notice that, in the dynamic model, the heap is modelled with three distinct variables (i.e. $HEAP_f, HEAP_{fg}$ and $HEAP_{fh}$), where the static scheme only has one. For this reason, the latter loses precision because information flows through *HEAP* from function h to g.

Typically, they are implemented on top of `malloc` and provide extra functionality such as pooling or error checking. The problem arises because the analysis has no way to spot these and, thus, can create only one constraint variable (arising from the `malloc` call inside the wrapper) to model the entire heap. As we will find later on in this thesis, such wrappers are a real problem, although it remains unclear what can be done without resorting to the more expensive dynamic model.

In the literature, we are aware of only one study on the effects of heap model on the precision and cost of pointer analysis. This is due to Nystrom *et al.* who use a context-sensitive, set constraint-based analysis and a heap model that supports varying degrees of specialisation, ranging from static to fully dynamic [NKH04b] . Their results indicate, unsurprisingly, that the static model generally introduces a lot of inaccuracy and that a fully dynamic model can dramatically increase runtime. Therefore, they experimented with restricting the amount of specialisation by manually limiting the maximum length of the context strings used to name heap objects. This showed that, while some heap specialisation always improves precision, there is typically a threshold after which further specialisation offers little gain. Thus, their overall conclusion was that, to achieve scalability, it is necessary to somehow limit the amount of specialisation that can occur.

2.2.5 Arrays, Conditionals and Loops

There are a few components of modern programming languages which remain to be discussed. The first is the array, which typically can be statically or dynamically sized. The usual approach is to model an array using a single constraint variable to represent all elements. The difficulty with modelling elements separately is that, to do this we must model integer variables to some extent. Generally speaking, this is regarded as expensive to do properly and a waste of time otherwise. The following clarifies the approach we take and highlights how precision is lost by this:

`int *A[2],b,c;`	
`A[0] = &b;`	$A \supseteq \{b\}$
`A[1] = &c;`	$A \supseteq \{c\}$
Conclude	$A \mapsto \{b, c\}$

Another programming language construct affecting precision is the if-statement, which constrains the values of variables inside the conditional body. For example:

`int c,d,**p,**q,*a,*b;`	
`a=&c;`	$a \supseteq \{c\}$
`p=&a;`	$p \supseteq \{a\}$
`if(...) { p = &b; }`	$p \supseteq \{b\}$
`if(p != &a) { *p = &d; }`	$*p \supseteq \{d\}$
Conclude	$a \mapsto \{c, d\}$

In reality a never points to d and, thus, we see that ignoring the constraining effect of conditionals

gives rise to imprecision. As discussed in Section 2.2.2, this is related to a lack of flow-sensitivity, although it is important to realise that this goes beyond what is commonly regarded as the flow-sensitivity problem. Indeed, we are unaware of any previous work which looks at this effect and, thus, no data is available to help assess the impact of this design choice.

The final language feature relevant to our discussion is the loop construct. One approach here might be to *unroll* any loops before performing the analysis. This has several drawbacks: firstly, if the loop has many iterations the resulting expansion will be large; secondly, unrolling dynamically bounded loops requires modelling the integer variables involved which is costly (as before); lastly, flow-insensitive analyses would not gain from this anyway. For these reasons, loops are usually modelled without knowledge of the loop bounds and, thus, some precision is inevitably lost here.

2.2.6 Metrics

In the previous pages, we have considered various ways in which our analysis can be imprecise and, with the aid of previous work, have attempted to quantify this. As we have seen, the metric used for comparing the precision of pointer analyses is of great import here. Unfortunately, it still remains unclear what metrics should be used to compare analyses when considering specific problem domains (e.g. optimisation and verification). Some authors have gone to the extreme of discarding metrics altogether, instead showing the improvements obtained for a particular client (e.g. [SH97b, LPH01, GLS01, Guy03, HP00]). One problem with this approach is that limited space usually means only a few, specific clients are considered, with the reader being left unclear about the broad picture.

An interesting effort in this regard, is the work of Das *et al.*, who present a metric called *alias frequency* for comparing pointer analyses in the domain of compiler optimisations [DLFR01]. The idea is that alias frequency should be a good indicator for all likely optimisations and, thus, can be used instead of studying specific optimisations such as constant propagation or live variable analysis. Roughly speaking, the alias frequency is the percentage of all possible alias queries which are determined as aliased. An alias query being a request to determine whether two expressions refer to the same object. For example, consider the following program:

```
   int *p,a,b;
1. a=1;
   ...;
2. b=*p;
```

Now, let us imagine a compiler pass which (for whatever reason) desires to move the first statement past the second. To do this, those instructions in between must be examined to check for any dependencies. For example, if `p` points to `a` then there is a *Read-After-Write (RAW)* dependence, prohibiting the move. Thus, the compiler pass formulates the alias query $?<b,*p>$, passing it over to the pointer analysis component to be resolved. This will return either *unaliased* or *aliased* and only in the first case can the reordering go ahead. Generally speaking, it is always desirable for the analysis to return *unaliased* as this will enable whatever optimisation is being

attempted. Intuitively, the precision of the analysis determines the likelihood of *unaliased* being returned. For example, a simple and highly imprecise approach might be to always return *aliased*, but this would likely lead to many missed optimisations. So, the purpose of the alias frequency metric is to estimate the probability of the analysis returning *unaliased*. Of course, the set of actual queries generated will differ between each optimisation. To overcome this, the alias frequency is computed over the set of all possible alias queries for a program. In our example, this would be $\{?<a,b>,?<p,a>,?<p,b>,?<*p,a>,?<*p,b>,?<*p,p>\}$.

Perhaps the most interesting aspect of this work is that the authors compare their analysis against a lower bound analysis, which (unsoundly) returns unaliased for all queries involving a pointer dereference. The results of this show that their analysis generally produces results with an alias frequency within 5% of the lower bound, suggesting it is close to optimal. Note, the analysis itself was roughly equivalent to a flow-, context- and field-insensitive, set-constraint system. They conclude from this that investing in more precise analyses can offer only poor returns. Indeed, a separate study concurs (to a reasonable degree) with this finding [GLS01]. The key explanation appears to be that the majority of alias queries can be resolved *without using pointer analysis at all*. Furthermore, the experimental data presented also shows little or no correspondence between alias frequency and the actual speedup observed. From this, we draw two conclusions: firstly, the value of pointer analysis for enabling simple compiler optimisations may be limited; secondly, the usefulness of alias frequency as a metric remains uncertain. However, contrasting with the conclusion of [DLFR01], we do not believe that flow- and context-insensitive pointer analysis is 95% accurate, only that it may offer little benefit for some applications.

2.2.7 Concluding Remarks

In this section, we have examined what is known about the trade-off between precision and scalability for pointer analysis. Generally speaking, we have found it difficult to draw firm conclusions about the real benefits of a particular form of sensitivity. We feel the reason for this essentially comes down to two factors: firstly, it is always difficult to compare results from different works; secondly, the metrics used to quantify precision can be misleading. Typically, we find the most insight regarding a particular technique comes from studies which directly compare it against the alternatives. However, these are time consuming to perform, since multiple implementations are required and, thus, are likely to always be in short supply.

Regardless of these issues we feel that, in spite of conflicting reports, the benefits in precision from context-, field- and heap-sensitivity are becoming clear. Furthermore, we strongly believe that future studies will also show flow-sensitivity to offer significant gains in accuracy. The question, then, is whether or not these techniques can be combined efficiently to realise the dream of high precision, scalable pointer analysis.

2.3 Alternative Approaches to Pointer Analysis

In the previous sections, we have examined the use of set constraints for efficient pointer analysis, looked at improving the base system and speculated what yields, in terms of precision, might be obtained from doing this. We now divert our attention from set constraints to briefly consider the main alternatives and our aim here is purely to give the reader a broader overview of the field.

2.3.1 Abstract Interpretation

By far the most widely used technique for program analysis is *abstract interpretation* and much has been written in the literature about this (e.g. [CC77, Cou78, CC79, Myc81, BHA85, MJ86, JS87, BJCD87, Mel87, MH87, Wad87, WH87, Bru91, CC91, CC92a, CC92b, HM94]). The attraction of this approach is that it provides a general framework for validating termination and partial correctness. In the early days, abstract interpretation was the preferred choice for analysing pointer variables, although this has been in steady decline over the past decade. The main reason for this, as we shall see, is that the obvious implementation is very inefficient in both time and space.

We describe abstract interpretation in terms of a labelled digraph, which is somewhat unorthodox. However, our description is more expressive, subsumes the traditional approach and aligns better with this thesis. Let us define V to be the set of all variables in the source program and $P \subseteq V$ be the set of pointer variables. For simplicity, we assume no two variables have the same name. Now, for each program point p_x, we create a unique node x in the graph and associate with it an *abstract store*, denoted by σ_x, mapping each pointer variable to its solution. We can think of the abstract store as modelling the machine store at the corresponding program point, for all possible executions. For each program statement S, we construct a *transfer function*, written f_S, taking as input an abstract store and producing an updated version as output. Thus, the effect of S is captured in the difference between input and output. For example, a statement `x=y` is modelled by the transfer function $f_z(\sigma) = \sigma[x \mapsto \sigma(y)]$, where $\sigma[\ldots]$ yields an abstract store defined by:

$$\forall z \in P.\ \sigma[\ p \mapsto q\ ](z) = \begin{cases} q & \text{if } p = z \\ \sigma(z) & \text{otherwise} \end{cases}$$

Thus, applying f_z to an abstract store σ, gives a new abstract store differing only in that x now has the same target set as y. The edges of the graph capture control-flow information. For example, if p_a and p_b are the program points before and after some statement s, then an edge $a \xrightarrow{f_s} b$ will exist. This is labelled with f_s to mean that σ_b is constructed from σ_a by applying f_s. This makes sense, as the program state after the statement is executed is a function of the state before plus the statement semantics. In general, it is possible for a program point p_x to have multiple paths leading into it. In this case, we construct σ_x by *joining* each of the transformed stores from the incoming edges. The join operator, $\sqcup$, is defined as:

$$\sigma_1 \sqcup \sigma_2 = \{x \mapsto y \mid x \in P \wedge y = \sigma_1(x) \cup \sigma_2(x)\}$$

In the initial graph, every variable of each store is mapped to $\emptyset$. To solve the graph, we repeatedly

```
    int a,b;
1.  int *r,*q=&a;
2.  int **p=&q;
3.  if(...) *p=&b;
4.  r=q;
```

$$f_1(\sigma) = \sigma[q \mapsto \{a\}]$$
$$f_2(\sigma) = \sigma[p \mapsto \{q\}]$$
$$f_3(\sigma) = \bigsqcup_{x \in \sigma(p)} \sigma[x \mapsto \sigma(x) \cup \{b\}]$$
$$f_4(\sigma) = \sigma[r \mapsto \sigma(q)]$$

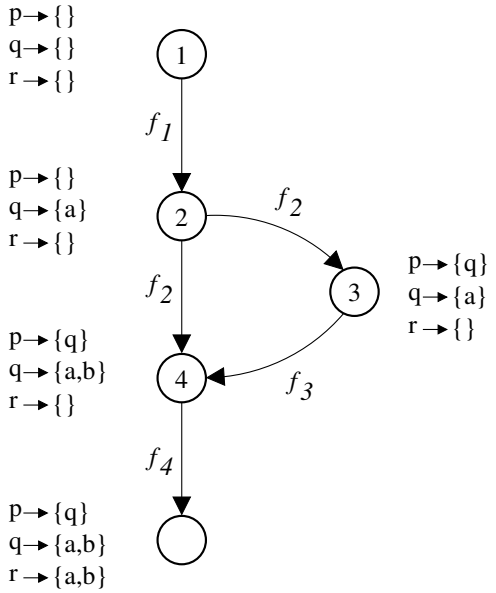

Figure 2.4: Here, we see a simple C program, its transfer functions and the *solved* graph. The transfer function for statement 3 is the most interesting part. Essentially, this adds b to the target set of all targets of p. Notice that it doesn't overwrite the target sets for the targets of p, as this would be unsafe.

procedure solve()
  $W = V$; *// W is the Worklist*
  while $|W| > 0$ **do**
    $n =$ select(W);
    // propagate solution to successors of n
    foreach $n \xrightarrow{f} w \in E$ **do**
      $tmp = f(Sol(n))$;
      if $Sol(q) \not\supseteq tmp$ **then**
        $Sol(w) = Sol(w) \sqcup tmp$;
        $W \cup = \{w\}$;
  // end while

Figure 2.5: A simple worklist solver. Note, we assume that, to start with, Sol contains the initial values for each node and selecting a node removes it from the worklist. Note, this algorithm is almost identical to that found in [NNH99] on page 367.

propagate the store for each node along its outgoing edges, until no change is observed. Propagating σ_x across $x \xrightarrow{f} y$ is defined as $\sigma_y = \sigma_y \sqcup f(\sigma_x)$. We now put all this together with some examples, shown in Figures 2.4 and 2.5. The latter gives a typical procedure for solving the graph, called the *worklist* algorithm.

One property of this analysis is that, by modelling each variable separately for each program point, it is implicitly flow-sensitive. In fact, most previous pointer analyses using this approach (e.g. [WL95, Wil97, EGH94, HBCC99, Lan92a]) go beyond this, by treating indirect assignments with a single destination in the same manner as a static assignment. This means previous values of the destination are overwritten (not included as is done above), which is commonly known as a *strong update*. Unfortunately, none of these analyses have been shown to operate on programs over 50,000LOC and the main reason for this is that each abstract store must model every variable in the program. In fact, this this can be reduced to a certain degree, for example, by ignoring variables outside the current scope. Furthermore, many stores will hold identical solutions for each variable, as a statement typically only affects one variable. While these issues have received some attention (e.g. [BCC$^+$02, BCC$^+$03, Bur90]), the general problem of efficient abstract interpretation has yet to be properly addressed and it remains interesting to see what can be achieved here.

An interesting study investigating the cost of using abstract interpretation for pointer analysis is that of Hind and Poli [HP00]. They provide an empirical comparison of several context-insensitive pointer analyses, including a flow-insensitive set-constraint algorithm and also the flow-sensitive abstract interpretation algorithm from [CBC93, HBCC99]. The reader may find it strange, then, that their results do not really support our claims. While the abstract interpretation algorithm was (on average) at least twice as slow as the set-constraint system, this reduced to a 20% margin when the execution time taken for a client analysis was also considered. This latter point may seem curious, but it is well known that a more precise analysis can often speed up the clients using it [SH97b, HP00]. However, a glaring problem with this experiment is that the set-constraint system did not use any of the crucial techniques, such as online cycle detection, which are known (and demonstrated in this thesis) to provide orders of magnitude speedup. In fact, the authors comment on this and caution about drawing conclusions from their performance data.

Unfortunately, there are no other fair comparisons of the two approaches to pointer analysis being considered. For example, the work of Ryder *et al.* [RLS$^+$01, SRLZ98] compares the context- and flow-sensitive, dataflow analysis from [Lan92a] against the context- and flow-insensitive analysis from [Zha98]. Their results show the former struggling to operate on programs with more than ≈ 7000LOC, while the latter scales up to ≈ 29000LOC with ease. Of course, the use of context-sensitivity interferes with a direct comparison of the dataflow approach since it is likely to be very expensive.

Finally, there is an important point to make about our description. We have suggested that, for each statement, there is one transfer function, which would imply the outgoing edges of a given node have the same label. This is in fact the normal approach taken, but we prefer to relax this constraint as it allows us to account for the effect of conditional statements. For example:

```
    int *p;
    ...
1.  p=q;
2.  if(p != NULL) { ... }
```

$f_{1a}(\sigma) = \sigma[p \mapsto \sigma(q)]$
$f_{1b}(\sigma) = \sigma[p \mapsto \sigma(q) - \{NULL\}]$

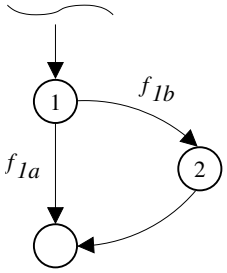

So, we see the transfer function f_{1b} models the conditional by ensuring that $p \not\mapsto \{NULL\}$ inside the body. Note that, under a traditional formulation of abstract interpretation, the effects of conditional statements cannot be accounted for.

2.3.2 Unification

The algorithms presented by Steensgaard [Ste95, Ste96b, Ste96a] were the first example of the unification approach to pointer analysis. This technique achieves a time complexity almost linear in program size, at the cost of being somewhat less precise than using set constraints. Curiously, unlike the others, unification does not appear to have expanded into other areas of program analysis. The general idea is to enforce the invariant that $|Sol(x)| \leq 1$ for each pointer variable x. This has subtle implications which are best explained by considering the *points-to* graphs involved. These differ from the set-constraint graphs focused on so far, because an edge $a \rightarrow b$ indicates that a points-to b (i.e. $b \in Sol(a)$). The invariant means that each statement need only be examined once, giving a fast time complexity. Thus, in the following example, each diagram shows the analysis solution after the corresponding statement has been processed:

Statement Processed	Unification Points-To graph
`1. int a,b,*p,*q`	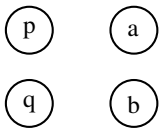
`2. p=&a;`	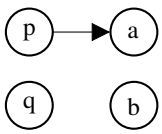
`3. p=&b;`	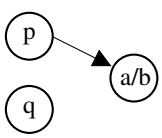
`4. q=&a;`	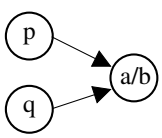

What we see is that, in order to maintain the invariant, we must *unify* two nodes together if one

pointer targets them both. We can also see that this reduces precision, since q must point to the combined node for a and b, instead of just a. Recall that the set-constraint analyses discussed previously do not impose such restrictions. Thus, they precisely conclude that $p \mapsto \{a, b\}$ and $q \mapsto \{a\}$, which corresponds to the following *points-to* graph:

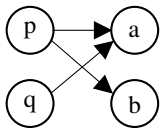

The intriguing aspect of unification is that we never need to visit a statement twice, while for the other types of pointer analysis we certainly do. This makes it very efficient and, in Figure 2.6, we attempt to uncover how this is possible. Of course, we have already seen that this efficiency comes at some cost to precision and this was generally perceived to be quite high. In fact, there is now overwhelming evidence to support this with many studies showing large differences compared with using set constraints (e.g. [LH99, Das00, FFA00, HP00, SS00, LPH01]). To that end, most previous work on unification has focused on improving precision whilst maintaining fast runtimes. A good example is that of Das *et al.* [Das00, DLFR01] who have extended unification in several directions. In [Das00], it is argued that the greatest use of pointers in C programs is in implementing call-by-reference parameters. Thus, their first extension, called *One Level Flow (OLF)*, attacks this case specifically by preventing unification of nodes at the top level of the points-to graph. For example, in Figure 2.6 this would mean c and d were not unified, while a and b (and any reachable from them) still would be. Their evaluation of this technique suggests it increases precision up to a level only marginally worse than using set constraints. Their results also show it maintains efficiency and, although comparative timing data is not provided for a set-constraint system, it seems likely that OLF would be much faster on large programs. Their case is supported by experimental data over a number of sizeable C programs and, in particular, one benchmark has over 2 million LOC and needs only 10 seconds for OLF to complete.

Das *et al.* take this further in [DLFR01], by introducing a limited amount of context-sensitivity, at the cost of roughly doubling the runtime. Their results show, firstly, that little precision was gained from introducing context-sensitivity and, secondly, that it was only slightly worse than a previous, fully context-sensitive unification algorithm [FRD00]. The new technique, called *Generalised One Level Flow (GOLF)*, aims to prevent values flowing into a function from some callsite x and flowing out to a different call site (i.e. along unrealisable paths). However, to that end, they are only able to restrict values flowing out of a function via the `return` statement. Thus, outgoing flow through global variables and call-by-reference parameters is not treated context-sensitively. This may be important and, in fact, it has been argued elsewhere that C functions largely side effect global variables and heap objects [FFA00].

Continuing this theme, Liang and Harold have also developed two context-sensitive unification algorithms [LH99, LH01]. The most interesting of these is MoPPA [LH01], which appears to provide slightly better precision than set constraints whilst maintaining reasonable efficiency. The technique used differs greatly from that found in [DLFR01, FRD00] and, in particular, we believe

Statement Processed	Unification Points-To graph	Set-Constraint Graph
`1. int a,b,*c,*d,**p`	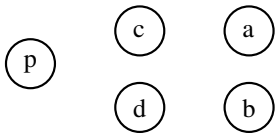	
`2. c=&a;`	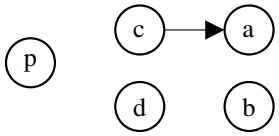	
`3. p=&c;`	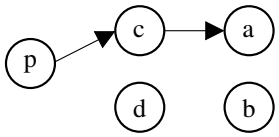	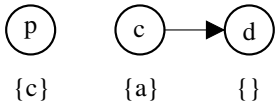
`4. d=c;`	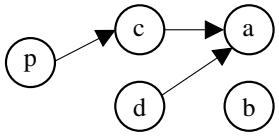	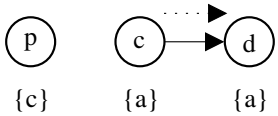
`5. *p=&b;`	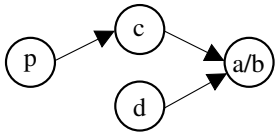	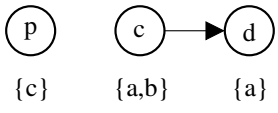

Figure 2.6: Illustrating how unification avoids revisiting statements. Note that the graphs shown for unification are *points-to* graphs, while for set constraints we draw the constraint graphs (as done in most prior examples). Also, the set-constraint approach first parses the program, producing a set of constraints which then form the initial graph shown. We have omitted the intermediate constraints, since they should be clear from the program statements. We see that the set-constraint system chooses to propagate from c (represented by the dotted line) before processing the complex constraint $*p \supseteq \{a\}$. This means that, in the final diagram, the solution is not yet obtained because c must be revisited to propagate b into $Sol(d)$. Thus, in a sense, it is revisiting statement 4 to do this. In contrast, the unification system is complete once the last statement is processed. This is because, by updating the value for c, we indirectly update that of any variable which c has flowed into before processing the current statement.

it treats all value-flow context-sensitively. In addition, MoPPA is the only analysis considered so far which implements a *dynamic heap model* (see Section 2.2.4). Thus, it seems likely that MoPPA offers higher precision than the algorithms from [DLFR01, FRD00].

The final piece of work we consider is by Foster *et al.* [FFA00]. Like the previous works, they present a context-sensitive variant, described as a *polymorphic analysis*. They experimentally compare this with the original Steensgaard algorithm, concluding theirs to be significantly more precise. However, they go against the trend by suggesting that this still falls some way short of that obtainable through set constraints. One reason for this might be explained by their inability to achieve context-sensitivity through indirect function calls, although this remains uncertain.

And so, in spite of these works, we must conclude that much remains unclear about the relative precision of unification, although it certainly offers faster solving times. There are many other interesting works on unification not covered here, which roughly fall into the following categories: those introducing context-sensitivity [LPH01, FRD00]; those studying precision [SH97b, SH97a, DMM98, HP00]; and, finally, those attempting to improve unification in other directions [Zha98].

2.4 Concluding Remarks

In this chapter, we have looked at the broad spectrum of techniques available to those developing pointer analyses. Our aim in doing this has been, firstly, to lay the foundations for the following chapters and, secondly, to give the reader a full understanding of how this work ties in with what has gone before. In the next chapter, we divert our attention away from pointer analysis entirely to examine online algorithms for maintaining a topological sort and identifying strongly connected components. Later, in Chapter 4, we return to consider how these can be used for speeding up pointer analysis.

Chapter 3

Online Topological Order

For a directed acyclic graph (DAG), $D = (V, E)$, a topological ordering, ord, maps each vertex to a priority value such that, for all edges $x \rightarrow y \in E$, $ord(x) < ord(y)$ holds. For cyclic digraphs, no valid topological ordering is possible. However, by collapsing each *strongly connected component (SCC)* or cycle into a single node we can obtain a DAG, often called the *condensation graph*, for which a valid ordering exists. There are well known linear time (i.e. $O(v + e)$, where $v = |V|$ and $e = |E|$) algorithms for computing the topological order of a DAG (e.g. [CLRS01]) and for identifying SCC's (see Appendix B). However, these are considered offline as they must compute a new solution from scratch when the graph is changed.

In this chapter, we examine efficient algorithms for updating the topological order of a DAG after some graph change (e.g. edge insertion) and we refer to this as the *Online Topological Order (OTO)* problem. We also consider the related issue of identifying strongly connected components after edge insertions/deletions, which we call the *Online Strongly Connected Components (OSCC)* problem. We say that an online algorithm is *fully dynamic* if it supports both edge insertions and deletions. A partially dynamic algorithm is termed *incremental/decremental* if it supports only edge insertions/deletions. Furthermore, an algorithm is described as *unit change* if it offers no advantage to processing updates in batches rather than one at a time. The main contributions of this chapter are:

1. A fully dynamic, unit change algorithm for maintaining the topological order of a DAG. While this has marginally inferior time complexity, compared with a previous algorithm, it is far simpler to implement. For this reason, we find it to be faster in practice and provide an experimental study on random graphs to support this.

2. The first batch algorithm for maintaining the topological order of a DAG. For a batch of b edge insertions, this has an optimal $O(b + v + e)$ bound on its runtime, which improves upon the best previous bound of $O(b(v+e))$ obtained by any unit change algorithm. We also provide an experimental comparison of this algorithm against the alternatives.

3. Extensions to these and a previous algorithm for the incremental OSCC problem.

Please note, the fully dynamic, unit change algorithm along with relevant background material and a similar experimental study have been previously published in [PK04].

procedure add_edges(B) *// B is a batch of updates*
  if $\exists x \rightarrow y \in B.[ord(y) < ord(x)]$ **then** *perform standard topological sort*

Figure 3.1: Algorithm SOTO, a simple solution to the OTO problem where ord is implemented as an array of size $|V|$.

3.1 Background

At this point, it is necessary to clarify some notation used throughout the remainder. In the following, we assume $D = (V, E)$ is a digraph:

Definition 1. We say that x *reaches* a node y, written $x \rightsquigarrow y$, if $x = y$ or $x \rightarrow y \in E$ or $\exists z.[x \rightarrow z \in E \ \wedge \ z \rightsquigarrow y]$. We also say that y is *reachable* from x.

Definition 2. The *set of outedges* for a vertex set, $S \subseteq V$, is defined as $E^+(S) = \{x \rightarrow y \mid x \rightarrow y \in E \wedge x \in S\}$. The *set of inedges*, $E^-(S)$ is defined analogously and the *set of all* edges is $E(S) = E^+(S) \cup E^-(S)$.

Definition 3. The extended size of a set of vertices, $K \subseteq V$, is denoted $||K|| = |K| + |E(K)|$. This definition originates from [AHR$^+$90].

The offline topological sorting problem has been widely studied and optimal algorithms with $\Theta(||V||)$ (i.e. $\Theta(v + e)$) time are known (e.g. [CLRS01]). However, the problem of maintaining a topological ordering online appears to have received little attention. A simple and well known solution, based upon a standard topological sort, is shown in Figure 3.1. This algorithm implements ord using an array of size $|V|$, which maps each vertex to a unique integer from $\{1 \ldots |V|\}$. Thus, ord is a total and contiguous ordering of nodes. The idea is to perform a full topological sort only when an edge $x \rightarrow y$ is inserted which breaks the ordering (i.e. when $ord(y) < ord(x)$). Therefore, SOTO traverses the entire graph for half of all possible edge insertions and, for a single edge insertion, has a lower and upper bound on its time complexity of $\Omega(1)$ and $O(||V||)$ respectively. An important observation is that edge deletions are trivial, since they cannot invalidate the ordering.

In practice, SOTO performs poorly unless the batch size is sufficiently large and several works have attempted to improve upon it [AHR$^+$90, MSNR96, Hoo87, ZM03, RR94]. Of these only two are of interest, since they provide the key results in this field. Henceforth, these are referred to as AHRSZ [AHR$^+$90] and MNR [MSNR96]. We examine these algorithms in some detail later on, but first we compare the known results on their time complexity. For MNR, an amortised time complexity of $O(v)$ over $\Theta(e)$ edge insertions has been shown [MSNR96]. One difficulty is that it remains unclear how optimal this result is. To that end, the work of Alpern *et al.* is more enlightening as they used an alternative mechanism for theoretically evaluating their algorithm [AHR$^+$90]. Their approach was to develop a complexity parameter which captured the *minimal* amount of work needed to update a topological order:

Definition 4. Let $D = (V, E)$ be a directed acyclic graph and ord a valid topological order. For an edge insertion, $x \rightarrow y$, the set K of vertices is a cover if $\forall a, b \in V.[a \rightsquigarrow b \wedge ord(b) < ord(a) \Rightarrow a \in K \vee b \in K]$.

This states that, for any a and b connected by some path which are incorrectly prioritised, a cover K must include a or b or both. We say a cover is minimal, written K_{min}, if it is not larger than any valid cover. Thus, K_{min} captures the least number of nodes any algorithm must reorder to obtain a solution. Alpern *et al.* recognised it is difficult to do this without traversing edges adjacent to those being reordered. They used a variation on this parameter, which we call K^*_{min}, where $||K^*_{min}|| \leq ||K||$ for any valid cover K. Therefore, $||K^*_{min}||$ captures the minimal amount of work required, *assuming adjacent edges must be traversed*. It remains an open problem as to whether this assumption is true of all algorithms for this problem. Certainly, it holds for those being studied here[1]. Algorithm AHRSZ obtains an $O(||K^*_{min}|| \log ||K^*_{min}||)$ bound on the time required for a single edge insertion. In contrast, we show in Section 3.1.2 that MNR is not bounded by $||K^*_{min}||$ and, thus, it has inferior time-complexity.

This approach to theoretically evaluating online algorithms is known as *incremental complexity analysis* and is a natural extension of complexity analysis based on input size. It recognises that, for an online problem, there is typically no fixed input capturing the minimal amount of work to be performed. Instead, work is measured in terms of a parameter δ representing the (minimal) *change* in input and output required. For example, in the OTO problem, input is the current topological order, while output is (any) valid ordering after an edge insertion. Thus, δ is the (minimal) set of nodes which must be reordered (i.e. $\delta = K_{min}$). Incremental complexity analysis is about identifying the parameter δ for the online problem in question. Furthermore, an algorithm is described as *bounded*, if its time complexity can be expressed only in terms of $||\delta||$ for all inputs and outputs. Otherwise, it is said to be *unbounded*. The use of $||\delta||$ here, as opposed to $|\delta|$, is simply to include algorithms which depend upon visiting the edges of nodes in δ. This is necessary to obtaining a bounded algorithm for all online graph problems we are aware of. The ideas of incremental complexity were developed over several previous works [Ber92, RR96, Ram96] and there many examples of its use (e.g. [Rep82, AHR$^+$90, RMT86, Wir93, FMSN94, Yeh83, Ram96]).

An alternative way of comparing online algorithms is *competitive analysis*. Essentially, the idea is to assume a sequence of operations (edge insertions in our case) for which an algorithm performs the most work. Then, the algorithm is regarded as *k-competitive* if it never performs more than *k* times the least amount of work needed to process this sequence. Here, *k* is the *competitive ratio* and it is used to compare against other algorithms for the problem in question. Unfortunately, Ramalingam and Reps have shown that no algorithm for the OTO problem can have a constant competitive ratio [RR94]. This suggests that competitive analysis is unsuitable for comparing algorithms of this problem.

Regarding the OSCC problem, it turns out that algorithm SOTO can be used if we replace the topological sort with Tarjan's algorithm for detecting strongly connected components (see Appendix B). In this way it still maintains a topological ordering as before, but with cycles repre-

[1] Strictly speaking, only if a refined notion of extended size (see Definition 7) is used.

sented as a single node in the ordering. The key point is that only edge insertions which invalidate the ordering can introduce cycles into the graph. Again, this means that it traverses the entire graph for half of all possible edge insertions. The approach used in [Shm83] is similar to this, but offers an improvement in that, when an edge $x \rightarrow y$ is inserted it will either do nothing or will search the entire reachable subgraph from y. In the worse-case, it will still search the entire graph for half of all edge insertions, but this is unlikely. Fähndrich *et al.* use a technique similar to this, demonstrating its ability to speed up pointer analysis [FFSA98]. In general, these approaches are inferior to MNR, AHRSZ and the algorithms presented later which, when extended to this problem, can prune the search dramatically. Finally, there has been a certain amount of work on dynamic cycle detection in labelled digraphs (e.g. [RS88, FMSN98, CBL01]), but this is a different and fundamentally harder problem than that studied in this thesis.

In general, online algorithms for directed graphs have received scant attention, of which the majority has focused on shortest paths and transitive closure (e.g. [KS99, DI00, DPZ00, DFMSN00, FMSN98, BHS02]). For undirected graphs, there has been substantially more work and a survey of this area can be found in [IEG99].

3.1.1 The Complexity Parameter δ_{xy}

In the above, we introduced the complexity parameter $||K^*_{min}||$ as a measure of the least work any algorithm must perform to update an invalidated topological order. Unfortunately, the time complexity for most of the algorithms examined in this chapter cannot be expressed in terms of $||K^*_{min}||$. Therefore, we must use an alternative to evaluate and understand them:

Definition 5. Let $D = (V, E)$ be a directed acyclic graph and ord a valid topological order. For an edge insertion $x \rightarrow y$, the affected region is denoted AR_{xy} and defined as $\{k \in V \mid ord(y) \leq ord(k) \leq ord(x)\}$.

Definition 6. Let $D = (V, E)$ be a directed acyclic graph and ord a valid topological order. For an edge insertion $x \rightarrow y$, the set δ_{xy} is defined as $\delta^+_{xy} \cup \delta^-_{xy}$, where $\delta^+_{xy} = \{k \in AR_{xy} \mid y \rightsquigarrow k\}$ and $\delta^-_{xy} = \{k \in AR_{xy} \mid k \rightsquigarrow x\}$.

Notice that, $\delta_{xy} = \emptyset$ only when x and y are already correctly prioritised (i.e. when $ord(x) < ord(y)$). Also, it is fairly easy to see that no member of δ^+_{xy} reaches any in δ^-_{xy}, since this would introduce a cycle. To understand δ_{xy}, it is useful to consider its meaning in a graphical manner:

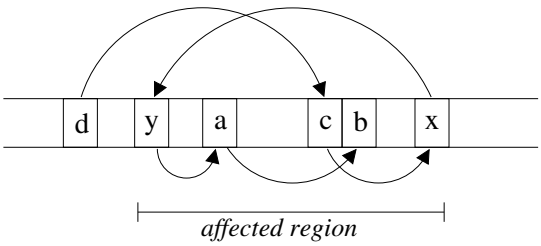

Here, nodes are laid out in topological order (i.e. increasing in ord value) from left to right and the gaps may contain nodes, which we have omitted to simplify the presentation. The edge

$x \to y$ invalidates the topological order (i.e. it has just been inserted) and is referred to as a *invalidating edge*, since $ord(y) < ord(x)$. Thus, $\delta_{xy} = \{y, a, b, c, x\}$ since it must include all those nodes in the affected region which reach x or are reachable from y. One feature common to all the algorithms we will consider is that they only reorder nodes *within the affected region*. This is possible because, for any edge $v \to w$ where $v \notin AR_{xy}$ and $w \in AR_{xy}$, we can reposition w anywhere within the affected region without breaking the invariant $ord(v) < ord(w)$. A similar argument holds when $v \in AR_{xy}$ and $w \notin AR_{xy}$. Another interesting property is the following:

Lemma 2. *Let $D = (V, E)$ be a directed acyclic graph and ord a valid topological order. For an edge insertion $x \to y$, it holds that $K_{min} \subseteq \delta_{xy}$.*

Proof. Suppose this were not the case. Then there must be a node $v \in K_{min}$, where $v \notin \delta_{xy}$. By Definition 4, v is incorrectly prioritised with respect to some node w. Thus, either $w \rightsquigarrow v$ or $v \rightsquigarrow w$. Consider the case when $w \rightsquigarrow v$ and, hence, $ord(v) < ord(w)$. Since ord is valid for all edges except $x \to y$, any path from w to v must cross $x \to y$. Therefore, $y \rightsquigarrow v$ and $w \rightsquigarrow x$ and we have $v \in AR_{xy}$ as $ord(y) \leq ord(v) \leq ord(w) \leq ord(x)$. A contradiction follows as, by Definition 6, $v \in \delta_{xy}$. The case when $v \rightsquigarrow w$ is similar. □

In fact, $K_{min} = \delta_{xy}$ only when both are empty. Now, $||K^*_{min}|| \leq ||K_{min}|| \leq ||\delta_{xy}||$ and, hence, we know $||\delta_{xy}||$ is not strictly a measure of minimal work for the OTO problem. Nevertheless, we choose δ_{xy} as it facilitates a meaningful comparison between the algorithms being studied. Finally, it turns out that a refinement on the notion of *extended size* is actually more useful when comparing algorithms for the OTO problem:

Definition 7. Let $D = (V, E)$ be a directed acyclic graph and ord a valid topological order. For some set $K \subseteq V$ and invalidating edge insertion $x \to y$, the *forward search cost*, $||\overrightarrow{K}||$, is defined as $|K_F| + |E^+(K_F)|$, where $K_F = \{z \in K \mid y \rightsquigarrow z\}$. Likewise, the *backward search cost* is $||\overleftarrow{K}|| = |K_B| + |\overleftarrow{E^-}(K_B)|$, where $K_B = \{z \in K \mid z \rightsquigarrow x\}$. Finally, the *total search cost* is $||\overleftrightarrow{K}|| = ||\overrightarrow{K}|| + ||\overleftarrow{K}||$.

Intuitively, the difference between $||K||$ and $||\overleftrightarrow{K}||$ is that the former assumes *all* edges adjacent to a node must be iterated, while the latter assumes only *inedges* or *outedges* (not both) need to be. This makes sense as the set of nodes to reorder can always be found by searching *forward* from y and *backward* from x. Furthermore, a forward (backward) search does not need to traverse the inedges (outedges) of those visited. Generally, we take the view that $O(||\overleftarrow{K}||) = O(||\overrightarrow{K}||) = O(||\overleftrightarrow{K}||) = O(||K||)$. While this does not hold for an individual edge insertion, it will on average across a sufficiently long sequence of (random) insertions. In particular, all four parameters are expected to be small on sparse graphs, but large on dense graphs. Finally, in what follows, we often reuse the term K^*_{min} to represent a cover where $||\overleftrightarrow{K^*_{min}}|| \leq ||\overleftrightarrow{K}||$ holds for any valid cover K. While this usage is slightly ambiguous, since a set K which minimises $||\overleftrightarrow{K}||$ does not necessarily minimise $||K||$, our meaning should always be clear from the context.

3.1.2 The MNR Algorithm

The algorithm of Marchetti-Spaccamela *et al.* [MSNR96] implements ord as a total, contiguous ordering of nodes using an array of size $|V|$, which maps each vertex to a (unique) integer in $\{1 \ldots |V|\}$. In addition, a second array ord^{-1} of size $|V|$ is used, which is the reverse of ord — it maps each index in the order to the corresponding vertex. Hence, both $ord^{-1}(ord(x)) = x$ and $ord(ord^{-1}(i)) = i$ always hold. Note, for the moment, we assume to be working with directed acyclic graphs (i.e. solving the OTO problem) and we will return to consider general digraphs in Section 3.5. Now, consider the following example arising from an edge insertion $x \rightarrow y$:

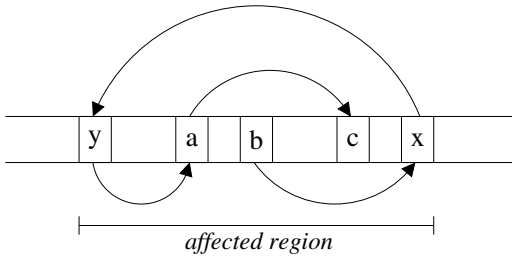

Here, nodes are laid out in topological order as before and, as ord is a total and contiguous ordering, the gaps must contain nodes, omitted to simplify the discussion. We know that y must come after x in the final ordering. So, a simple idea is to place y immediately after x, whilst left-shifting those in between. However, this is insufficient as a and c would now be left of y. So, the approach taken by MNR is to first identify all those reachable from y in the affected region (i.e. δ^{+}_{xy}) using a depth-first search and then shift them to positions immediately right of x. For the above example, this gives the following (valid) ordering:

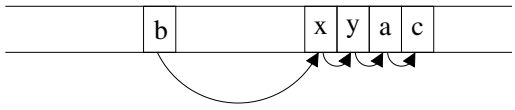

Pseudo-code for the algorithm is presented in Figure 3.2. The time needed for the DFS (discovery) phase is exactly $\Theta(||\overrightarrow{\delta_{xy}}||)$. The reassignment phase (i.e. procedure *shift*) requires $\Theta(AR_{xy})$ time as each element of AR_{xy} is visited. Therefore, we obtain an $\Theta(||\overrightarrow{\delta_{xy}}|| + AR_{xy})$ bound on the time for a single edge insertion. Note, only an amortised result was given by Marchetti-Spaccamela *et al.* and we feel that this new result provides a better reflection of MNR's performance. In particular, it suggests that MNR will perform poorly on sparse graphs, where $|AR_{xy}|$ is expected to be much greater than $||\overrightarrow{\delta_{xy}}||$. Finally, MNR is a unit change algorithm (i.e. it offers no advantage to processing in batches) and thus requires $O(b(v + e))$ time, in the worse case, to process a batch of b insertions.

```
procedure add_edge(x, y)
  lb = ord[y]; // lb = lower bound
  ub = ord[x]; // ub = upper bound
  if lb < ub then
    // invalidating edge
    dfs(y); // discovery phase
    shift(); // reassignment phase

procedure dfs(n)
  visited(n) = true; // mark n as member of δ+xy
  forall n → s ∈ E do
    if ord[s] = ub then abort; // cycle detected
    // visit s if not already and is in affected region
    if ¬visited(s) ∧ ord[s] < ub then dfs(s);

procedure shift()
  L = ∅;
  shift = 0;
  // shift nodes in affected region down order
  for i = lb to ub do
    w = ord^-1[i]; // w is node at topological index i
    if visited(w) then
      // w ∈ δ+xy so reposition after x
      visited(w) = false;
      push(w, L);
      shift = shift + 1;
    else allocate(w, i − shift);
  // now place members of δ+xy in their original order
  for j = 0 to |L| − 1 do
    allocate(L[j], i − shift);
    i = i + 1;

procedure allocate(n, i) // place n at index i
  ord[n] = i;
  ord^-1[i] = n;
```

Figure 3.2: The MNR algorithm.

3.1.3 The AHRSZ Algorithm

The algorithm of Alpern *et al.* [AHR$^+$90] employs a special data structure due to Dietz and Sleator to implement a priority space [DS87, BCD$^+$02]. This permits new priorities to be created between existing ones in $O(1)$ worse-case time. A side effect of using it is that AHRSZ maintains a partial, not total, ordering of vertices. Thus, the topological ordering, ord, is implemented as an array of size $|V|$, mapping vertices to priority values. Like MNR, this algorithm operates in two stages: *discovery* and *reassignment*. We now examine these (assuming $x \rightarrow y$ is an invalidating edge):

Discovery: The set of nodes, K, to be reprioritised is determined by simultaneously searching forward from y and backward from x. During this, nodes queued for visitation by the forward (backward) search are said to be on the forward (backward) frontier. At each step the algorithm extends the frontiers toward each other. The forward (backward) frontier is extending by visiting a member with the lowest (largest) priority. The following diagrams aim to clarify this:

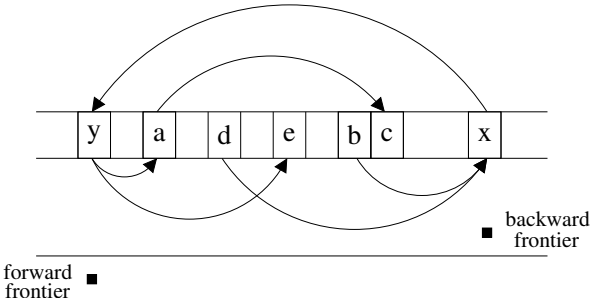

In the above, members of the forward/backward frontiers are marked with a dot. Initially, each frontier consists of a single starting node, determined by the invalidating edge. The algorithm proceeds by extending each frontier:

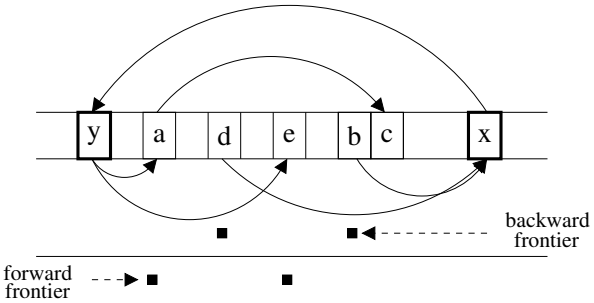

Here we see that the forward frontier has been extended by visiting y and this results in a, e being added and y removed. In the next step, a will be visited as it has the lowest priority of any on the frontier. Likewise, the backward frontier has been extended by visiting x and, next time, b will be visited as it has the *largest* priority. Thus, we see that the two frontiers are moving toward each other and the search stops either when one frontier is empty or they "meet" — when each node on the forward frontier has a priority greater than any on the backward frontier. The set of nodes, K, to be reprioritised contains exactly those visited before this happens. We refer to this procedure as *lock-step search*, since both frontiers move in unison.

Lemma 3. *Let $D = (V, E)$ be a directed acyclic graph and ord a valid topological order. For an invalidating edge insertion $x \to y$, the set $K \subseteq V$ found by lock-step search is a cover.*

Proof. Assume it is not. By Definition 4, some $a, b \notin K$ exist where $a \rightsquigarrow b \wedge ord(a) \geq ord(b)$. Partition K into $K^+ = \{z \in K \mid y \rightsquigarrow z\}$ and $K^- = \{z \in K \mid z \rightsquigarrow x\}$. Let $F_F = \{w \mid \exists v \in K^+ \wedge v \to w\}$ and $B_F = \{v \mid \exists w \in K^- \wedge v \to w\}$. Now, $\forall v \in F_F, w \in B_F.[ord(v) > ord(w)]$ as the search stops only when this holds. This implies $\forall v \in (\delta^+_{xy} - K^+), w \in (\delta^-_{xy} - K^-).[ord(v) > ord(w)]$, as ord is valid for all edges except $x \to y$. The contradiction follows as, by a similar argument to that of Lemma 2, $b \in (\delta^+_{xy} - K^+)$ and $a \in (\delta^-_{xy} - K^-)$. □

Lemma 4. *Let $D = (V, E)$ be a directed acyclic graph, ord a valid topological order and $x \to y$ an invalidating edge insertion. The set $K \subseteq V$ found by lock-step search contains $O(K_{min})$ nodes.*

Proof. Partition K into $K^+ = \{z \in K \mid y \rightsquigarrow z\}$ and $K^- = \{z \in K \mid z \rightsquigarrow x\}$. The lock-step search guarantees $|K^+| = |K^-|$ (since both frontiers extend simultaneously) and $\forall v \in K^+, w \in K^-.\big[ord(v) < ord(w)\big]$. Thus, either $K^+ \subseteq K_{min}$ or $K^- \subseteq K_{min}$ must hold, as every node in K^+ is incorrectly prioritised with every node in K^-. This implies $|K^+| \leq |K_{min}| \leq |K| \leq 2.|K^+| \leq 2.|K_{min}|$. □

Thus, we obtain an $O(||\overleftrightarrow{K_{min}}|| \log ||\overleftrightarrow{K_{min}}||)$ bound on discovery using the lock-step search. The $\log$ factor arises from the use of priority queues to implement the frontiers, which we assume are heaps. In fact, Alpern *et al.* use a clever strategy to reduce work further. Consider:

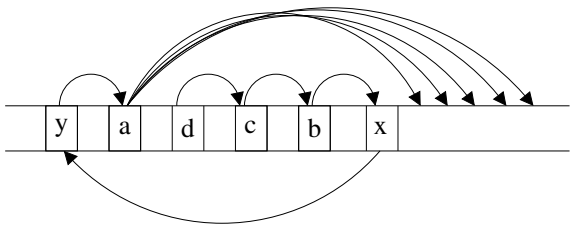

Here, node a has high outdegree (which can be imagined as much larger than shown). Thus, visiting node a is expensive as its outedges must be iterated. Instead, we could visit b, c, d in potentially much less time and still update the order correctly. The lock-step search algorithm described so far cannot do this because it moves both frontiers in each step. The full AHRSZ search algorithm, however, allows them to move independently to capitalise on situations like the above. Essentially, the frontier whose next node has the least number of adjacent edges is moved at each step. If it is a draw, then both are moved simultaneously. Thus, in the above, the backward frontier would be repeatedly extended. To ensure the amount of work done is still strictly bounded by $O(||K_{min}||)$, a counter $C(n)$ is maintained for each node n. This is initialised by the total number of edges incident on n (i.e. both inedges and outedges). At each step, $min(C(f), C(b))$ is subtracted from $C(f)$ and $C(b)$, where f and b are next on the forward and backward frontiers respectively. Thus, the forward frontier is extended if $C(f) = 0$ and the backward if $C(y) = 0$. Alpern *et al.* proved that this ensures an $O(||K^*_{min}|| \log ||K^*_{min}||)$ bound on the work done in this

stage [AHR+90]. This can be improved to $O(||\overleftrightarrow{K^*_{min}}|| \log ||\overleftrightarrow{K^*_{min}}||)$ by initialising $C(n)$ more appropriately [KB05]. Specifically, if n is on the forward frontier, then $C(n)$ is initialised with $E^+(n)$, otherwise $E^-(n)$ is used.

Reassignment: The reassignment process also operates in two stages. The first is a depth-first search of all nodes in K which computes a ceiling on the new priority of each:

$$ceiling(x) = min(\{ord(y) \mid y \notin K \ \wedge \ x \rightarrow y\} \cup \\ \{ceiling(y) \mid y \in K \ \wedge \ x \rightarrow y\} \cup \{+\infty\})$$

In a similar fashion, the second stage of reassignment computes the floor using ord', the new topological order formed so far:

$$floor(y) = max(\{ord'(x) \mid x \rightarrow y\} \cup \{-\infty\})$$

Once the floor has been computed for a node, the algorithm assigns a new priority, $ord'(k)$, such that $floor(k) < ord'(k) < ceiling(k)$. An important consideration here, is to minimise the number of new priorities created [AHR+90]. Otherwise, the underlying Deitz and Sleator ordered list structure may not achieve peak performance. Alpern *et al.* pointed out that, if an arbitrary topological order is used to compute the floor and priority of each $v \in K$, more priorities may be created than necessary. The following example highlights this, where members of K are shaded and the (fixed) priorities of non-members are shown below:

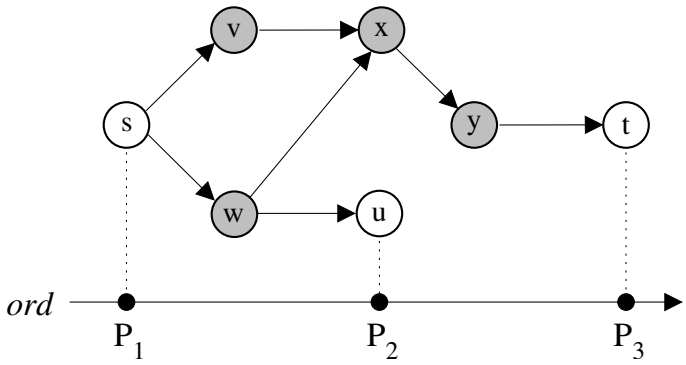

The problem is that more priorities are created if v, rather than w, is reassigned first. This is because v must be assigned a priority between it's floor $ord(s)$ and it's ceiling $ord(t)$, *reusing existing priorities whenever possible*. Thus, the new assignment must be $ord(v) = P_2$. This implies each of w, x and y require a new priority to be created, which is suboptimal since a valid reassignment is possible that creates only two new priorities. To address this, Alpern *et al.* use a mechanism similar to breadth-first search to ensure nodes with the same floor get the same priority. Specifically, they employ a min-priority queue with $floor(k)$ as the priority of each member k. Initially, this contains all nodes $k \in K$ with no predecessor in K. The algorithm proceeds by popping all nodes z with the lowest floor off the queue and determining the minimum ceiling, z_{min}, between them. Each z is then assigned the same priority P_z, where $floor(z) < P_z < z_{min}$. In doing this, the lowest existing priority is always used when possible, otherwise a new priority

is created. At this point, all remaining nodes whose predecessors are either not in K or have already been reassigned are pushed onto the queue. The whole process is repeated until all of K is reassigned. For the above example, this procedure creates the minimum number of new priorities. However, Alpern *et al.* did not prove that this holds for the general case, although it seems likely.

Finally, since all edges touching nodes in K must be scanned to generate the floor and ceiling information, the time needed for this stage is bounded by $O(||\overleftrightarrow{K^*_{min}}|| + K^*_{min} \log K^*_{min})$. The $\log$ factor arises from the use of a min-priority queue. In fact, Katriel and Bodlaender showed that this can be reduced to $O(K^*_{min})$, using a simpler mechanism [KB05]. However, this does not minimise the number of new priorities created and, thus, is expected to perform worse in practice.

The original bound given by Alpern *et al.* on the total time needed to process an edge insertion was $O(||\overleftrightarrow{K^*_{min}}|| \log ||\overleftrightarrow{K^*_{min}}||)$ [AHR+90, RR94]. However, it is easy to see that this reduces to $O(||\overleftrightarrow{K^*_{min}}|| \log ||\overleftrightarrow{K^*_{min}}||)$ if the improved discovery algorithm and the simple $O(K^*_{min})$ approach to reassignment are used. Pseudo-code for our implementation is provided in Figure 3.3 and there are a few remarks to make about it. In particular, the improved discovery algorithm of Katriel and Bodlaender is used, although their simpler reassignment algorithm is not — *even though it offers lower time complexity*. As discussed above, this is because their approach does not minimise the number of new priorities created and, hence, is expected to perform poorly in practice [AHR+90].

There are also a few points to make about the Dietz and Sleator ordered list structure [DS87] which AHRSZ relies on: firstly, it is difficult to implement and suffers high overheads in practice (both in time and space); secondly, only a certain number of priorities can be created for a given word size, thus limiting the maximum number of nodes. In fact, the original paper by Dietz and Sleator developed three ordered list algorithms: the first has an amortised $O(\log n)$ time bound and holds up to 32768 priorities with 32 bit integers; the second has an amortised $O(1)$ time bound and holds 2^{20} priorities with 32bit integers; the third has a worst-case $O(1)$ time bound. Generally, we consider the second variant to be of most practical value for this work. In particular, while we find the first variant to have lower time overheads, its limit on the maximum number of priorities is too restrictive. For example, up to 63568 priorities are needed to analyse ghostscript with our basic flow-insensitive pointer analysis (see Table 4.1, Chap 4) and even more are required for the field-sensitive version. In addition, we choose the second ordered list variant over the third *in spite of its worse time complexity*, as Dietz and Sleator themselves expect it to perform better in practice.

Finally, while we have studied the main aspects of algorithm AHRSZ here, some additional results are known. Katriel and Bodlaender showed that $O(\mathit{min}\{m^{3/2} \log v, m^{3/2} + v^2 \log v\})$ time is needed to process a sequence of m edge insertions [KB05]. They also found that, for DAGs with treewidth k, the modified algorithm needs at most $O(mk \log^2 v)$ time to insert m edges and that, for the special case of trees, this reduces to $O(v \log v)$. Zhou and Müller have also shown the space requirements of AHRSZ can be reduced [ZM03].

```
procedure add_edge(x, y)
  if ord(y) ≤ ord(x) then K = ∅; discovery(); reassignment();

procedure discovery()
  ForwFron = {y}; f = y; BackFron = {x}; b = x;
  ForwEdges = OutDegree(f); BackEdges = InDegree(b);
  // extend frontiers until either one is empty or they meet
  while ord(f) ≤ ord(b) do
    u = min(ForwEdges,BackEdges);
    ForwEdges = ForwEdges − u;
    BackEdges = BackEdges − u;
    if ForwEdges = 0 then
      // extend forward frontier
      K ∪= {f}; ForwFron −= {f};
      forall f→y ∈ E do ForwFron ∪= {y};
      if ForwFron = ∅ then f = x;
      else f = ForwFron.top();
      ForwEdges = OutDegree(f);
    if BackEdges = 0 then
      // extend backward frontier
      K ∪= {b}; BackFron −= {b};
      forall y→b ∈ E do BackFron ∪= {y};
      if BackFron = ∅ then b = y;
      else b = BackFron.top();
      BackEdges = InDegree(b);

procedure reassignment()
  // compute ceilings
  forall x ∈ K in reverse topological order do
    ceiling(x) = +∞;
    forall x→y ∈ E do
      if y ∈ K then ceiling(x) = min(ceiling(y), ceiling(x));
      else ceiling(x) = min(ord(y), ceiling(x));
  // compute new priorities, whilst minimising number created
  Q = ∅;
  forall x ∈ K do
    deps(x) = |{u | u→x ∧ u∈K}|;
    if deps(x) = 0 then floor(x) = max({ord(y) | y→x ∈ E} ∪ {−∞}); Q.push(x);
  while Q ≠ ∅ do
    Z = {z ∈ Q | floor(z) = floor(Q.top())};
    P_z = compute_priority(floor(Q.top()), min({ceiling(z) | z∈Z}));
    forall z ∈ Z do
      ord(z) = P_z; Q.pop();
      forall z→u ∈ E where u∈K do
        deps(u) = deps(u) − 1;
        if deps(u) = 0 then floor(u) = max({ord(y) | y→u ∈ E} ∪ {−∞}); Q.push(u);

procedure compute_priority(floor, ceiling)
  // select lowest priority z where floor < z < ceiling
  // if none exists then create one in O(1) time
  return z;
```

Figure 3.3: Algorithm AHRSZ, an optimal solution for the (unit change) OTO problem. The forward frontier is represented by ForwFron, and implemented using a min-priority queue. BackFron is similar, but using a max-priority queue. Notice that *ForwEdges* and *BackEdges* implement the counter $C(n)$ discussed in the text. Finally, Q is implemented using a min-priority queue.

3.2 Algorithm POTO1

We now present our first algorithm for solving the OTO problem. The development of this came from efforts to improve upon MNR and, hence, they share many similarities. The main improvement is a much tighter bound on the time needed for an edge insertion. While this remains inferior to that of AHRSZ, our claim is that its simplicity makes it more efficient in practice. In particular, the complicated Dietz and Sleator ordered list structure is not used. Like the others, POTO1 is a unit change algorithm operating on directed acyclic graphs.

The topological ordering, ord, is implemented as a total and contiguous ordering using an array of size $|V|$. As with MNR, this maps each vertex to a unique integer in $\{1 \ldots |V|\}$, such that for any edge $x \rightarrow y$, $ord(x) < ord(y)$ always holds. A second array (i.e. ord^{-1}) is not used. Thus, POTO1 has the lowest storage requirements of any so far[2]. The main observation behind the algorithm is that, for an invalidating edge insertion $x \rightarrow y$, we can obtain a correct ordering by simply reorganising nodes in δ_{xy}. That is, in the new ordering ord', nodes in δ_{xy} are repositioned to ensure a valid topological ordering, *using only positions previously held by members of* δ_{xy}. All other nodes remain unaffected and this represents a significant departure from MNR, where the entire affected region is reorganised. Consider the following example, arising from an invalidating edge insertion $x \rightarrow y$:

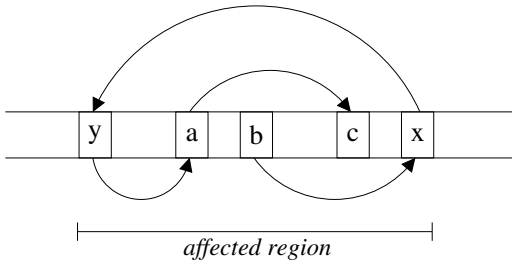

As before, nodes are laid out in topological order from left to right. Only members of δ_{xy} are shown and, as ord is total and contiguous, the gaps must contain nodes omitted to simplify the presentation. So, we have $\delta^+_{xy} = \{y, a, c\}$ and $\delta^-_{xy} = \{b, x\}$ and we obtain a correct ordering by repositioning nodes to ensure all of δ^-_{xy} are left of δ^+_{xy}:

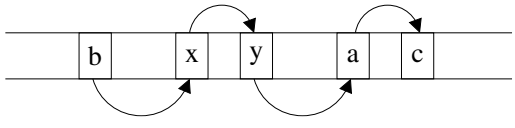

In doing this, the original (relative) order of nodes in δ^+_{xy} must be preserved and likewise for δ^-_{xy}.

[2]In fact, this is only true if the underlying graph data structure is an *adjacency matrix*. When an *adjacency list* is used, POTO1 may need more space than MNR (but not AHRSZ), because it necessitates a *bidirectional* adjacency list where MNR does not. This is because POTO1 relies on the ability to efficiently traverse both inedges and outedges, while MNR only ever traverses outedges.

This ensures that the following subtle invariant is maintained, where ord' is the new ordering being computed:

$$\forall x \in \delta^+_{xy}.[\ ord(x) \leq ord'(x)\ ] \wedge \forall y \in \delta^-_{xy}.[\ ord'(y) \leq ord(y)\ ]$$

The above states that members of δ^+_{xy} cannot be given lower priorities than they already have, whilst those in δ^-_{xy} cannot get higher ones. This is because, for any node in δ^+_{xy}, we have identified all in the affected region which must be higher than it (i.e. right of it). However, we have not determined all those which must come lower and, hence, cannot safely move them in this direction. A similar argument holds for δ^-_{xy}. Thus, we begin to see how the algorithm works: it first identifies δ^-_{xy} and δ^+_{xy}. Then, it pools the indices occupied by their nodes and, starting with the lowest, allocates increasing indices first to members of δ^-_{xy} and then δ^+_{xy}. So, in the above example, the algorithm proceeds by allocating b the lowest available index, like so:

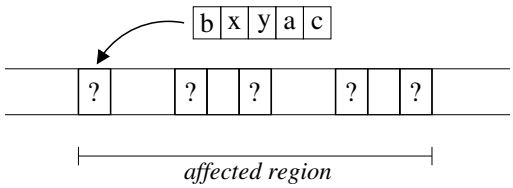

After this, it will allocate x to the next lowest index, then y and so on. The algorithm is presented in Figure 3.4 and the following summarises the two stages:

Discovery: The set δ_{xy} is identified using a forward depth-first search from y and a backward depth-first search from x. Nodes outside the affected region are not explored. Those visited by the forward and backward search are placed into δ^+_{xy} and δ^-_{xy} respectively. Thus, exactly $\Theta(||\overleftrightarrow{\delta_{xy}}||)$ time is needed for this stage.

Reassignment: The two sets are now sorted separately into increasing topological order (i.e. according to ord), which we assume takes $\Theta(\delta_{xy} \log \delta_{xy})$ time. We then load δ^-_{xy} into array L followed by δ^+_{xy}. In addition, the pool of available indices, R, is constructed by merging indices used by elements of δ^-_{xy} and δ^+_{xy} together. Finally, we allocate by giving index $R[i]$ to node $L[i]$. This whole procedure takes $\Theta(\delta_{xy} \log \delta_{xy})$ time.

Therefore, algorithm POTO1 has time complexity $\Theta((\delta_{xy} \log \delta_{xy}) + ||\overleftrightarrow{\delta_{xy}}||)$, which is a good improvement over MNR, but remains marginally inferior to AHRSZ. As it is a unit change algorithm (i.e. it offers no advantage to processing in batches) POTO1, like the others studied so far, requires $O(b(v+e))$ time to process a batch of b insertions. Elsewhere, Katriel has also demonstrated this algorithm to be worse-case optimal with respect to the number of nodes reordered over a series of edge insertions [Kat04a]. Finally, we provide the necessary correctness proof of algorithm POTO1:

Lemma 5. *Assume $D = (V, E)$ is a DAG and ord an array, mapping vertices to unique values in $\{1 \ldots |V|\}$, which is a valid topological order. If an inserted invalidating edge, $x \rightarrow y$, does not introduce a cycle then algorithm POTO1 obtains a correct topological ordering.*

Proof. Let ord' be the new ordering found by the algorithm. To show this is a correct topological order we must show, for any two vertices a, b where $a \rightarrow b$, that $ord'(a) < ord'(b)$ holds. An important fact to remember is that the algorithm only uses indices of those in δ_{xy} for allocation. Therefore, $z \in \delta_{xy} \;\Rightarrow\; ord(y) \leq ord'(z) \leq ord(x)$. There are six cases to consider:

(i) $a, b \notin AR_{xy}$. Here neither a nor b have been moved as they lie outside affected region. Thus, $ord(a) = ord'(a)$ and $ord(b) = ord'(b)$ which (by defn of ord) implies $ord'(a) < ord'(b)$.

(ii) $(a \in AR_{xy} \wedge b \notin AR_{xy}) \vee (a \notin AR_{xy} \wedge b \in AR_{xy})$. When $a \in AR_{xy}$ we know $ord(a) \leq ord(x) < ord(b)$. If $a \in \delta_{xy}$ then $ord'(a) \leq ord(x)$. Otherwise, $ord'(a) = ord(a)$. A similar argument holds when $b \in AR_{xy}$.

(iii) $a, b \in AR_{xy} \;\wedge\; a, b \notin \delta_{xy}$. Similar to case 1 as neither a or b have been moved.

(iv) $a, b \in \delta_{xy} \;\wedge\; x \rightsquigarrow a \;\wedge\; x \neq a$. Here, a reachable from x only along $x \rightarrow y$, which means $y \rightsquigarrow a \;\wedge\; y \rightsquigarrow b$. Thus, $a, b \in \delta^{+}_{xy}$ and their relative order is preserved in ord' by sorting.

(v) $a, b \in \delta_{xy} \;\wedge\; b \rightsquigarrow y \;\wedge\; y \neq b$. Here, b reaches y along $x \rightarrow y$, so $b \rightsquigarrow x$ and $a \rightsquigarrow x$. Therefore, $a, b \in \delta^{-}_{xy}$ and their relative order is preserved in ord' by sorting.

(vi) $x = a \;\wedge\; y = b$. Here, we have $a \in \delta^{-}_{xy} \wedge b \in \delta^{+}_{xy}$ and $ord'(a) < ord'(b)$ follows because all elements of δ^{-}_{xy} are allocated lower indices than those of δ^{+}_{xy}.

□

```
procedure add_edge(x, y)
  lb = ord[y];
  ub = ord[x];
  if lb < ub then
    // Discovery
    dfs-f(y);
    dfs-b(x);
    // Reassignment
    reorder();

procedure dfs-f(n)
  visited(n) = true;
  δ+_xy ∪= {n};
  forall n→w ∈ E do
    if ord[w] = ub then abort; //cycle
    // is w unvisited and in affected region?
    if ¬visited(w) ∧ ord[w]<ub then dfs-f(w);

procedure dfs-b(n)
  visited(n) = true;
  δ−_xy ∪= {n};
  forall w→n ∈ E do
    // is w unvisited and in affected region?
    if ¬visited(w) ∧ lb<ord[w] then dfs-b(w);

procedure reorder()
  // sort sets to preserve original order of elements
  sort(δ−_xy);
  sort(δ+_xy);
  L = ∅;

  // load δ−_xy onto array L first
  for i = 0 to |δ−_xy|−1 do
    w = δ−_xy[i];
    δ−_xy[i] = ord[w];
    visited(w) = false;
    push(w, L);
  // now load δ+_xy onto array L
  for i = 0 to |δ+_xy|−1 do
    w = δ+_xy[i];
    δ+_xy[i] = ord[w];
    visited(w) = false;
    push(w, L);
  merge(δ−_xy, δ+_xy, R);
  // allocate nodes in L starting from lowest
  for i = 0 to |L|−1 do ord[L[i]] = R[i];
```

Figure 3.4: The POTO1 algorithm. The "sort" function sorts an array such that x comes before y iff $ord[x] < ord[y]$. "merge" combines two arrays into one whilst maintaining sortedness (i.e. merge sort).

3.3 Algorithm POTO2

We now present our second algorithm, referred to as POTO2, for maintaining the topological order of a DAG online. This is the first batch algorithm for this problem and, hence, it can be considerably more efficient than any considered so far when edges are added in batches. Like POTO1, it is similar in design to MNR, this time employing both arrays, ord and ord^{-1}, to map nodes to indices and vice-versa. In fact, when only a single edge is added at a time, the algorithm operates in an identical fashion to MNR. So, our starting point is to identify where MNR performs redundant work when processing in batches. Consider the following, where there are two invalidating edges:

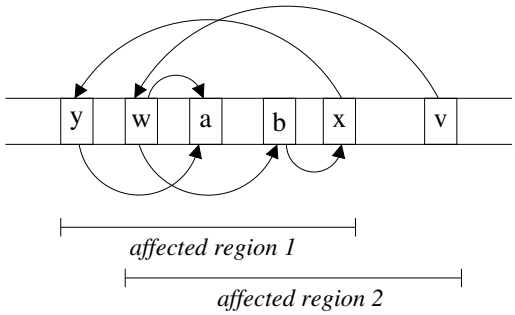

To deal with this batch update problem, each edge must be passed to MNR one at a time. If $x \rightarrow y$ is first, then applying MNR yields the following intermediate solution:

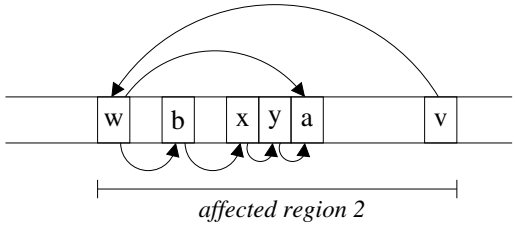

As expected, y and a were visited during the discovery (i.e. depth-first search) phase of MNR and then shifted past x. Now, inserting the second edge $v \rightarrow w$ means that w, b, x, y and a are all visited by the discovery phase and shifted past v to obtain the final solution:

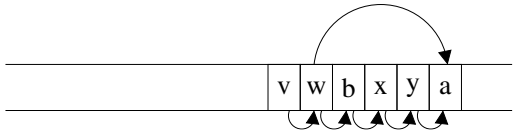

Thus, we see that a is discovered and shifted twice — once when $x \rightarrow y$ was added and then again for $v \rightarrow w$. Furthermore, every node which was originally in both affected regions has also been shifted twice. This is unnecessary as, by looking at the final solution, we know that every node which was originally left of and reachable from v must be shifted right of it. Hence, had we

somehow determined this set of nodes beforehand then only one shift would have been required. Note that, inserting $v \rightarrow w$ before $x \rightarrow y$ does not prevent nodes from being shifted twice.

The key feature of algorithm POTO2 is that it *never visits or shifts a node more than once* when inserting a batch of edges. In order to achieve this, we must alter our notion of the *affected region*, which was previously defined as the set of nodes between the head and tail of an invalidating edge. This is done by treating overlapping regions as one — so, although a batch of insertions can still define several affected regions, they are all distinct and can be processed independently. The following aims to clarify the new definition of an affected region:

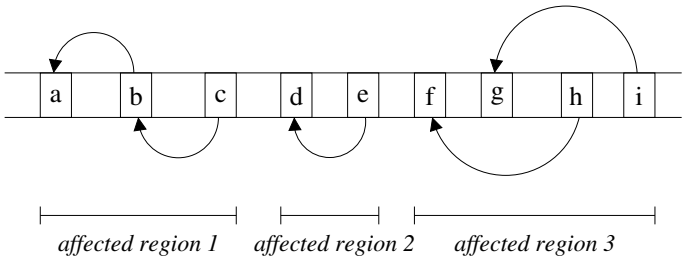

Here, each affected region can be correctly ordered independently of the others, by simply rearranging its contents. The difficulty then, lies in rearranging an individual region without visiting or shifting any node twice. This is complicated by the fact that we must now shift nodes to different points within an affected region, instead of only to the rightmost positions (as done in MNR). For example, in the above, f must be positioned just right of h, whilst g must go next to i. In fact, the reader may wonder why we don't simply shift both f and g past i. Doing this, it turns out, requires more work as we must also identify and shift any node reachable from f between h and i. Therefore, we introduce the *shift queue* which is a LIFO queue of tuples, $< x, d >$, where x is to be shifted past d (its destination). For example, the shift queue for processing region 3 above would be: $\{< f, h >, < g, i >\}$. The shifting process operates in much the same way to that of MNR — by scanning the region from left-to-right whilst filling up vacant slots by moving those not being shifted to the left. One difference is that, after moving a node, we check whether it is the destination of any on the shift queue and, if so, place them immediately after it. The following elaboration of region 3 from above shows how it would be shifted using this process:

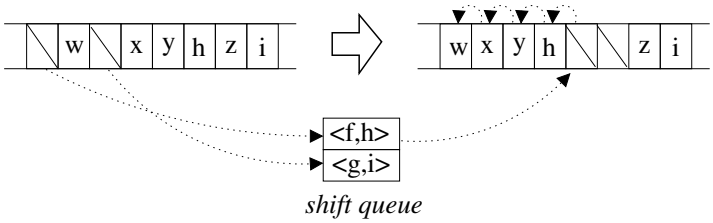

At this point, the algorithm has just moved h to the left and, as its destination has been reached, f will be placed into the free slot following it. The algorithm will then proceed by moving z and i one slot to the left and then placing g. Notice how the queue is carefully arranged so tuples whose

destinations will be encountered first are on top. Thus, only a constant-time check is needed to determine whether nodes on the queue need to be placed or not.

At this point, the remaining difficulty is with the discovery stage of the algorithm which is responsible for loading the shift queue before each region is reordered. The goal is to ensure each node in the region is visited at most once and the key to achieving this lies in the order with which invalidating edges are processed. Recall the discovery procedure of MNR consists of searching from the head of the invalidating edge to identify and mark those which must be shifted past its tail. The new procedure remains similar to this, in that we pick an invalidating edge $x \rightarrow y$ and then search forward from y. This time, however, discovered nodes are placed onto the shift queue, raising the question of what destination to give them. Unfortunately, the obvious answer of using the tail of the invalidating edge does not necessarily work. For example, consider the following graph:

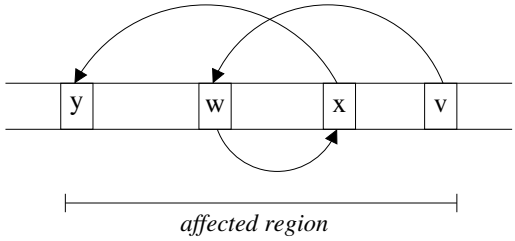

Now, suppose we begin with $x \rightarrow y$ by searching forward from y (within the affected region) and adding all encountered to the shift queue. The problem is that the destination for these nodes is actually v, not x, but we cannot know this before processing $v \rightarrow w$. Therefore, POTO2 processes invalidating edges in decreasing order by the topological index of their tail. In other words, it processes them from right to left. This guarantees it to always start at the rightmost point of any series of connected invalidating edges. Furthermore, if an invalidating edge is traversed (e.g. $x \rightarrow y$ above) whilst processing another (e.g. $v \rightarrow w$ above) then it will not be considered again.

A subtle point, worth mentioning here, is the way in which the searching is pruned. In the original MNR algorithm, each search was simply restricted to be within the affected region. However, using this rule with our new definition of an affected region leads to some inefficiency:

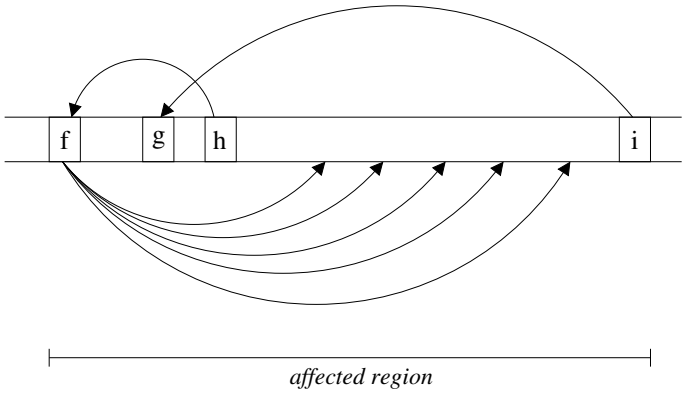

Here, f connects to a number of nodes right of h and, as they lie in the affected region, it seems that a search from f should visit them. However, it turns out that, since h is the destination

of those discovered from f, only nodes between f and h need to be visited. Therefore, algorithm POTO2 restricts the search to all nodes whose index is lower than the current destination (h in this case).

Pseudo-code for algorithm POTO2 is provided in Figure 3.5 and we now consider its worse-case time complexity over a batch of b edge insertions. If we assume that *sort* is implemented using a merge sort, then the worse case runtime is $O(v + e + b.\log b)$ as the algorithm can visit each node at most twice (once whilst searching and once whilst shifting). In fact, thanks must go to Irit Katriel for pointing out that this can be improved to $O(v + e + b)$ if a bucket sort is used instead [Kat04b]. Thus, we see that POTO2 offers a dramatic improvement over the $O(b(v + e))$ bound obtained for the other algorithms studied in this chapter.

The final part remaining in our discussion of algorithm POTO2 is to provide the necessary correctness proof. Perhaps unsurprisingly, this is a difficult undertaking and, as is customary, we aim only to provide enough detail to convince the reader of the algorithm's correctness. The center piece of the proof is the shift queue since this is really the glue connecting the discovery stage of the algorithm with the shifting stage.

Lemma 6. *Assume $D = (V, E)$ is a DAG and ord an array mapping each vertex to a unique index from $\{1 \ldots |V|\}$, with ord^{-1} implementing its reverse map. If a batch B of edge insertions does not introduce a cycle, then algorithm POTO2 produces a valid topological ordering.*

Proof. Let *ord'* be the new value of ord computed by the algorithm. Now, let us assume that *ord'* is not a valid topological ordering of nodes. Hence, there must exist two nodes, v and w, for which $v \rightsquigarrow w$ and *ord'*$(w) <$ *ord'*(v) is true. There are five cases to consider and we now demonstrate how each yields a contradiction of our assumptions:

(i) Neither v nor w were placed on the shift queue, Q, and $ord(v) < ord(w)$. Since $shift$ is only incremented when a visited node (i.e. a member of Q) is reached, any two nodes $i, j \notin Q$ must retain their relative ordering and, hence, $ord'(v) < ord'(w)$.

(ii) Neither v nor w were placed on the shift queue and $ord(v) > ord(w)$. Since ord is a valid ordering for all edges except those in B, v can only reach w by some series of invalidating edges. Let $x \rightarrow y$ be the invalidating edge whose tail has the highest priority of any on a path from v to w. As invalidating edges are sorted into decreasing order by the priority of their tail, it follows that dfs$(y, ord(x))$ will be invoked before dfs$(z, \ldots)$, for any other node z on a path from v to w. Furthermore, it must hold that $ord(v) \leq ord(x)$ — otherwise v could not reach w as (by definition of x) there are no invalidating edges higher up than x. From this and the basic properties of depth-first search it follows that dfs$(y, ord(x))$ invoked dfs$(w, ord(x))$, thus placing w onto the shift queue and contradicting our assumption.

(iii) $< w, z >$ was placed on the shift queue, but $< v, \ldots >$ wasn't. From this, $ord(w) < ord(z)$ immediately follows. Now, if $ord(v) \leq ord(z)$ then the contradiction follows easily as w is placed (possibly along with other members of the shift queue) immediately after z. If $ord(v) > ord(z)$ then there must be an invalidating edge $x \rightarrow y$ where $ord(z) < ord(x)$

```
procedure add_edges(B)
  // remove forward edges from B
  forall x→y ∈ B do if ord[x] < ord[y] then B −= {x→y}
  // sort invalidating edges into descending order by index of their tail
  sort(B);
  Q = ∅; // the shift queue
  lb = |V|; // lowerbound of current affected region
  // process invalidating edges
  for i = 0 ... |B| do
    x→y = B[i];
    // if index of tail less than lower bound, current region finished, so shift
    if ord[x] < lb then shift(lb);
    // dfs from head if edge not already traversed
    if ¬visited(y) then dfs(y, ord[x]);
    lb =min(ord[y], lb);
  // shift final affected region
  shift(lb);

procedure dfs(n, ub)
  visited(n) = true;
  forall n→s ∈ E do
    if ord[s] = ub then abort; // cycle detected
    // visit s if not already and is in affected region
    if ¬visited(s) ∧ ord[s]<ub then dfs(s, ub);
  // place n and current destination in topological order on queue
  push(<n, ord^-1[ub]>, Q)

procedure shift(i)
  shift = 0;
  while Q≠∅ do
    w = ord^-1[i]; // w is node at topological index i
    if visited(w) then
      visited(w) = false;
      shift=shift+1;
    else allocate(w, i − shift);
    // now insert all nodes associated with index i
    <n, t> = top(Q);
    while Q≠∅ ∧ w = t do
      shift=shift−1;
      allocate(n, i − shift);
      pop(Q);
      <n, t> = top(Q);
    i = i+1;

procedure allocate(n, i)
  // place n at index i
  ord[n] = i; ord^-1[i] = n;
```

Figure 3.5: Algorithm POTO2. This first marks those nodes reachable from y in AR_{xy} and then shifts them to lie immediately after x in $i2n$. Note that, initially all nodes are marked *unvisited*.

and $x \rightsquigarrow w$, because otherwise $v \not\rightsquigarrow w$. As invalidating edges are sorted into decreasing order by the priority of their tail, dfs$(y, ord(x))$ must have been invoked before dfs$(u, \ldots)$, for any other node on a path $v \rightsquigarrow w$. Thus, it again follows from the basic properties of depth-first search that dfs$(y, ord(x))$ invoked dfs$(w, ord(x))$. This gives the contradiction, since it implies that $< w, x >$ was placed onto the shift queue (not $< w, z >$).

(iv) $< v, z >$ was placed on the shift queue, but $< w, \ldots >$ wasn't. From this, $ord(v) < ord(z)$ immediately follows. Now, if $ord(w) < ord(z)$ then dfs$(v, ord(z))$ (which must have been called for v to be on the shift queue) would have lead to dfs$(w, ord(z))$ and w being pushed on the shift queue, giving the contradiction. If $ord(z) \leq ord(w)$ then $< z, x >$ was not placed on the shift queue, for any node x. This holds because otherwise $< v, x >$ would have been pushed onto the queue (since $x \rightsquigarrow v \wedge ord(z) < ord(x)$ and a similar argument to that used in (ii) and (iii) applies). Furthermore, since neither z nor w are placed on the shift queue, the argument from (i) gives $ord'(z) < ord'(w)$. Thus, a contradiction is obtained as v is placed (possibly with other members of the shift queue) immediately after z.

(v) Both $< v, x_1 >$ and $< w, x_2 >$ were placed on the shift queue. Again, $ord(v) < ord(x_1) \wedge ord(w) < ord(x_2)$ follows immediately. If it can be shown that $< v, x_1 >$ is pushed onto the queue after $< w, x_2 >$, then the contradiction follows easily because nodes are allocated in LIFO order. Thus, it remains only to show this. Let $x_1 \rightarrow y_1$ and $x_2 \rightarrow y_2$ be the two invalidating edges responsible for pushing $< v, x_1 >$ and $< w, x_2 >$ onto the queue respectively. If $x_1 = x_2$ then either dfs$(v, ord(x_1))$ invoked dfs$(w, ord(x_1))$ or the latter had already been called (due to some path $x_1 \rightsquigarrow w$ not involving v). Either way, $< w, ord(x_1) >$ is pushed first. If $x_1 \neq x_2$ then either $ord(x_1) < ord(x_2)$ and dfs$(w, ord(x_2))$ was invoked first, or $ord(x_1) > ord(x_2)$ and dfs$(v, ord(x_1))$ failed to call dfs$(w, ord(x_1))$. For the latter to hold, it must be that $ord(x_1) < ord(w)$ (otherwise w was already visited). But, this implies $ord(x_1) < ord(x_2)$ and, hence, that dfs$(w, ord(x_2))$ was invoked before dfs$(v, ord(x_1))$. Again, both cases result in $< w, ord(x_1) >$ being pushed first.

□

3.4 Experimental Study

In this section, we experimentally compare five algorithms for the OTO problem: MNR, AHRSZ, POTO1, POTO2 and SOTO (recall Figure 3.1). The experiments measure how the *Average Cost Per Insertion (ACPI)* varies with *graph density* and batch size, over a large number of randomly generated DAGs.

Definition 8. For a DAG with v nodes and e edges, define its density to be $\frac{e}{\frac{1}{2}v(v-1)}$. Thus, it is the ratio of actual edges to the maximum possible.

Furthermore, in an effort to correlate with our theoretical analysis, we also investigated how $||\overleftrightarrow{\delta_{xy}}||$, $|AR_{xy}|$ and $||\overleftrightarrow{K}||$, where K is the actual cover computed by AHRSZ, vary on average with graph density.

3.4.1 Generating a Random DAG

The standard model for generating a random *undirected* graph is $G(v, p)$, which defines a graph with v vertices where each edge is picked with probability p. Erdös and Rényi were the first to study this random graph model [ER60]. They found that, for certain properties such as connectedness, graphs whose edge count was below a certain threshold were very unlikely to have the property, whilst those with just a few more edges were almost certain to have it. This is known as the *phase transition* and is a curious and pervasive phenomenon (see [JLR00, Chapter 5] for more on this). Several other random graph models exist, such as one for generating graphs which obey a power law [ACL00]. For this work, we are only concerned with generating random DAGs and the model $G_{dag}(v, p)$, first defined by Barak and Erdös [BE84], is used here:

Definition 9. The model $G_{dag}(v, p)$ is a probability space containing all graphs having a vertex set $V = \{1, 2, \ldots, v\}$ and an edge set $E \subseteq \{(i, j) \mid i < j\}$. Each edge of such a graph exists with a probability p independently of the others.

For a DAG in $G_{dag}(v, p)$, we know that there are at most $\frac{v(v-1)}{2}$ possible edges. Thus, we can select uniformly from $G_{dag}(v, p)$ by enumerating each possible edge and inserting with probability p. In our experiments, we used $p = x$ to generate a DAG with v nodes and expected density x.

The approach to generating random DAGs suggested here is by no means the only method. One alternative is to use a *Markov Chain* where each step consists of picking two nodes at random and either deleting the edge between them (if one is present) or inserting an edge between them (if one is not) [MBMD01, IC02]. Note that, if inserting an edge would introduce a cycle then nothing is done. In general, it remains unclear how the two generation methods compare and further work could examine this in more detail.

An interesting aspect of our random DAGs is how they are affected by the phase transition and this issue was addressed by Pittel and Tungol [PT01]. They showed that, if $p = \frac{c(\ln\ v)}{v}$, then the size of the largest transitive closure of any vertex is asymptotic to $v^c \ln\ v$, $\frac{2v(\ln\ \ln\ v)}{v}$ and $v(1 - \frac{1}{c})$, when $c < 1$, $c = 1$ and $c > 1$ respectively. This means the phase transition occurs roughly at a graph density of $\frac{\ln\ v}{v}$, after which point it is likely that a path exists from the root (i.e. that with

procedure measure_acpi(v, d, b, s)
// v = number of nodes, d = density, b = batch size, s = sample Size
$ES = \ldots$; // *generate* $d.\frac{1}{2}v(v-1)$ *random (acyclic) edges*
$S =$ randomly select $s.\frac{1}{2}v(v-1)$ edges from ES;

$G = (\{1 \ldots v\},\ ES-S)$;
$start =$ timestamp();
while $S \neq \emptyset$
  $T =$ randomly select b edges from S;
  $S = S - T$;
  add_edges(T, G);

return $\frac{1}{|S|}.(\text{timestamp}() - start)$;

Figure 3.6: Our procedure for measuring insertion cost over a random DAG. Note that, through careful implementation, we have minimised the cost of the other operations in the loop, which might have otherwise interfered. In particular, the order in which edges are picked from S is precomputed, using a random shuffle.

the lowest index in our model) to every other node. In the experiments which follow, the graphs normally have 2000 nodes and, thus, the phase transition should occur around 0.0038. For this reason, we consider graphs with density below this threshold as sparse, and those over it as dense.

3.4.2 Experimental Procedure

Our general procedure for measuring the Average Cost Per Insertion (ACPI) for an algorithm was to generate, for some v and density, a random DAG and measure the time taken to insert a sample of edges whilst maintaining a topological order. Figure 3.6 outlines the procedure. Note, the sample size was fixed at 0.0001 (i.e. 0.01% of all $\frac{1}{2}v(v-1)$ possible edges). Although this seems like a small number, it is important to realise that most of the interesting observations occur between 0.001 and 0.02 density and, thus, larger sample sizes would swamp our results. To generate each data point, we averaged over 100 runs of this procedure (i.e. over 100 random DAGs). An important aspect of our procedure is that the sample may include non-invalidating edges and these dilute our measurements, since all five algorithms do no work for these cases. Our purpose, however, was to determine what performance can be expected in practice, where it is unlikely all edge insertions will be invalidating.

As mentioned already, some of our experiments measured the average set size of our complexity metrics, instead of ACPI. The procedure for doing this was almost identical to before except, instead of measuring time, exact values for $||\overleftrightarrow{K}||$, $||\overleftrightarrow{\delta_{xy}}||$ and $|AR_{xy}|$ were recorded. These were obtained from the corresponding algorithm (AHRSZ for $||\overleftrightarrow{K}||$, POTO1 for $||\overleftrightarrow{\delta_{xy}}||$ and MNR for $|AR_{xy}|$) by counting nodes visited and edges iterated where appropriate.

Finally, all experiments were performed on a 900Mhz Athlon based machine with 1GB of main memory, running Redhat Linux 8.0. The executables were compiled using gcc 3.2, with optimisation level "-O3" and timing was performed using the `gettimeofday` function, which gives

microsecond resolution. The implementation itself was in C++ and took the form of an extension to the *Boost Graph Library* [SLL02] and utilised the `adjacency_list` class to represent the DAG. Our implementation of AHRSZ employs the $O(1)$ amortised (not $O(1)$ worse-case) time structure of Dietz and Sleator [DS87]. This seems reasonable as they themselves state it likely to be more efficient in practice.

3.4.3 Single Insertion Experiments

The purpose of these experiments was to investigate the performance of the three unit change algorithms, *AHRSZ*, *POTO1* and *MNR*. Specifically, we looked at how ACPI varied with graph density and we report our findings here. Furthermore, we include data for a control experiment (labelled as CTRL), whose purpose is to indicate the best possible performance any algorithm could obtain. To generate data for our control, we perform exactly the same steps as for the other algorithms, except that no work is done to actually maintain the topological order. Thus, the control measures the cost of inserting edges into our underlying graph data structure.

Figure 3.7 shows the effect on ACPI and the complexity parameters of varying density, whilst maintaining $|V|$ constant. Although the highest density shown is 0.1, we have explored beyond this and found the plots extend as expected. Therefore, we limit our attention to this density range as it is most interesting. From the topmost graphs, we see that all three algorithms have quite different behaviour. The main observations are: firstly, MNR performs poorly on sparse graphs, but is the most efficient on dense graphs; secondly, POTO1 performs well on very sparse and dense graphs, but not as well on those inbetween; finally, AHRSZ is relatively poor on very sparse graphs, but otherwise has constant performance which is reasonably competitive with the others. By looking at the middle two graphs of Figure 3.7, a clear resemblance can be seen between the plots of ACPI for POTO1 and $||\overleftrightarrow{\delta_{xy}}||$, between that for MNR and $|AR_{xy}|$ and between that for AHRSZ and $||\overleftrightarrow{K}||$. Also, it is interesting to note that, while $||\overleftrightarrow{K}||$ is generally much smaller than $||\overleftrightarrow{\delta_{xy}}||$, AHRSZ still performs worse than POTO1 and this reflects the larger constants involved in its implementation.

Clearly, the curves observed for the three complexity metrics are key to understanding the performance of the algorithms. Their shape can be explained if we consider the number of invalidating edges in the insertion sample. The bottom two graphs of Figure 3.7 plot this and they show that the proportion of invalidating edges goes down rapidly with density. But, why is this? Well, we know that as density increases, the chance of a path existing between any two nodes must also increase. From this, it follows that the number of possible invalidating edges must go down as density goes up. This is because an edge $x \rightarrow y$ is invalidating only if there is *no* path from x to y. The steepness of these plots is governed by the phase transition phenomenon, which dictates that the chance of a path existing between two nodes quickly approaches 1 as soon as the 0.0038 density threshold is passed. From these facts, the curves seen for $|AR_{xy}|$ and $||\overleftrightarrow{\delta_{xy}}||$ can be explained: firstly, the average size of an affected region must go down as density increases, since $|AR_{xy}| = 0$ for non-invalidating edges; secondly, the average size of $||\overleftrightarrow{\delta_{xy}}||$ must (initially)

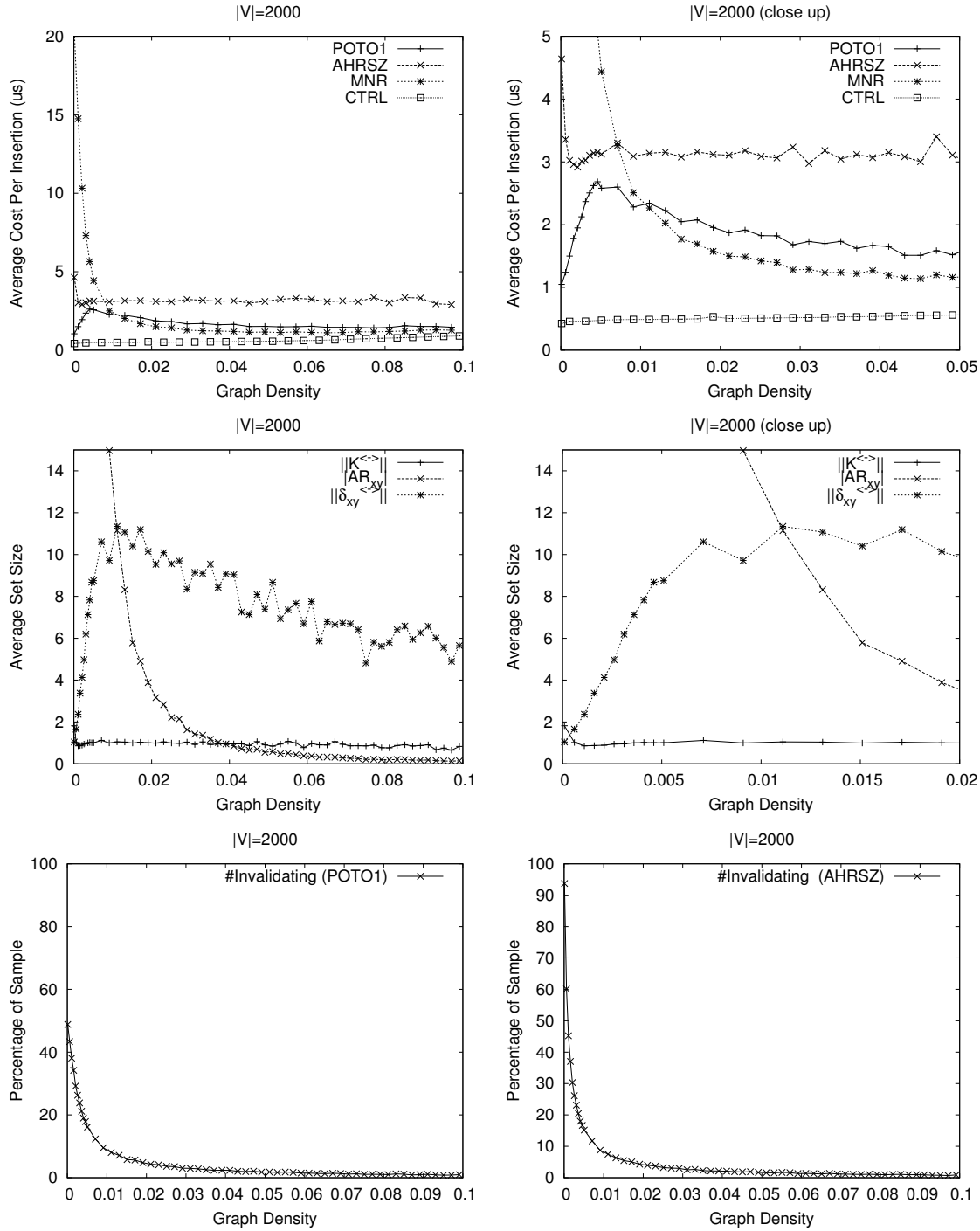

Figure 3.7: Experimental results for random DAGs with 2000 nodes of increasing density. The topmost plots show ACPI against density for the three unit change algorithms and our control. The middle plots show the complexity metrics which measure the work done by each algorithm. Finally, the bottom plots illustrate how the proportion of the insertion sample which is invalidating decreases with density for POTO1 and AHRSZ.

increase with density, since its size is determined by the chance of a path existing between two nodes. However, the decreasing number of invalidating edges will eventually overpower this and, hence, $||\overleftrightarrow{\delta_{xy}}||$ is determined by the trade-off between these two factors. The shape seen for $||\overleftrightarrow{K}||$ is more subtle. We had expected to see something more closely resembling that of $||\overleftrightarrow{\delta_{xy}}||$. That is, we had expected to see $||\overleftrightarrow{K}||$ go up initially and then fall. In fact, a small positive gradient can be seen roughly between 0.001 and 0.005 density which, we argue, corresponds to the increasing chance of a path existing between two nodes at this point. The most important feature of this plot, namely the negative initial gradient, is more curious. In particular, it seems strange that $||\overleftrightarrow{K}||$ is ever larger than $||\overleftrightarrow{\delta_{xy}}||$. This does make sense, however, if we contrast the bottom two graphs of Figure 3.7 against each other. What we see is that the proportion of invalidating edges for AHRSZ starts at a much higher point than for POTO1. This arises because, on very sparse graphs, AHRSZ will assign most nodes the *same priority* — so most insertions are invalidating. In contrast, for POTO1, all nodes have a different priority, regardless of density. This means there is (roughly) a 50% chance that any edge insertion $x \to y$ will be invalidating, since y is equally likely to come after x in the ordering than before it. Thus, as both $||\overleftrightarrow{K}||$ and $||\overleftrightarrow{\delta_{xy}}||$ are empty on valid insertions, we can see that $||\overleftrightarrow{\delta_{xy}}||$ is smaller than $||\overleftrightarrow{K}||$ on very sparse graphs simply because it is measured over fewer invalidating edges. Unfortunately, it still remains somewhat unclear why a negative gradient is seen for $||\overleftrightarrow{K}||$.

3.4.4 Experiment 2 - Batch Insertions

The purpose of these experiments was to investigate the benefits offered by algorithm POTO2, compared with the others, when edges are inserted in batches. Furthermore, we were also interested in seeing how it would compare against SOTO, which you may recall from Figure 3.1 uses a standard (offline) topological sort. So, following the same experimental procedure as before, we measured ACPI for all five algorithms for varying batch sizes on sparse and dense graphs.

Figure 3.8 shows the performance of POTO1, POTO2, MNR, AHRSZ and SOTO across varying batch sizes at densities 0.0001, 0.001 and 0.01. The plots of the three unit change algorithms (i.e. POTO1, MNR and AHRSZ) are flat as they can only process one edge at a time and, hence, obtain no advantage from seeing the edge insertions in batches. There are two overall conclusions from these graphs: firstly, POTO2 is always a better choice than either MNR or SOTO and, in many cases, offers a significant speedup; secondly, we find that POTO1 is very competitive with POTO2, even at large batch sizes, which is perhaps unexpected. In particular, the topmost four graphs of Figure 3.8 illustrate that, on sparse graphs, POTO1 performs significantly better than POTO2. This stems from the fact that POTO2 is a batch variant of MNR and, hence, shares its limitations on sparse graphs — especially when the batch size is small. However, the bottom two graphs of Figure 3.8 confirm that, on dense graphs, POTO2 is always the best choice when edges are inserted in batches.

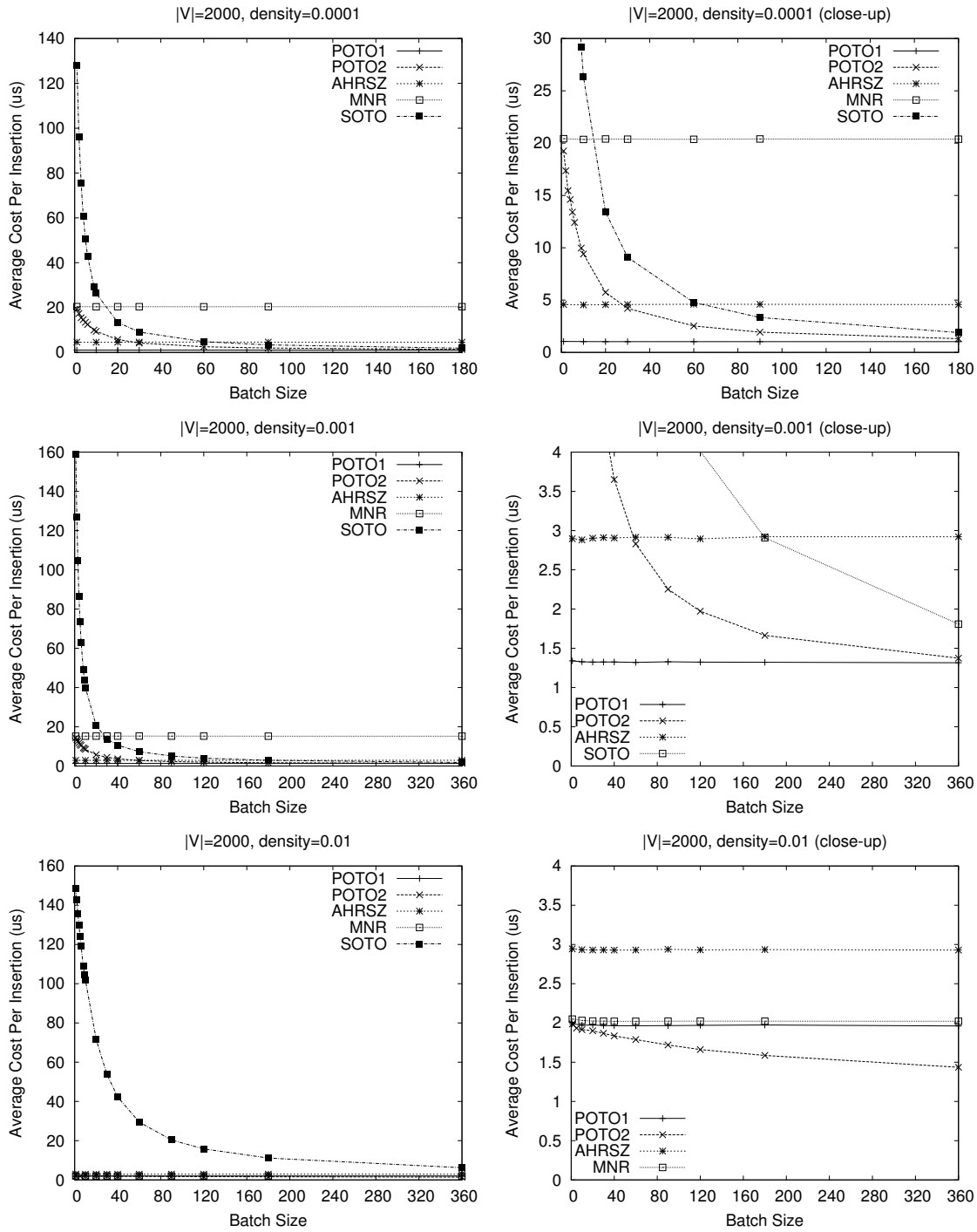

Figure 3.8: Experimental results looking at the effect of increasing batch size for all five algorithms on random DAGs with 2000 nodes at densities 0.0001, 0.001 and 0.01. In each case, batch size is plotted against ACPI and we provide close ups at each density to capture interesting features. We were unable to explore batch sizes greater than 180 at density 0.0001, since these graphs must have ≈ 200 edges after the insertion sample is completed. This limits the maximum batch size accordingly, since it cannot be larger than the insertion sample.

```
procedure dfs(n) // new edge is x → y
  visited(n) = true;
  forall n → s ∈ E do
    // visit s if not already and is in affected region
    if ¬visited(s) ∧ ord[s] < ub then dfs(s);
    // back propagate component information
    component(n) = component(n) ∨ component(s);
```

Figure 3.9: The depth-first search component of MNR, modified to back-propagate *component* information.

3.5 Online Strongly Connected Components

In this section, we adapt algorithms MNR, POTO1 and POTO2 to the problem of (incremental) *Online Strongly Connected Components (OSCC)*. Henceforth, we refer to the new algorithms as MOSCC, POSCC1 and POSCC2 respectively. Furthermore, while the modifications are straightforward and do not affect the complexity bounds obtained, we are unaware of any previous effort to use this type of algorithm for online cycle detection.

We begin by considering MNR and POTO1, since they are both extended in a similar way, based on the following observation: *if a new edge $x \rightarrow y$ introduces a cycle then x must be visited during a forward depth-first search from y.* Thus, it is easy enough to tell whether a cycle has been created during the discovery stage of MNR or POTO1. The real question is: how can we identify members of that cycle? By definition, all nodes reachable from y and reaching x are in the cycle, since there is a path from each through $x \rightarrow y$ back to itself. Therefore, we maintain an extra bit of storage for each node, referred to as the *component* bit, indicating whether a node is in the cycle or not. Initially, it is false for all nodes and, before starting the forward search from y, we set $component(x) = true$. The idea now is to back-propagate *component* information along edges traversed by the depth-first search. Figure 3.9 shows how the depth-first search used in MNR can be modified for doing this.

Once a cycle has been detected we collapse its members into a single node and, hence, we are effectively maintaining the topological order of the condensation graph. One issue is that, since the topological ordering is maintained using arrays of size $|V|$, the collapsing process will leave "unused slots" in the ordering — one per cycle member, less one for the representative. The temptation maybe to reduce the size of the array in order to eliminate these, but doing so would break our complexity bounds. Therefore, we simply leave them as is, since they can do no harm. Figure 3.10 walks through an example, whilst Figure 3.11 provides pseudo-code for the extended *shift* procedure from MNR. The extension for POTO1 is much the same, although care must be taken to reset the visited flag for any nodes reached in `dfs-f` before moving onto `dfs-b` since all predecessors of nodes in the component must be found to update the topological order correctly.

Detecting cycles with POTO2 is slightly harder, since multiple edges can introduce multiple cycles, and the technique used for MNR and POTO1 no longer works. The solution is to combine POTO2 with the original algorithm by Tarjan for detecting strongly connected components [Tar72]. Since both algorithms use a depth-first search, it is very easy to compose them and this

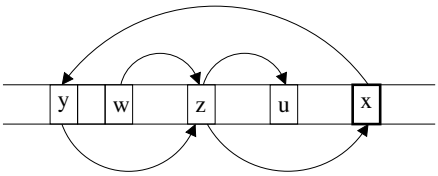

1. Initially, x is marked as *component*.

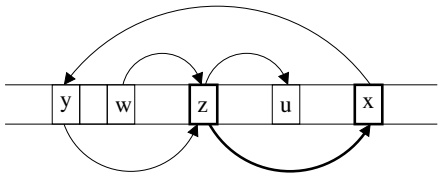

2. z is marked *component*, since it touches a node marked *component*.

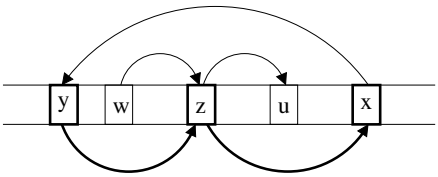

3. Likewise, y is marked *component*, since it also touches a node marked *component*.

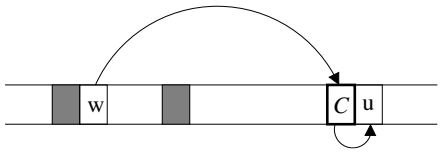

4. Finally, x, y, z are collapsed into one node C and shifted right as usual. This leaves two blank slots which are not removed to preserve the complexity bound.

Figure 3.10: Illustrating algorithm MOSCC operating on an example graph.

```
procedure shift() // new edge is x → y
  visited(x) = false; component(x) = false;
  L = ∅; C = ∅; shift = 0;
  for i = lb to ub do
    w = ord^{-1}[i]; // w is node at topological index i
    if visited(w) ∧ ¬component(w) then
      push(w, L);
      shift = shift+1;
      visited(w) = false;
    else
      if component(w) then
        push(w, C); // w is member of cycle
        component(w) = false;
        visited(w) = false;
      allocate(w, i−shift);
  // end for
  // place visited nodes after t in ordering
  for j = 0 to |L| − 1 do
    allocate(L[j], i−shift);
    i = i+1;
  // check if new cycle detected
  if |C| > 0 then collapse(x, C);
```

Figure 3.11: The extended *shift* procedure for algorithm MOSCC. The "collapse(x,C)" function merges nodes in $\{x\} \cup C$ such that x becomes the representative in the underlying graph.

does not affect the complexity bound obtained for POTO2. The main disadvantage over the simpler method used for POTO1 and MNR is that Tarjan's algorithm requires $v(2+3w)$ additional storage bits, where w is the word size and v the number of nodes. Note, Appendix B examines Tarjan's algorithm in detail and discusses some recent efforts to reduce the space requirements.

3.6 Concluding Remarks

In this chapter, we have presented two new algorithms for maintaining a topological order online and have shown, through theoretical and experimental evaluation, that they improve upon the best previously known works. In particular, we are the first to experimentally compare algorithms for this problem. Furthermore, we have demonstrated that these algorithms can be extended to detect strongly connected components dynamically, which is an important and well-known optimisation for pointer analysis.

While we have provided a detailed and rigorous analysis of algorithms for the OTO problem, there remains several avenues which could be explored further. These include:

- *Experimenting with real-world graphs*. We are aware that uniform random graphs do not necessarily reflect real life structures. Therefore, it would be interesting to experiment with real-world graphs in an effort to see whether any difference arises. Indeed, any alternative approach to generating the random graphs would also be interesting here.

- *A bounded complexity result for POTO2*. The reader may have noticed something interesting about our analysis of algorithm POTO2 — we did not provide a result in terms of $||\overleftrightarrow{\delta_{xy}}||$ and $|AR_{xy}|$. This was not because we could not find one, but that we simply did not have time to try. Furthermore, while the $O(v+e+b)$ bound we give does improve upon that of the three unit change algorithms, it does not in fact improve upon that of SOTO (recall Figure 3.1) which uses a standard (offline) topological sort, but achieves the same worse case bound. Nevertheless, we are confident that a result distinguishing POTO2 from SOTO can be found, probably without much effort.

- *Developing a batch variant of POTO1*. Since we were able to find a batch variant of the MNR algorithm, it seems plausible that a batch variant of POTO1 exists. In fact, while we have not obtained a complete algorithm, we have made some progress in this direction and we discuss this further in Chapter 6.

- *Improving algorithm POTO1*. Although not mentioned so far, there remains several opportunities to improve the POTO1 algorithm and it will be interesting to see whether a similar complexity bound to AHRSZ can be obtained. Again, we discuss this further in Chapter 6.

Finally, we must make some comments regarding the relationship this work has with that we have previously published. In [PK04], algorithm PK corresponds directly with POTO1 and the theoretical analysis also remains essentially the same, except that the refined notion of extended

size was not used. However, the experimental procedure for generating data has changed somewhat in light of several issues. Perhaps the main difference is that, since the publication of [PK04], an error in our implementation of algorithm AHRSZ was found. As a result, the performance data reported for AHRSZ in that paper differs substantially from that shown here.

Another difference from this work is that the experimental procedure used in [PK04] maintained a constant number of edges in the graph during the experiment. This was achieved by deleting edges from the graph within the inner loop (see [PK04, Figure 4]). However, we eventually found the overhead of doing this interfered with the results and, thus, we abandoned this method. However, this means that added edges now remain in the graph during an experiment and, hence, we must take care to use small enough sample sizes to prevent any dramatic change in density between the first and last insertion. Also, in the paper the sample size was a fixed constant, but we now prefer it as a proportion of the maximum possible. This ensures the graph density at the start and end of each individual experiment (i.e. each invocation of the procedure in Figure 3.6) remains the same, regardless of what value for $|V|$ is used.

Chapter 4

Efficient Pointer Analysis

Having spent the last chapter developing some directed graph algorithms in a more general context, we now return to consider their application to pointer analysis. Specifically, the focus of this chapter is on finding efficient methods for solving set constraint-based pointer analyses. To this end, we provide a theoretical and practical investigation into several specific solving algorithms. Furthermore, we extend a previous technique called *difference propagation* to our problem domain. Our starting point in all these endeavours is the Worklist algorithm (recall Section 2.3.1), since this is the classical approach to solving set-constraint systems.

To summarise, the main contributions of this chapter are:

1. A large experimental study, looking at numerous set-constraint solvers across different online cycle detection algorithms and iteration orders. Our benchmark suite contains 11 common C programs, ranging in size from 15,000 to 200,000 lines of code.

2. A theoretical and practical investigation into a technique called *difference propagation*. We show how this permits practical, cubic time solving algorithms.

Much of the work contained here-in has been previously published as [PKH03, PKH04b] and we return to discuss the relationship with this work at the end of the chapter.

4.1 Worklist Solvers

In this section, we consider how a traditional worklist solver, such as that introduced in Chapter 2, can be extended to solve constraints from our set-constraint language. In particular, we examine the importance of *iteration strategy* and also present a technique called *difference propagation*, which has been adapted from previous work [FS98] to the pointer analysis problem. We begin with an examination of what is already known about worklist algorithms in general.

```
procedure solve()
  W = V; // W is the worklist
  while |W| > 0 do
    n = select(W);
    // propagate Sol(n) to successors of n
    foreach n -f-> w ∈ E do
      tmp = f(Sol(n));
      if Sol(w) ⊉ tmp then
        Sol(w) = Sol(w) ∪ tmp;
        W = W ∪ {w};
```

Figure 4.1: Algorithm W, a traditional worklist solver. Note, we assume that, to start with, Sol contains the initial values for each node and selecting a node removes it from the worklist.

4.1.1 Background

In Chapter 2, we introduced the worklist algorithm (see Section 2.3.1) and we now discuss its operation in more detail. Figure 4.1 provides pseudo-code for such an algorithm, henceforth named W, which is a specialised version of that given in Chapter 2 (i.e. $\sqcup$ and $\sqsupseteq$ are implemented as $\cup$ and $\supseteq$). Note that, as it stands, algorithm W is not sufficient to handle our set-constraint language, since complex constraints are not dealt with. Thus, we are only considering in this section the case for solving a static constraint graph. In fact, almost all the previous work on worklist algorithms has assumed this. Recall from Section 2.3.1, that the problem domain solved by the worklist algorithm associates *transfer functions* with edges. In what follows, we assume these are the identity function, unless otherwise stated. An integral part of algorithm W is the strategy for choosing which node to process next, often referred to as the *iteration order* or *iteration strategy*. In Figure 4.1, the logic for implementing the iteration strategy is contained within the `select` function and a poor strategy can dramatically affect performance. For example, consider the following constraint graph prior to solving:

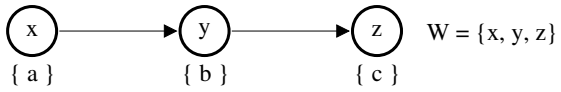

Notice that all nodes are present on the worklist. Suppose algorithm W begins solving the graph by visiting (i.e. selecting) node y first. This results in $Sol(y)$ being propagated into $Sol(z)$ and y being removed from the worklist:

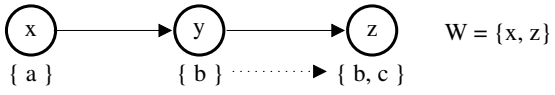

Since x remains on the worklist, it must be visited at some point in the future. When this happens, $Sol(x)$ will be propagated into $Sol(y)$ adding a to it. As $Sol(y)$ is now changed, y is placed back onto the worklist to ensure this is propagated to successors of y. Therefore, we must *revisit* y and *repropagate* $Sol(y)$ into $Sol(z)$. Had algorithm W begun by visiting x instead of y,

this redundancy would have been avoided. The obvious solution is to visit nodes in topological order. For acyclic digraphs, this provides a simple and optimal solution. For those containing cycles, one problem is that no valid topological order exists. To overcome this, an approximate topological ordering known as *reverse postorder (RPO)* can be used where $ord(y) < ord(x)$ must hold if $y \rightsquigarrow x \wedge x \not\rightsquigarrow y$. In other words, the usual topological ordering rules apply, except that nodes in the same cycle may be ordered arbitrarily with respect to each other. Note, this is also known as a *weak topological order* and can be computed using a depth-first search in the same way as a topological sort. So, for the following graph a valid reverse postorder would be $x \sqsubset y \sqsubset z \sqsubset w$:

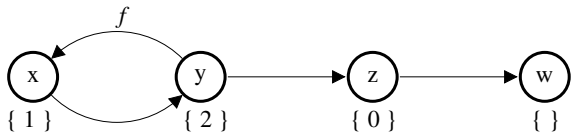

Another valid order would be $y \sqsubset x \sqsubset z \sqsubset w$. A simple strategy, henceforth S-RPO, is to visit nodes in RPO by implementing the worklist as a priority queue, with nodes prioritised by their index in the order. Assuming the RPO $x \sqsubset y \sqsubset z \sqsubset w$ and, for example, that $f(X) = \{y{+}1 \mid y{\in}X \ \wedge \ y{<}10\}$, then this strategy solves the above graph in an optimal number of visits. We write $(xy)^*zw$, to describe the general visitation order of S-RPO on this graph. As expected, this describes the set of strings $\{xyzw, xyxyzw, \ldots\}$. To the best of our knowledge, S-RPO was first presented by Horwitz *et al.* [HDT87] and, to highlight a limitation with it, they used an example similar to the following:

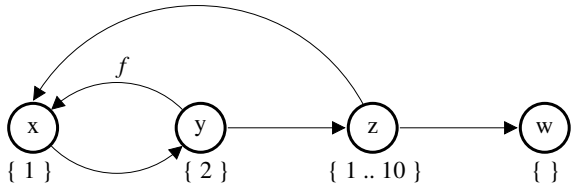

Here, assuming f as before, S-RPO visits nodes according to $((xy)^*z)^*w)$. Thus, x and y are iterated until their solutions have stabilised (known as reaching a *fixpoint*) before the others are considered. However, if z is chosen first then the inner cycle will stabilise immediately, resulting in fewer visitations. To overcome this, Horwitz *et al.* suggested a scheme, henceforth called S-SCC, where the (maximal) strongly connected components are first identified using Tarjan's algorithm. The idea is that, instead of iterating inner cycles to a fixpoint before considering others, all nodes in the same (outermost) cycle are visited one after the other, in RPO until a fixpoint is reached. For the above graph, this gives an iteration order of $(xyz)^*w$, an improvement on S-RPO. However, it is easy to construct problem cases for S-SCC. For example:

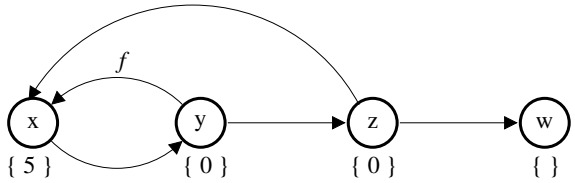

For this graph, S-RPO follows $((xy)^*z)^*w$ and visits fewer nodes than the order $(xyz)^*w$, used by S-SCC because z is visited only once.

An important work on this subject is that of Bourdoncle, who refers to the S-SCC approach as an *iterative strategy* [Bou93b]. He also proposes a *recursive strategy* (similar to S-RPO), where inner loops are always iterated to a fixed point before moving on to other nodes, and suggests this almost always outperforms the iterative strategy in practice. Thus, it seems reasonable to conclude that the previous example, where S-SCC outperforms S-RPO, may be somewhat artificial. The reader is referred to [NNH99, Bou93b, CH94, Bur90, FS96, Sch95] for more discussion on this subject.

4.1.2 Algorithm PW1, a Simple Worklist Solver

We now extend algorithm W to our set-constraint language. As mentioned already, the fundamental issue is the lack of support for complex constraints. This limitation can be addressed in several ways and we explore the obvious approach in this section. Furthermore, we demonstrate how complex constraints change the nature of the problem, rendering the iteration strategies of the previous section largely obsolete. Figure 4.2 provides pseudo-code for our new solver. The main observation is that complex constraints involving $*q$ are processed when q is visited. As before, iteration strategy greatly affects performance. One issue is that, as the graph is now dynamic in nature (i.e. new edges can be added during solving), the S-RPO and S-SCC strategies require online algorithms for maintaining reverse post-order to operate efficiently. The algorithms developed in Chapter 3 can be used for this. However, even with these available to us, there remains another problem not found in the static case. To understand this, let us consider how S-RPO will deal with the following graph:

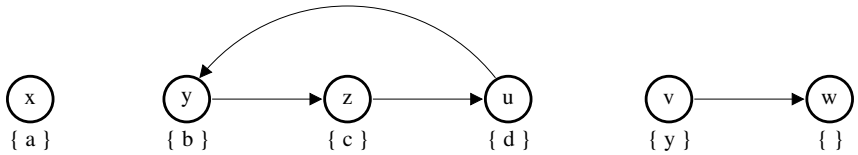

We assume there is also a single complex constraint, $*w \supseteq x$. The left-to-right layout of nodes constitutes a (weak) topological ordering and let us presume that this is used by S-RPO. Therefore, the complete order in which S-RPO will visit nodes to solve the graph is $xyzuyzvwyzu$. The key point is that, having visited v, processing w adds a new edge $x \rightarrow y$ to the graph (because of the complex constraint). In turn, this causes the revisitation of y, z and u to propagate a into each of their solutions. However, if S-RPO visits v and w first, then a visitation order such as $vwxyzuyz$ (which performs less work) is possible. To avoid redundant work, we must examine the solution

```
procedure solve()
  W = V;

  while |W| > 0 do
    n = select(W);

    // process constraints involving *n
    foreach c ∈ C(n) do
      case c of
      *n ⊇ w:
        foreach k ∈ Sol(n) do
          if w→k ∉ E then
            E = E ∪ {w→k};
            // invoke POSCC1/MOSCC add_edge here
            if Sol(k) ⊉ Sol(w) then
              Sol(k) = Sol(k) ∪ Sol(w);
              W = W ∪ {k};
      w ⊇ *n:
        foreach k ∈ Sol(n) do
          if k→w ∉ E then
            E = E ∪ {k→w};
            // invoke POSCC1/MOSCC add_edge here
            if Sol(w) ⊉ Sol(k) then
              Sol(w) = Sol(w) ∪ Sol(k);
              W = W ∪ {w};
      *n ⊇ {w}:
        foreach k ∈ Sol(n) do
          if w ∉ Sol(k) then
            Sol(k) = Sol(k) ∪ {w};
            W = W ∪ {k};

    // invoke POSCC2 add_edge here
    // propagate Sol(n) to successors of n
    foreach n→w ∈ E do
      // propagate Sol(n) across n→w.
      if Sol(w) ⊉ Sol(n) then
        Sol(w) = Sol(w) ∪ Sol(n);
        W = W ∪ {w};
  // end while
```

Figure 4.2: Algorithm PW1. The algorithm assumes that Sol has been initialised with all trivial constraints of the form $p \supseteq \{q\}$. The set $C(n)$ contains all complex constraints involving "$*n$". Selecting a node automatically removes it from the worklist.

sets to determine the hidden ordering they imply and supplement the topological order with this information. Strategies such as S-RPO and S-SCC do not do this and so, in general, cannot avoid revisiting nodes. We refer to such strategies as *solution-blind*. So, it becomes clear that finding an optimal iteration strategy for a dynamic graph differs greatly from the static case.

One approach to improving solution-blind strategies is to take the assumption that *any node may ultimately result in a new edge*. This can either be directly, via a complex constraint involving the node, or indirectly, where propagating its solution to some other node is a prerequisite (e.g. v in the above). This leads to a conclusion that nodes must be visited *fairly* to maximise the chance of processing one which actually does result in a new edge. Let us reconsider the visitation order $xyzuyzvwyzu$, obtained for S-RPO on the above graph. We see that S-RPO is *unfair*, because y is visited twice before v is visited once. In fact, imposing upon S-RPO the rule that each node must be visited once before any are revisited gives a near-optimal visitation sequence of $xyzuvwxyzu$.

In general, there has been little work on this issue of optimal iteration strategies in the dynamic setting (see [KW94, FS96]). However, we have found the simple scheme suggested in [KW94], called *least recently fired (LRF)*, to be very effective in practice. The idea is to prioritise nodes by when they were last visited, so that one is chosen over another if it was visited less recently. Essentially, this is identical to the *least recently used* paging policy and the key feature is that nodes are visited fairly. In contrast, we find that S-RPO and S-SCC perform poorly in practice, even when extended with the online topological ordering algorithms from Chapter 3. The reason for this is simply that, for every new edge added to the graph, the worklist must be reprioritised to reflect the new topological ordering and this is expensive. Although it is perhaps not apparent yet, this problem is really a limitation with the design of algorithm PW1, rather than with the efficiency of our online algorithms. In Section 4.2, we return to consider an improved algorithm which uses a fair, solution-blind topological iteration strategy and does perform well.

A tricky point is combining algorithm PW1 with the online cycle detection algorithms from Chapter 3. This is relevant to the experimental study which follows, since the full range of cycle detectors is used. For the unit change algorithms, this is straightforward as we simply invoke the corresponding "add_edge" function in MOSCC or POSCC1 when an edge is added by PW1. This means that any cycles which arise during solving are collapsed immediately. For POSCC2, however, things are more complicated since it must operate on insertion batches to gain any advantage. Therefore, its "add_edge" function is called by PW1 after all complex constraints for a node are processed — so all edges added whilst visiting a node are treated as a single batch. A side effect of this is that cycles are not collapsed immediately, but only once all complex constraints for a node have been processed. The corresponding places at which each "add_edge" function is called have been identified in the pseudo-code of Figure 4.2.

One important issue, neglected so far, is the computational complexity of algorithm PW1. In fact, it is fairly easy to show that, irrespective of the iteration strategy, at most $O(v^4)$ time is needed in the worst case, where v is the number of nodes in the constraint graph. This result underlines the inefficiency of PW1, since we already know from Chapter 2 that an $O(v^3)$ result is possible. In the next section, we demonstrate how a technique called *difference propagation* can be used to improve PW1 and obtain this optimal bound.

Lemma 7. *Let $D = (V, E, Sol)$ be a directed constraint graph, where $Sol(n) \subseteq V$ is the solution set for each $n \in V$. Algorithm PW1 needs at most $O(v^4)$ time to solve D, where $v = |V|$, regardless of the iteration strategy employed.*

Proof. Let $x \rightarrow y$ be any edge in E. We know that propagating $Sol(x)$ into $Sol(y)$ takes at most $O(v)$ time. Furthermore, $Sol(x)$ will be repropagated into $Sol(y)$ only when $Sol(x)$ changes. Therefore, since $Sol(x)$ can be changed at most $O(v)$ times, it follows that there will be at most $O(v)$ propagations across $x \rightarrow y$. From this the result is obtained easily, since we have $O(v)$ propagations across $O(e)$ edges, each of which takes $O(v)$ time, giving $O(v^2 e) = O(v^4)$. Furthermore, each node can have up to $2v$ complex constraints. This means at most $O(v^4)$ time is spent processing complex constraints, since each node can be visited $O(v)$ times and processing a constraint involves iterating $Sol(n)$. Note, we don't consider the cost of propagating across a new edge, since this happens at most $O(e)$ times and, thus, has already been accounted for. □

An interesting question is whether a specific iteration strategy can improve the worse-case bound of PW1. For this to be possible, the strategy must ensure that each node is visited once only. This is because we cannot avoid the cost of propagating a solution across each edge once, which takes $O(ve)$ time. Unfortunately, the following example demonstrates the impossibility of a cubic result for PW1:

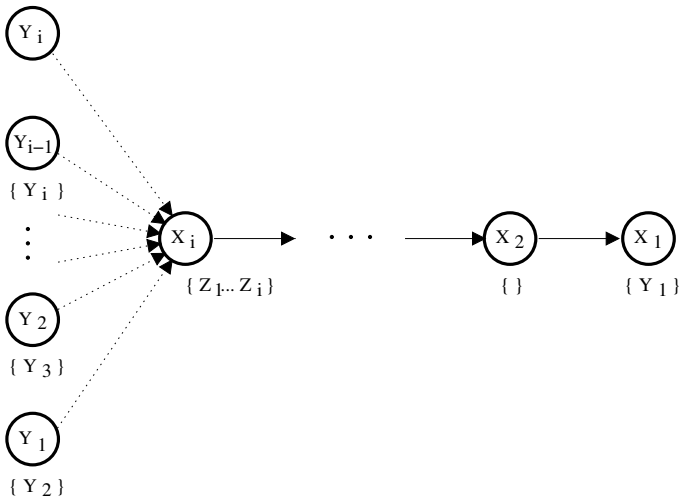

Here, $i = \frac{1}{3}v$ and we omit nodes $Z_1 \ldots Z_i$ for brevity and simply assume their solutions remain empty. Note, the nodes $X_1 \ldots X_i$ form a chain. Accompanying the graph is a single complex constraint, $X_i \supseteq *X_1$ and the dotted edges represent those which will be added during solving. The point about this example is that we simply cannot avoid repropagating the values $\{Z_1 \ldots Z_i\}$ across each edge in the chain $X_i \rightsquigarrow X_1$, every time a new edge is added. Now, there are $\frac{1}{3}v$ edges in the chain, each propagation takes at least $\frac{1}{3}v$ time and there will be $\frac{1}{3}v$ new edges. Thus, $O(v^3)$ time is needed to solve the graph. Furthermore, the example can be upgraded to require $O(v^4)$ solving time, simply by ensuring that $|E|$ is $O(v^2)$. This can be done, for example, by adding the edges given by $\{X_n \rightarrow X_{m-1} \mid 2 \leq m < n \leq i\}$.

4.1.3 Algorithm PWD, a Difference Propagation Solver

Difference propagation (also called incremental sets) is a technique first introduced by Fecht and Seidl [FS98]. They developed a general framework for applying it to (distributive) dataflow analysis systems, such as those discussed in Section 4.1.1 above and Section 2.3.1. Here, we show how this technique can be applied to our problem to obtain an $O(v^3)$ algorithm which, in some sense, can be considered an instance of their framework. One issue is that their system cannot describe constraints with a dereferenced variable on the left hand side, although this is not difficult to fix. However, our main contribution is in providing a theoretical and experimental study of the technique applied to our problem domain.

An important question is *where does algorithm PW1 perform redundant work?* By studying the proof of Lemma 7, it becomes apparent that a factor of v time is wasted repropagating solution values across edges. Therefore, the aim of difference propagation is to enforce an invariant that each value is only ever propagated across an edge once. Consider the following:

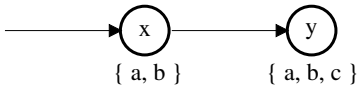

Here, we assume $Sol(x)$ has already been propagated along $x \rightarrow y$ once. Now, suppose a new value is propagated from some node into $Sol(x)$. Then, $Sol(x)$ must be repropagated across $x \rightarrow y$ to obtain a valid solution, like so:

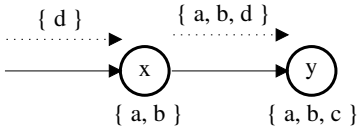

The key point is that a and b have already been propagated across $x \rightarrow y$ and doing so again is redundant. In fact, only the change in $Sol(x)$ (in this case $\{d\}$) must be propagated into $Sol(y)$. Difference propagation exploits this by maintaining the change in solution for each node, so it can be used in place of $Sol(x)$.

The new solver, PWD, is an extension of PW1 and its pseudo-code is given in Figure 4.3. A key component is the difference set, $\Delta(n)$, containing the change in solution for a node n. Thus, when visiting a node n, it is now $\Delta(n)$, not $Sol(n)$, which is propagated to all successors. A subtle point is the processing of complex constraints. When a new edge $x \rightarrow y$ is added to the graph, we cannot simply propagate $\Delta(x)$ into $Sol(y)$. This is because no member of $Sol(x)$ has been propagated across the edge yet. Therefore, we must propagate the entire of $Sol(x)$ across the edge. Notice that this does not break our invariant, since it will be the first time any member of $Sol(x)$ is propagated across the edge.

An important aspect of PWD is the implementation of $Sol(n)$ and $\Delta(n)$. In particular, to obtain the desired complexity bound, it must be possible to propagate $\Delta(x)$ into $Sol(y)$, for some edge $x \rightarrow y$, in $O(|\Delta(x)|)$ time. This rules out the use of a sorted array to implement $Sol(y)$, which needs $O(max(|\Delta(x)|, |Sol(y)|)$ for this operation. Likewise, we cannot use a bit vector

```
procedure solve()
  foreach n ∈ V do
    W = W ∪ {n};
    Δ(n) = Sol(n);

  while |W| > 0 do
    n = select(W);
    δ = Δ(n);
    Δ(n) = ∅;

    // process complex constraints involving *n
    foreach c ∈ C(n) do
      case c of
      *n ⊇ w:
        foreach k ∈ δ do
          if w→k ∉ E then
            E = E ∪ {w→k};
            // invoke POSCC1/MOSCC add_edge here
            δ_w = Sol(w) − Sol(k);
            if δ_w ≠ ∅ then
              Sol(k) = Sol(k) ∪ δ_w;
              Δ(k) = Δ(k) ∪ δ_w;
              W = W ∪ {k};
      w ⊇ *n:
        foreach k ∈ δ do
          if k→w ∉ E then
            E = E ∪ {k→w};
            // invoke POSCC1/MOSCC add_edge here
            δ_k = Sol(k) − Sol(w);
            if δ_k ≠ ∅ then
              Sol(w) = Sol(w) ∪ δ_k;
              Δ(w) = Δ(w) ∪ δ_k;
              W = W ∪ {w};
      *n ⊇ {w}:
        foreach k ∈ δ do
          if w ∉ Sol(k) then
            Sol(k) = Sol(k) ∪ {w};
            Δ(k) = Δ(k) ∪ {w};
            W = W ∪ {k};

    // invoke POSCC2 add_edge here
    // propagate δ to successors of n
    foreach n→w ∈ E do
      // propagate δ across n→w
      foreach x ∈ δ do
        if x ∉ Sol(w) then
          Sol(w) = Sol(w) ∪ {x};
          Δ(w) = Δ(w) ∪ {x};
      if Sol(w) changed then
        W = W ∪ {w};
  // end while
```

Figure 4.3: Algorithm PWD. Sol and C are initialised the same as for Figure 4.2.

to implement $\Delta(x)$, since this requires $O(v)$ time for the propagation, irrespective of $|\Delta(x)|$ and $|Sol(y)|$. Therefore, we recommend using a bit vector to implement $Sol(y)$ and an array to implement $\Delta(x)$. Note, the latter can be unsorted, since the algorithm guarantees that no element is ever added to $\Delta(x)$ more than once. Also, δ and δ_w should follow the implementation of $\Delta(x)$.

Lemma 8. *Let $D = (V, E, Sol)$ be a directed constraint graph, where $Sol(n) \subseteq V$ is the solution set for each $n \in V$. Algorithm PWD needs at most $O(v^3)$ time to solve D, where $v = |V|$, regardless of the iteration strategy employed.*

Proof. Assuming that each element is only propagated across an edge once, we obtain a trivial worse-case bound of $O(ve) = O(v^3)$ on the runtime of PWD, since we cannot avoid propagating $O(v)$ elements across each edge of the graph once. Note, the time spent processing complex constraints is also at most $O(v^3)$, since the inner loop of each complex case now iterates δ and not $Sol(n)$. What remains is to show that an element cannot be repropagated across an edge. Therefore, suppose some value a is propagated across an edge $x \rightarrow y$ twice. This implies that, before the first propagation, $a \in \Delta(x)$ must have held and, hence, also that $a \in Sol(x)$ — since at no point can $\Delta(x)$ be updated without $Sol(x)$ being so accordingly. After a is propagated across the edge for the first time, we know that $\Delta(n) = \emptyset$ as the propagation can only occur when x is visited. Hence, we have a contradiction, since at no point can an element already in $Sol(n)$ be loaded into $\Delta(n)$ (which is a prerequisite for propagation). □

There are a few final points to make regarding previous work on the idea of using difference propagation to speed up pointer analysis. In fact, we were not quite the first to introduce this idea. Independently to us, the work of Lhoták and Hendren provided the first experimental evaluation of the technique in conjunction with pointer analysis [LH03]. Their results showed significant reductions in solving time were obtained from using difference propagation. However, they do not discuss the algorithm used and, in particular, make no claims regarding improved worse-case complexity (as we have done) and, hence, it remains unclear how their system compares with ours. At the same time, Berndl *et al.* also used this idea in the context of pointer analysis based upon *Binary Decision Diagrams* [BLQ$^+$03]. In this case, they concluded that difference propagation was required for their system to analyse programs efficiently. However, their setting differs from ours somewhat, because the cost of redundant propagation is far greater with BDDs than it is for conventional methods. The last piece of related work is an unpublished report by Deepak Goyal, who considers difference propagation for the harder, flow-sensitive pointer analysis problem [Goy99]. In particular, he demonstrates how it can improve the worse-case time complexity of a worklist algorithm from $O(n^5)$ to $O(n^3)$. Unfortunately, an experimental evaluation of the technique was not provided and, again, it remains unclear how his system compares.

4.1.4 Experimental Study

In this section, we provide empirical data over a range of benchmarks, looking at the effects of iteration strategy, online cycle detection and difference propagation. Our objective is to facilitate

			Constraints			Variables		
	Ver	LOC	Triv	Simp	Comp	Total	Addr	Heap
uucp	1.06.1	15501 / 10255	784	2898	1470	3306	199	20
make	3.79.1	22366 / 15401	1394	4489	2340	4773	259	69
gawk	3.1.0	27526 / 19640	2181	7978	4520	7288	331	96
147.vortex	SPEC95	52624 / 40247	9706	11582	8287	11921	2201	21
bash	2.05	70913 / 50947	3392	12423	5228	10831	696	36
sendmail	8.11.4	68106 / 49053	5223	10115	5063	10218	727	13
emacs	20.7	128859 / 93151	10613	12540	16864	17961	3844	172
126.gcc	SPEC95	193752 / 132435	7269	36347	24984	27878	1113	231
cc1 (gcc)	2.95.1	271053 / 188535	13330	55308	35873	42822	1455	258
named	9.2.0	109001 / 75599	17325	30023	35366	34649	4279	24
ghostscript (gs)	6.51	215605 / 159853	18927	50377	65493	63568	8579	17

Table 4.1: LOC measures lines of code, with the first figure reporting total and the second only non-comment, non-blank lines. The constraint counts are from the initial (i.e. unsolved) constraint set and show Trivial ($p \supseteq \{q\}$), Simple ($p \supseteq q$) and Complex (involving '*'). The breakdown of constraint variables shows the total count, the number of address-taken and the number modelling the heap.

an understanding of how effective the various techniques are in practice. To achieve this, we experimented with algorithms PW1 and PWD and various combinations of the following:

- *Iteration strategy* - We consider LIFO, FIFO and Least Recently Fired (LRF) (recall Section 4.1.2).

- *Online cycle detection* - Algorithms MOSCC, POSCC1 and POSCC2 are evaluated.

We investigate the commonly used LIFO and FIFO iteration strategies in an effort to show whether they are a sensible choice or not. Their implementation uses simple stacks and, thus, permit multiple copies of a node to be on the worklist at once. This degrades performance but, we argue, reflects a typical implementation. In contrast, our LRF algorithm allows only one copy of a node to be on the worklist at any given time. Note, we have found that improving the LIFO and FIFO strategies along these lines makes no difference to the overall conclusion.

Table 4.1 provides information on our benchmark suite. With two exceptions, all are available under open source licenses and can be obtained online (e.g. `http://www.gnu.org`). Note that `cc1` is the C compiler component of `gcc`, while `named` is distributed in the BIND package. While both `147.vortex` and `126.gcc` are not available under open source licences, they form part of the SPEC95 benchmark suite and have been included to aid comparison with previous work. Looking at Table 4.1, a few interesting observations can be made: firstly, `named` and `ghostscript` have noticeably fewer constraint variables modelling the heap than others of similar size; secondly, while `emacs` has more lines of code than `named`, it generates far fewer constraints overall and, thus, should be considered the smaller of the two. In fact, it turns out that ghostscript uses a malloc wrapper (recall Section 2.2.4) called `png_malloc` and this certainly explains the small heap variable count. We suspect that `named` does as well, although this has not been verified.

The SUIF 2.0 research compiler from Stanford [SUI] was deployed as the frontend for generating constraint sets. In all cases, we were able to compile the benchmarks with only superficial modifications, such as adding extra "`#include`" directives for missing standard library headers or updating function prototypes with the correct return type. The constraint generator operates on the full 'C' language and a few points must be made about this:

- *Heap model* - The static model discussed in Section 2.2.4 was used. Recall that this uses a single constraint variable to represent all heap objects created from a particular call to `malloc` and other related heap allocation functions.
- *Structs* - These were modelled using a *field-insensitive* scheme (recall Section 2.2.3), where all elements of a structure are mapped to a single constraint variable.
- *Arrays* - Treated in a similar fashion to structs, by ignoring the index expression and, hence, representing all elements of an array with one constraint variable.
- *String Constants* - A single constraint variable was used to represent all string constants. In other words, we consider the right hand side of `p="foo"` and `q="bar"` as referring to the same object.
- *Indirect Calls* - Indirect function calls were handled using a special mechanism, which we will describe in the next chapter.
- *External Library Functions* - These, almost entirely, came from the GNU C library and were modelled using hand crafted summary functions, capturing only aspects relevant to pointer analysis.

Our experimental machine was a 900Mhz Athlon with 1GB of main memory, running Redhat 8.0 (Psyche). The executables were compiled using gcc 3.2, with compiler switches "`-O3`" and "`-fomit-frame-pointer`". Timing was performed using the `gettimeofday` function, which offers microsecond resolution on x86 Linux platforms. The implementation itself was in C++, making extensive use of the *Standard Template Library* and *Boost Library (version 1.30.2)*. Our implementation always applied *offline* cycle detection and subsumed node compaction (recall Section 2.1), but not the projection merging technique from [SFA00], as we find this degrades performance[1]. To implement the solution sets, our implementation used bit vectors, which we find offer the greatest performance in practice — especially on large benchmarks. It also employed the hash-based duplicate set compaction scheme from [HT01] (recall Section 2.1.1). This turns out to be necessary for solving the largest benchmark (ghostscript), which without compaction needs well over 1GB of memory to complete. Our measurements do not include the time needed for generating constraints and performing (offline) variable substitution. To validate our solvers we manually inspected the output produced on a test suite of small programs and also by ensuring that each algorithm produced the same output.

[1] Projection merging was originally designed for use with inductive form, which we do not use. Thus, we conclude that the technique is simply not suited for use with standard form.

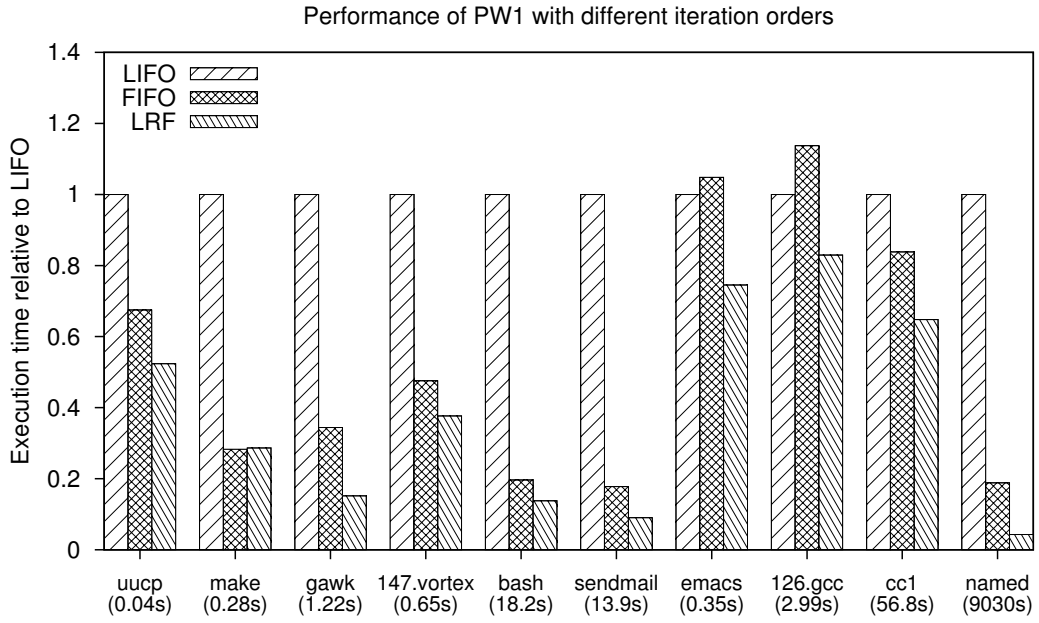

Figure 4.4: A chart of our experimental data investigating the effect of iteration strategy on the performance of algorithm PW1. Specifically, it shows the execution time of PW1 with each of the LIFO, FIFO and LRF iteration strategies. This is given relative to the LIFO implementation to allow data for different benchmarks to be shown on the same chart. Below each benchmark, the exact time taken by the LIFO is shown for reference. Finally, no form of online cycle detection was used here.

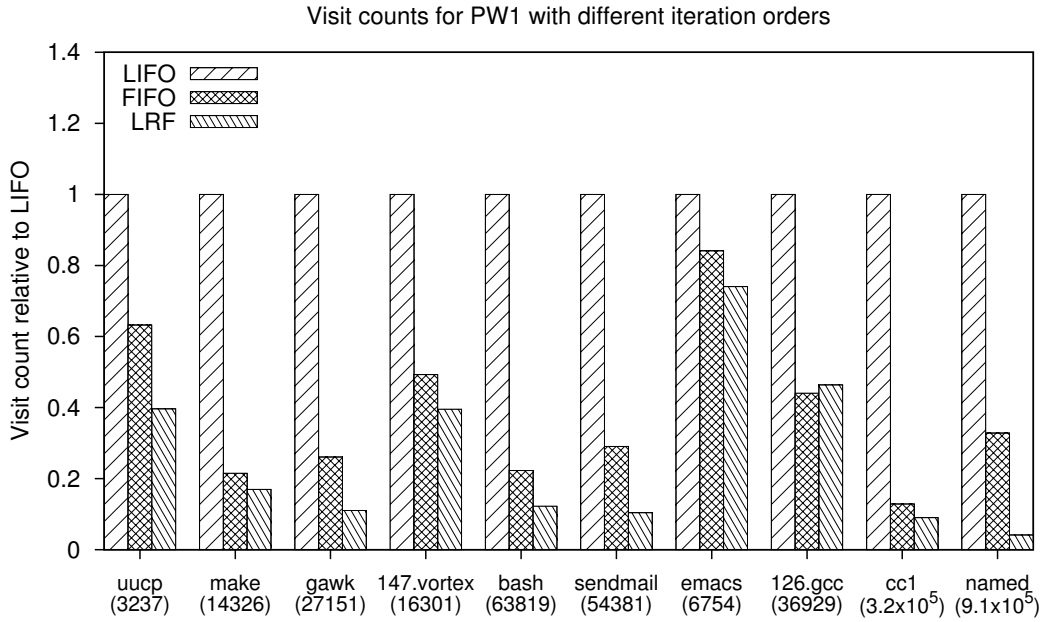

Figure 4.5: A chart of our experimental data looking at visit count for PW1. Specifically, it shows the number of nodes visited by PW1 with each of the LIFO, FIFO and LRF iteration strategies. Again, this is relative to the LIFO implementation and below each benchmark the exact visit count for LIFO is provided. All experimental parameters remain the same as for Figure 4.4.

The results are presented in Figures 4.4, 4.5, 4.6, 4.7, 4.8 and 4.9 we provide some discussion in the following paragraphs.

Iteration strategy: Figure 4.4 shows the effect of using different iteration strategies on the performance of algorithm PW1. The main observation is that LRF is invariably the best choice of iteration strategy. Figure 4.5 highlights the reason for this, as it shows that LRF almost always visits fewer nodes than the other strategies.

Comments: the LRF scheme requires the use of a priority queue, giving it a larger overhead than the other two strategies. While this can outweigh any saving in visit count on small applications (see [PKH03]), it is clear from Figure 4.4 that our benchmarks are sufficiently large to reap considerable benefits. Finally, we do not present data for ghostscript, as the time needed for generating it was prohibitive.

Online cycle detection: Figure 4.6 shows the effects on performance of using different online cycle detectors with algorithm PW1. The main observations are: firstly, that using Online Cycle Detection (OCD) is only beneficial on five benchmarks (`bash`, `sendmail`, `cc1`, `named` and `gs`); secondly, that POSCC1 is a better choice than the other two OCD algorithms on nine of the eleven benchmarks; finally, that POSCC2 is the worst performing cycle detector on six benchmarks.

Comments: online cycle detection is expensive and the cost of using it can easily outweigh the benefits on small benchmarks. This is confirmed by Figure 4.7, which shows that OCD almost always reduces the visit count. Thus, it becomes clear that although OCD does reduce the visit count, this is often insufficient to see a real performance gain in practice. We believe that larger benchmarks would benefit more. Indeed, Figure 4.6 supports this to some extent, since it shows significant gains on the two largest benchmarks. In fact, CTRL ran out of memory on the `gs` benchmark. To complete Figure 4.6, we simply used the time taken up to this point, although visit count information for Figure 4.7 was not available.

Turning our attention to POSCC1, the reason for its good performance arises from two facts: firstly, from the previous chapter we already know that MNR (hence MOSCC1) will perform badly unless the graphs are sufficiently dense; secondly, while POSCC2 benefits from processing edge insertions in batches, this can actually be disadvantageous. To understand why, we must recall that, unlike the others, POSCC2 does not detect cycles until after the loop for processing complex constraints in PW1. This allows time for a batch of insertions to accumulate. However, it also means that cycles are not detected immediately and this can lead to more edge insertions overall. For example, suppose processing $*p \supseteq q$ introduces three edges, with the first introducing a cycle and the others connecting members of that cycle. If cycles are collapsed immediately, only the first edge is added as the latter two now represent self loops and would be ignored. We can only conclude from Figure 4.6 that this effect outweighs the advantages of processing edges in batches in this case.

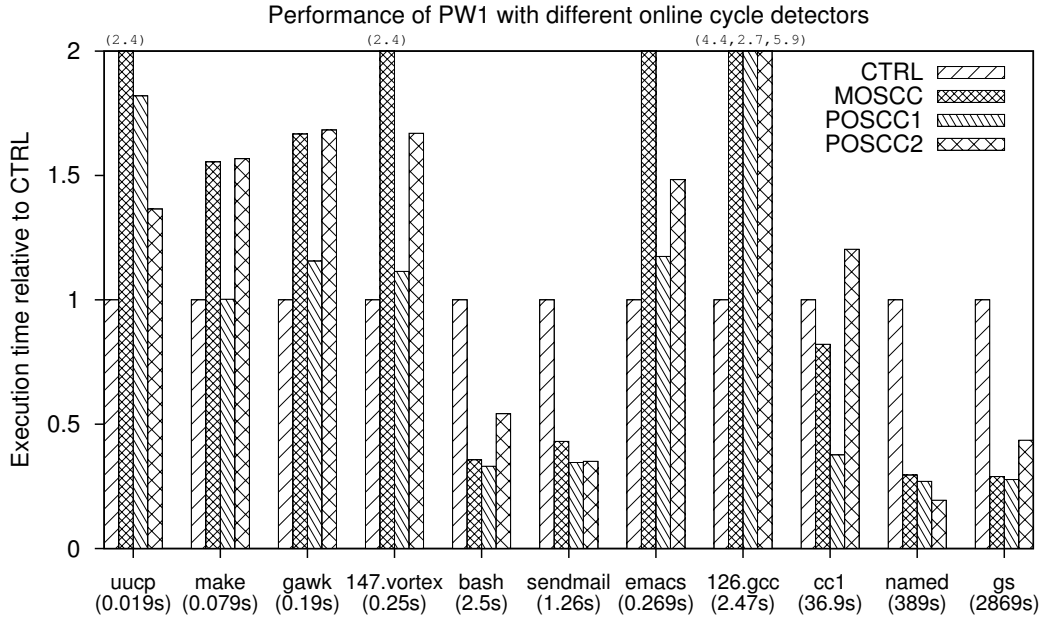

Figure 4.6: A chart of our experimental data looking at the effect of Online Cycle Detection (OCD) on the performance of PW1. It shows the execution time of PW1 without OCD (CTRL) and with each of the three OCD algorithms developed in the previous chapter. This is given relative to the CTRL implementation and below each benchmark the exact time taken by CTRL is given for reference. Note, the Least Recently Fired (LRF) iteration strategy was used here (hence, CTRL is identical to LRF from Figure 4.4).

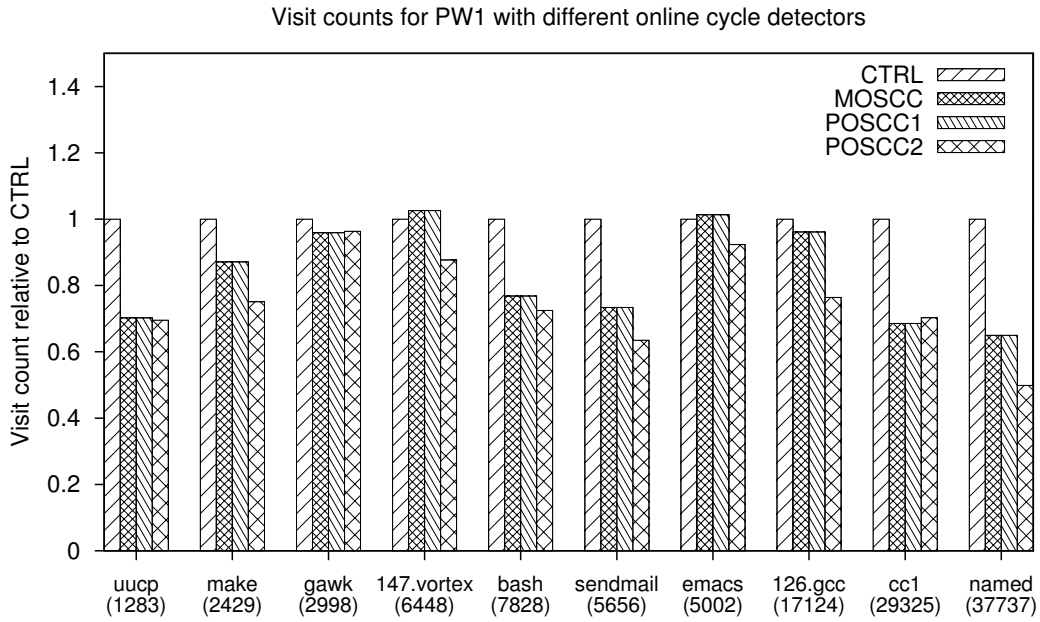

Figure 4.7: A chart of our experimental data looking at the effect of Online Cycle Detection (OCD) on visit count for PW1. It shows the number of nodes visited by PW1 without OCD (CTRL) and with each of the three OCD algorithms developed in the previous chapter. This is given relative to the CTRL implementation and below each benchmark the exact visit count for CTRL is given for reference. All experimental parameters remain the same as for Figure 4.6.

Difference propagation: Figure 4.8 compares solvers PW1 and PWD, in an effort to quantify the effect of difference propagation. The main observation is that difference propagation offers a benefit on eight of the eleven benchmarks. However, with three exceptions, the performance gains are fairly insignificant.

Comments: the advantage of difference propagation is that no element is propagated across an edge twice — meaning fewer elements should be involved, on average, in a set union operation. However, by looking at Figure 4.9 we see that, although this goal has been achieved, the reductions are generally small. This explains the relatively poor performance of difference propagation. Again, we believe that larger benchmarks would get more benefit from this technique. This is supported to some extent by the improvements for the two largest benchmarks seen in Figure 4.8.

4.2 Beyond the Worklist

At this point, we examine some alternatives to the traditional worklist algorithm. In particular, we present algorithm PW2 — a variation on PW1 designed to exploit a topological iteration strategy more effectively. We also look at the solver developed by Heintze and Tardieu [HT01]. Overall, we find the solving time for ghostscript can be reduced to a third of that obtained in the previous section.

4.2.1 Algorithm PW2

There are two main issues with algorithms PW1 and PWD: firstly, using a topological iteration strategy is impractical, since it requires reprioritising the worklist after every edge insertion; secondly, the batch sizes passed to the POSCC2 cycle detector may be rather small, since only a few edges will be added whilst visiting a single node. In fact, these could be overcome, for example, by reprioritising the worklist only after sufficient edges are added and delaying the call to POSCC2's "add_edge" until the batch is large enough. Indeed, this is what algorithm PW2 does in some sense. However, instead of making PW1 and PWD more complicated, we take the opportunity to simplify them in such a way that a topological iteration strategy becomes practical.

Pseudo-code for PW2 is presented in Figure 4.10 and the key difference from PW1 is that the worklist has been replaced with a boolean array, $changed$, which records when a solution set is updated. On each round of the outer loop, the algorithm begins by collapsing cycles and topologically sorting the nodes to obtain the desired iteration order. The inner loop of PW2 then traverses the nodes in order, visiting any marked as $changed$. The procedure for visiting a node remains essentially the same as for PW1 (i.e. process complex constraints and propagate to successors). A useful point to note here is that if either Tarjan's algorithm or those developed in Chapter 3 are used for cycle detection, then the topological sort comes for free as it is generated as part of their computation.

Another difference from PW1 is that, when POSCC2 is used as the cycle detector, "add_edge" is invoked only at the end of each round, instead of once per visit. This delay will (in most cases) increase the size of the insertion batch passed to POSCC2, thus capitalising on its ability to process

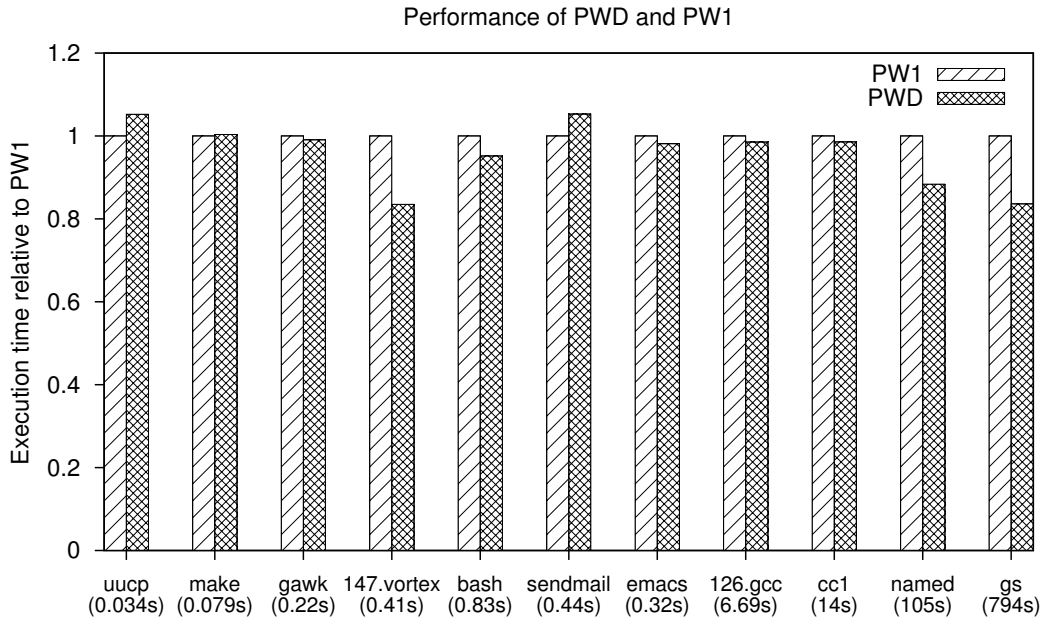

Figure 4.8: A chart of our experimental data looking at the effect of difference propagation on the performance of PW1. Specifically, PW1 is compared against PWD — a variation supporting difference propagation. Execution time is given relative to PW1 and below each benchmark the exact time taken by PW1 is given for reference. Both algorithms used the Least Recently Fired (LRF) iteration strategy and the POSCC1 online cycle detector (hence, PW1 is identical to POSCC1 from Figure 4.6).

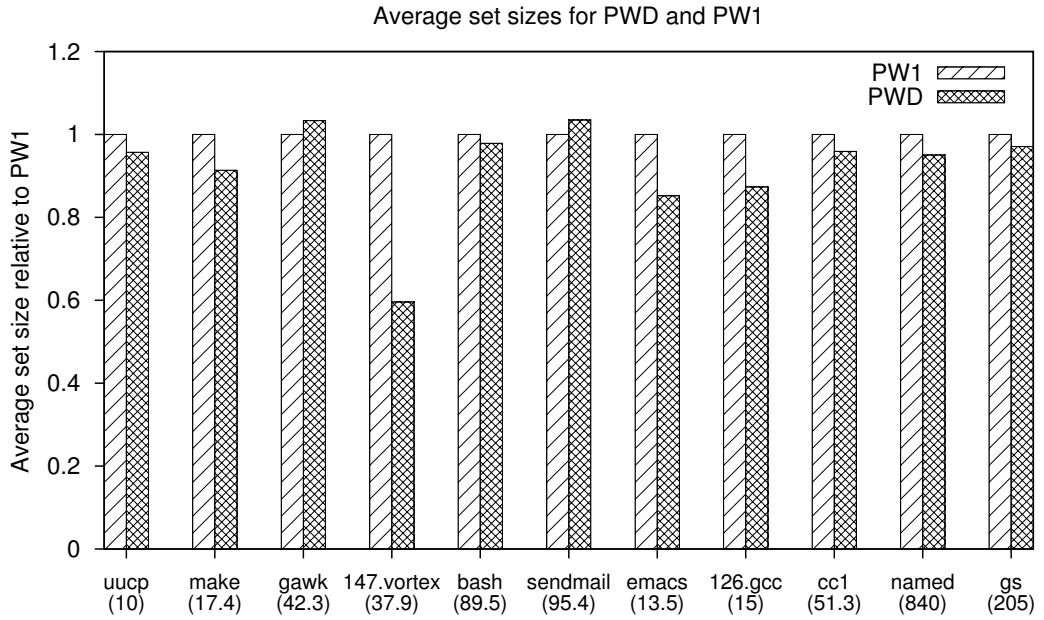

Figure 4.9: A chart of our experimental data looking at the effect of difference propagation on average set size for PW1. It shows the average set size involved in all set union operations for both PW1 and PWD. This is given relative to PW1 and below each benchmark the average set sizes for PW1 are given for reference. All experimental parameters remain the same as for Figure 4.8.

```
foreach x ∈ V do
  changed(x) = true;

while ∃x.changed(x) do
  // invoke Tarjan's cycle detection algorithm here
  // invoke POSCC2 add_edge here
  foreach n ∈ V in topological order do
    if changed(n) then
      changed(n)=false;
      foreach c ∈ C(n) do case c of
        *n ⊇ w:
          foreach k ∈ Sol(n) do
            if w→k ∉ E do
              E = E ∪ {w→k};
              // invoke POSCC1/MOSCC add_edge here
              if Sol(k) ⊉ Sol(w) then
                changed(k) = true;
                Sol(k) = Sol(k) ∪ Sol(w);
        w ⊇ *n:
          foreach k ∈ Sol(n) do
            if k→w ∉ E do
              E = E ∪ {k→w};
              // invoke POSCC1/MOSCC add_edge here
              if Sol(w) ⊉ Sol(k) then
                changed(w) = true;
                Sol(w) = Sol(w) ∪ Sol(k)
        *n⊇{w}:
          foreach k ∈ Sol(n) do
            if w∉Sol(k) do
              changed(k) = true;
              Sol(k) = Sol(k) ∪ {w};

      // propagate Sol(n) to successors
      foreach n→w ∈ E do
        if Sol(w) ⊉ Sol(n) then
          changed(w) = true;
          Sol(w) = Sol(w) ∪ Sol(n);
```

Figure 4.10: Algorithm PW2. The algorithm assumes that $Sol(p)$ has been initialised with all trivial constraints of the form $p \supseteq \{q\}$. The set $C(n)$ contains all complex constraints involving "$*n$". Notice that the actual code for collapsing cycles has been omitted for brevity. There are four different cycle detection algorithms which could be used here (i.e. Tarjan's, POSCC1,POSCC2 and MOSCC). We have marked the point at which the "add_edge" function of each should invoked, as this depends upon the algorithm being used.

batch updates more efficiently. As before, this means cycles will not be detected immediately. Furthermore, as the inner loop proceeds, the visitation order may not remain strictly topological, since edges added which invalidate the property will not be processed until the following round.

A subtle aspect of the algorithm is the choice to process complex constraints when a node is visited. The alternative is to split the inner loop in half, processing the complex constraints of every node before (or after) performing any propagation. This is essentially the approach taken in [LH03], although we argue it is less efficient. This is because, by processing complex constraints immediately (as PW2 does), edges added to nodes further down the order can be propagated across again in the current round. This may seem insignificant, but we find in practice that it has an observable effect on performance.

There are a few final points to make here. Firstly, as PW2 essentially operates in the same manner as PW1, Lemma 7 applies to it — meaning that the worse-case time is $O(v^4)$. Secondly, although pseudo-code is not provided, we have also implemented the difference propagation counterpart of PW2, and this is referred to as PWD2 in the experimental study later on. The implementation of this was in the expected manner, and can be inferred from PW1 and PWD.

4.2.2 The Heintze-Tardieu Algorithm

In this section we study an algorithm, henceforth called HT, which was developed by Heintze and Tardieu [HT01]. Our purpose here is to give the reader some background necessary to understanding the experimental comparison which follows.

The key idea behind the algorithm is that the constraint graph is maintained in *pre-transitive* form. In contrast, worklist algorithms, such as those we have been discussing, maintain their graph in transitive form, which means they are performing a computation similar in spirit to that of traversal-based *transitive closure* algorithms (e.g. [Nuu95, IRW93]). The difference between the pre-transitive and transitive forms is most easily explained with an example:

Let us suppose that there is also the complex constraint $*s \supseteq p$. Now, the solution a worklist solver would produce is (as expected) the following:

Here, we see that the appropriate propagations have taken place and that a new edge $p \rightarrow q$ has been added. This graph is referred to as being in transitive form, since the solution for each node is explicit. In contrast, the pre-transitive solution looks like this:

```
while change do
  change = false;
  Cache = ∅; // empty the cache
  foreach n ∈ V where |C(n)| > 0 do
    sol = getLvals(n);
    // collapse cycles
    ...
    // process complex constraints
    foreach c ∈ C(n) do case c of
      *n ⊇ w:
        foreach k ∈ sol do
          if w → k ∉ E do
            E = E ∪ {w → k};
            change = true;
      w ⊇ *n:
        foreach k ∈ sol do
          if k → w ∉ E do
            E = E ∪ {k → w};
            change = true;
      *n ⊇ {w}:
        foreach k ∈ sol do
          if w ∉ Sol(k) do
            Sol(k) = Sol(k) ∪ {w};
            change = true;
// end while
// collapse cycles with Tarjan's algorithm
...
// generate explicit solution
foreach n ∈ V in topological order do
  foreach n → w ∈ E do
    Sol(w) = Sol(w) ∪ Sol(n);

procedure getLvals(n)
  sol = Sol(n);
  Cache = Cache ∪ <{}, n>;
  ...
  foreach w → n ∈ E do
    if <S, n> ∈ Cache then sol = sol ∪ S;
    else sol = sol ∪ getLvals(w);
    ...
  // end for
  ...
  // cache the solution for n
  Cache = Cache ∪ <sol, n>;
  return sol;
```

Figure 4.11: Algorithm HT. Sol and $C()$ are initialised as for W1. Note that additional code is required for collapsing strongly connected components and dots mark places where this is needed.

This is identical to the original graph, except for the edge $p \rightarrow q$. This is known as pre-transitive form, since we must traverse the graph to obtain the solution for a node. This traversal operates in the expected manner — by searching backwards from the node in question, accumulating the solution of each visited.

Pseudo-code for HT is provided in Figure 4.11 and the main component to observe is the function *getLvals*. This is responsible for constructing the solution of a node via the backward graph traversal. One issue here is use of a cache, without which the algorithm would be hopelessly inefficient. This cache prevents *getLvals* from repeatedly generating the same solution during an iteration of the outer loop. Thus, we see the overall procedure is fairly straightforward: for each dereferenced variable, compute the current solution and add any edges which arise; repeat this until no change is observed. Note that, parts of the original algorithm relating to online cycle detection have been omitted from the pseudo-code. In fact, HT effectively gets online cycle detection for free. This is because Tarjan's algorithm for identifying strongly connected components can be integrated with *getLvals* at no cost. However, this does mean that HT cannot (in general) benefit from other cycle detectors, such as those developed in this work.

Finally, we note without proof that the worse-case complexity of algorithm HT is $O(v^4)$. This follows from the simple fact that no effort is made to prevent multiple propagations of a value across an edge.

4.2.3 Experimental Study

We now investigate the practical performance of algorithms PW2, PWD2 and HT using our benchmark suite. In what follows, the entire experimental setup including host machine, constraint generation, variable substitution, set implementation, timing, metrics and more remains identical to that previously used in Section 4.1.4. Therefore, a direct comparison with the results for PW1/PWD can be made. The experimental data is presented in Figures 4.12 and 4.13 and we now provide some discussion:

Online cycle detection: Figure 4.12 illustrates the effect of using different online cycle detectors on the performance of PW2. The main observation are: firstly, that POSCC2 is the best choice on nine of the eleven benchmarks; secondly, that Tarjan's offline algorithm for finding strongly connect components is surprisingly competitive.

Comments: the performance of POSCC2, compared with POSCC1, reverses the trend seen in the experimental study of Section 4.1.4, where POSCC1 was the clear winner. This can almost certainly be put down to the fact that, as POSCC2 now only detects cycles once all nodes have been visited during the current round, it can accumulate larger batches than were possible with PW1. This reduces the cost of using POSCC2 because it stands to gain from larger batches. Thus, it appears this seemingly small difference between PW1 and PW2 shifts the balance in favour of POSCC2, compared with POSCC1.

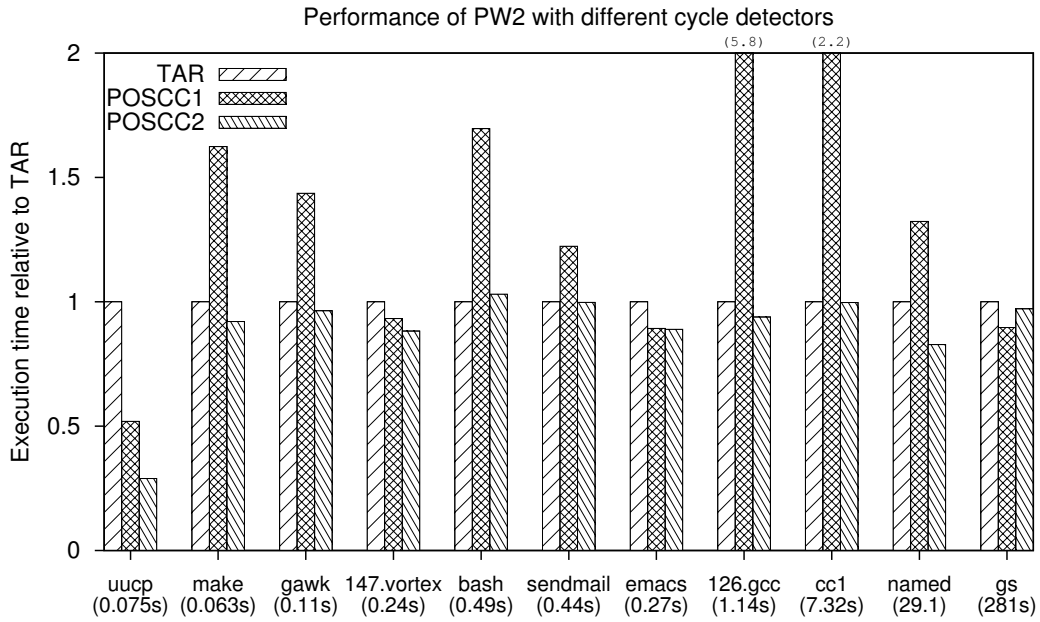

Figure 4.12: A chart of our experimental data looking at the performance of PW2 with different Online Cycle Detection (OCD) algorithms. It shows the execution time of PW2 when each of POSCC1, POSCC2 and TAR are used for online cycle detection. Here, TAR is Tarjan's algorithm for finding strongly connected components (see Appendix B). Execution time is given relative to the TAR implementation to allow data for different benchmarks to be shown on the same chart. Below each benchmark the exact execution time for TAR is given for reference.

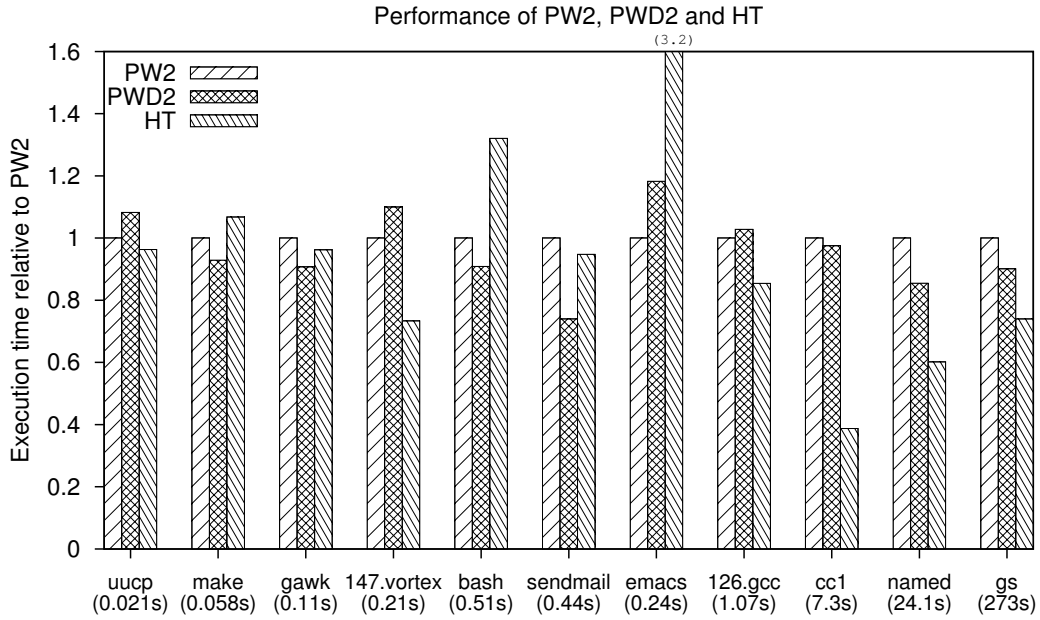

Figure 4.13: A chart of our experimental data comparing algorithms PW2, PWD2 (a variant of PW2 supporting difference propagation) and HT. It shows the execution time of each algorithm relative to the PW2 implementation. Below each benchmark the exact execution time for PW2 is provided. Finally, both PW2 and PWD2 used algorithm POSCC2 for online cycle detection.

The performance of Tarjan's algorithm when used as an online cycle detector is quite unexpected. We can only conclude that the cost of cycle detection is largely insignificant, compared with the propagation of values (i.e. the cost of set union operations) when solving the analysis.

Difference propagation and HT: Figure 4.13 compares the performance of algorithms PW2, PWD2 and HT. The main observations are: firstly, PWD2 outperforms PW2 on seven out of the eleven benchmarks; secondly, the Heintze-Tardieu solver (algorithm HT) is the optimal choice on six benchmarks.

Comments: the largely disappointing performance of PW2 with difference propagation (i.e. PWD2) appears to follow our previous findings with PW1 (see Section 4.1.4). Regarding algorithm HT, the reader might conclude from our observations that it is not much better than the other two. However, it is important to note that it is consistently fastest on the four *longest running* benchmarks, although the gap does narrow with size. The exact reasons for this remain largely unclear and further work is needed to understand the operation of this algorithm. In particular, it seems that combining this algorithm with difference propagation (if possible) to obtain $O(v^3)$ worse-case complexity might lead to a very fast solver.

4.3 Concluding Remarks

In this chapter, we explored three avenues for improving the execution times of worklist-style algorithms for solving pointer analysis. These were: *iteration strategy*, *difference propagation* and *online cycle detection*. We now summarise our overall findings for each:

Iteration strategy. In Section 4.1.2, we demonstrated how the problem of finding an optimal iteration strategy differs greatly for our dynamic setting, compared with the much-studied static case. We also proved that, regardless of iteration strategy, algorithm PW1 has a worse-case time complexity of $O(v^4)$. The experimental study at the end of Section 4.1 demonstrated how important iteration strategy is to solving performance. Furthermore, the study confirmed that the Least Recently Fired (LRF) strategy suggested by Kanomori and Weise [KW94] is highly effective. In Section 4.2, we took this a step further and showed that, through careful design, a topological iteration strategy can offer significant speedups.

Difference propagation. In Section 4.1.3, we adapted this technique to our problem domain to obtain a worklist solver with an optimal $O(v^3)$ worse-case time complexity. In the experimental comparisons which followed, we found this yielded consistent, but perhaps disappointing, improvements. While the exact reasons for this remain unclear, the data does appear to indicate that larger benchmarks would show more significant gains.

Online cycle detection. In the previous chapter, much effort was put into developing original and fast algorithms for dynamically maintaining a topological ordering of nodes. Furthermore, these had the useful property of being applicable to the problem of online cycle detection — a well known method for speeding up pointer analysis. In this chapter, we put these algorithms to practical use by integrating them with our pointer analysis solvers. To that end, the final results are largely disappointing in that, even on large benchmarks, they did not yield significant gains over the standard (and theoretically inferior) algorithm by Tarjan. Again, however, the data does suggest that with larger benchmarks we would see the gap widening. In general, we feel that POSCC1 is perhaps more exciting that POSCC2 — especially if a batch variant could be developed.

Another curious issue raised in this chapter is the performance of the Heintze-Tardieu solver. While we have invested a large amount of time examining the operation of this algorithm, we are still unable to draw any concrete conclusions as to why it performs so well. Certainly, the use of pre-transitive form appears to be relevant here, but we are unable to find any reason why this would offer an advantage when the complete analysis solution is required. Indeed, we are reduced to speculating that low-level effects, such as cache behaviour, may be a factor. In any case, it seems that much could be learnt from further study of this algorithm and its possible integration with other techniques such as difference propagation.

Finally, for completeness, we must make a few remarks regarding the relationship between that contained herein and our previously published material [PKH03, PKH04b]. In particular, the implementation of difference propagation differs somewhat in both papers from that presented here. This is significant only from a theoretical point of view, because an $O(v^3)$ result is unobtainable for the variants used in [PKH03, PKH04b]. In practice we find no real difference in performance. Otherwise, the main differences in the experimental results, compared with this chapter, arise purely from the choice of set implementation — bit vectors were not used in either [PKH03, PKH04b].

Chapter 5

Field-Sensitive Pointer Analysis

In this chapter, we extend our set-constraint language to support indirect function calls and field-sensitive pointer analysis. The former is a prerequisite for analysing real C programs and has been used in all our experimental studies so far. We have deferred discussing the mechanism until now, simply because it shares much in common with our approach to field-sensitivity. The main contributions of this chapter are:

1. A small extension to our language of set-constraints, which elegantly formalises a field-sensitive pointer analysis for the C language. As a byproduct, function pointers are supported for free with this mechanism.

2. The largest experimental investigation to date into the trade-offs in time and precision of field-insensitive and -sensitive analyses for C. Our benchmark suite from the previous chapter is reused for this purpose and, in all cases, we find that precision is greatly improved with field-sensitivity.

Our technique is not the first field-sensitive, constraint-based pointer analysis for C — previous work has covered this (see [YHR99, CR99a]). Our claim then, is that we go beyond their initial treatment by considering efficient implementation and some important algorithmic issues not adequately addressed. In particular, our technique is designed specifically to work with the *points-to* or solution sets (i.e. $Sol(n)$) implemented as integer sets. This permits the use of data structures supporting efficient set union, such as bit vectors or sorted arrays, which are necessary for scalable pointer analysis. Much of this work has been published in [PKH04a] and this is extended further here with more examples, a larger experimental study and a more detailed discussion of previous work.

5.1 Indirect Function Calls

In the literature, function pointers are either dealt with in ad hoc ways (e.g. [HT01, LH03]) or through the lam constructor (e.g. [FFA00, FFA97]). The latter uses a special rule for function application:

$$[func]\ \frac{\begin{array}{c} *p(\tau_1, \ldots, \tau_n) \\ p \supseteq \{\ lam_v(v_1, \ldots, v_n)\ \} \end{array}}{\forall 1 \leq i \leq n.\ v_i \supseteq \tau_i}$$

which is used to resolve indirect function calls in the following manner:

```
int f(int *p) { return p; }
```
(1) $f_* \supseteq f_p$

```
int (*p)(int*) = &f;
int *q = ... ;
p(q);
```
(2) $p \supseteq \{\ lam_f(f_p)\ \}$
(3) $q \supseteq \{\ \ldots\ \}$
(4) $*p(q)$

---

(5) $f_p \supseteq q$ $\quad (func,\ 2{+}4)$
(6) ...

Here, we see that constraints are introduced on-the-fly between the actual parameters and their caller values. The main issue here is the implementation of lam. Certainly, we don't wish to sacrifice the ability to implement solutions as integer sets. One approach is to place the lam constructs into a table, so they are identified by index. Thus, if care is taken to avoid clashes with the variable identifiers, the two element types can co-exist in the same solution set. However, this is inelegant as we must litter our algorithm with special type checks. For example, when dealing with $*p \supseteq q$, we must check for lam values in $Sol(p)$.

We now present our approach to modelling indirect function calls and, in the following section, we will build upon this to obtain a field-sensitive analysis. A crucial observation is that using integer identifiers allows us to reference a variable by an offset from another. Thus, we introduce the following forms:

$$p \supseteq *(q{+}k) \mid\ *(p{+}k) \supseteq q \mid\ *(p{+}k) \supseteq \{q\}$$

Here k is an arbitrary constant and $*(p + k)$ means "load $Sol(p)$ into a temporary set, add k to each element and dereference as before". To understand this more clearly, consider two variables x and y indexed by 2 and 3 respectively. If $p \mapsto \{x\}$ then $*(p{+}1) \supseteq q$ evaluates to $*(\{x\}{+}1) \supseteq q$, which is really $*(\{2\}{+}1) \supseteq q$, and applying the addition gives $*(\{2{+}1\}) \supseteq q \equiv *(\{3\}) \supseteq q \equiv *(\{y\}) \supseteq q \equiv y \supseteq q$. Of course, when $k = 0$, these new forms are equivalent to those of the original language. The corresponding inference rules are given in Figure 5.1, where idx maps variables to their index.

$$[deref_4]\ \frac{\tau_1 \supseteq *(\tau_2{+}k) \quad \tau_2 \supseteq \{\tau_3\} \quad idx(\tau_4) = idx(\tau_3){+}k}{\tau_1 \supseteq \tau_4} \qquad [deref_5]\ \frac{*(\tau_1{+}k) \supseteq \tau_2 \quad \tau_1 \supseteq \{\tau_3\} \quad idx(\tau_4) = idx(\tau_3){+}k}{\tau_4 \supseteq \tau_2}$$

$$[deref_6]\ \frac{*(\tau_1{+}k) \supseteq \{\tau_2\} \quad \tau_1 \supseteq \{\tau_3\} \quad idx(\tau_4) = idx(\tau_3){+}k}{\tau_4 \supseteq \{\tau_2\}}$$

Figure 5.1: Extended inference rules

Now, suppose in our source program there is some function $f(p_0, \ldots, p_i)$. If the address of f has been taken, we create a block of $i{+}1$ consecutively indexed variables, where the first represents p_0 and so on. This can be visualised in the following way:

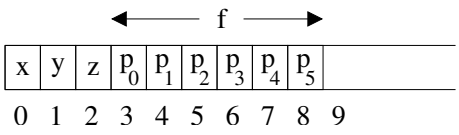

Here, x, y and z represent some other variables allocated before those of f. The key point is that each parameter of f can be accessed as an offset from p_0 and, thus, we model the address of f by that of p_0. The following example aims to clarify this:

```
void f(int **p,int*q) {
 *p = q;
}
void g(...) {
 void (*p)(int**,int*);
 int *a,*b,c;
 p = &f;
 b = &c;
 p(&a,b);
}
```

(1,2) $idx(f_p) = 0, idx(f_q) = 1$
(3) $*f_p \supseteq f_q$
(4,5) $idx(g_p) = 2, idx(g_a) = 3$
(6,7) $idx(g_b) = 4, idx(g_c) = 5$
(8) $g_p \supseteq \{f_p\}$
(9) $g_b \supseteq \{g_c\}$
(10) $*(g_p{+}0) \supseteq \{g_a\}$
(11) $*(g_p{+}1) \supseteq g_b$

---

(12)	$f_p \supseteq \{g_a\}$	$(deref_6, 8{+}10{+}1)$
(13)	$f_q \supseteq g_b$	$(deref_5, 1{+}2{+}8{+}11)$
(14)	$f_q \supseteq \{g_c\}$	$(trans, 9{+}13)$
(15)	$g_a \supseteq f_q$	$(deref_2, 3{+}12)$
(16)	$g_a \supseteq \{g_c\}$	$(trans, 14{+}15)$

Here, constraint 8 is the key as `&f` is translated into f_p — the first parameter of `f` — allowing us access to f_q through the offset notation in (11). In fact, return values can be modelled using this mechanism if we allocate the corresponding variable (e.g. f_*) the index following the

$$[add] \quad \frac{\tau_1 \supseteq \tau_2{+}k \quad \tau_2 \supseteq \{\tau_3\} \quad idx(\tau_4) = idx(\tau_3){+}k}{\tau_1 \supseteq \{\tau_4\}}$$

Figure 5.2: An inference rule for constraints of the form $q \supseteq x{+}1$

last parameter[1]. Thus, we can always determine the offset of the return value from the type of the function pointer being dereferenced. The final issue with this mechanism is the use of invalid casts:

```
void f(int *p) { ... }
int g(int *a,int *b) {
 void (*p)(int *,int*);
 p = (void(*)(int*,int*)) &f;
 *p(a,b);
}
```

$idx(f_p) = 0$
$idx(g_a) = 1, idx(g_b) = 2$
$idx(g_p) = 3$
$g_p \supseteq \{f_p\}$
$*(g_p{+}0) \supseteq g_a$
$*(g_p{+}1) \supseteq g_b$

According to the rules of Figure 5.1, $*(g_p{+}1) \supseteq b$ derives $g_a \supseteq b$ as $idx(g_a) = idx(f_p){+}1$. This seems somewhat unfortunate, although it is unclear how to model the above anyway. To prevent this type of unwanted propagation we can extend our mechanism with $end()$ information for each variable. This determines where the enclosing block of consecutively allocated variables ends. Thus, we only permit offsets which remain within the enclosing block of the variable in question. For example, in the above, $end(f_p) = 0$ and $end(g_a) = end(g_b) = 2$ and we can identify the problem as $idx(*(g_p{+}1)) > end(*g_p)$.

5.2 Field-Sensitive Pointer Analysis

In this section, we further extend the language of set-constraints to support field-sensitive pointer analysis of C. Although this problem has been addressed by a number of previous works, we go beyond them by considering specific details relating to efficient implementation. In particular, our formulation can be regarded as an instance of the general framework for field-sensitive pointer analysis of C by Yong *et al.* [YHR99]. In fact, it is equivalent to the most precise, but portable analysis their system can describe and we consider here some important algorithmic issues which they did not address.

For Java, there are also several existing extensions to the set-constraint language which support field-sensitive analysis [RMR01, LH03, WL02, LPH01]. However, Java presents a simpler problem than C in this respect, since it does not permit the address of a field to be taken. Indeed, it turns out the language of the previous section is sufficient for field-sensitive analysis of Java. This works by using blocks of constraint variables, as we did for functions, to represent aggregates. For example:

[1]Note, using the first parameter for the return value causes problems when the function is incorrectly typed. This commonly occurs in C, when a function has multiple prototypes of which some incorrectly assign a `void` return type.

```
typedef struct { int *f1; int *f2; } aggr;
```

`aggr a,*b;`	$idx(a.f1)=0, idx(a.f2)=1, idx(b)=2$
`int *p,**q,c;`	$idx(p)=3, idx(q)=4, idx(c)=5$
`b = &a`	$b \supseteq \{a.f1\}$
`b->f2 = &c;`	$*(b+1) \supseteq \{c\}$
`p = b->f2;`	$p \supseteq *(b+1)$

To analyse C, however, we must also be able to translate "`q=&(b->f2);`". This is a problem since we want to load the *index* of $a.f2$ into $Sol(q)$, but there is no mechanism for this. So, we extend the language to permit the translation: $q \supseteq b+1$, meaning *load* $Sol(b)$ *into a temporary, add 1 to each element and merge into* $Sol(q)$. Note the inference rule in Figure 5.2. This form can be represented by turning the constraint graph into a weighted multigraph, where weight determines increment — so $p \supseteq q+k$ gives $q \xrightarrow{k} p$. One difficulty with this new form is the *Positive Weight Cycle (PWC)* problem. For example:

`aggr a,*p; void *q;`	
`q = &a;`	$q \supseteq \{a\}$
`p = q;`	$p \supseteq q$
`q = &(p->f2);`	$q \supseteq p+1$
`/* now use q as int* */`	

This is legal and well-defined C code. Here, the cycle arises from flow-insensitivity, but other forms of imprecision can also cause them. For example:

`void *f(int s){return malloc(s);`	(1) $f_* \supseteq \{HEAP0\}$
`}`	
`aggr **p,*t1;  int **q,*t2;`	
`p=(aggr **) f(sizeof(aggr *));`	(2) $p \supseteq f_*$
`q=(int **) f(sizeof(int *));`	(3) $q \supseteq f_*$
`*p = ... ;`	(4) $*p \supseteq \ldots$
`t1 = *p;`	(5) $t1 \supseteq *p$
`t2 = &t1->f2;`	(6) $t2 \supseteq t1+1$
`*q = t2;`	(7) $*q \supseteq t2$

---

(8) $p \supseteq \{HEAP0\}$	$(trans, 1+2)$
(9) $q \supseteq \{HEAP0\}$	$(trans, 1+3)$
(10) $t1 \supseteq HEAP0$	$(deref_2, 5+8)$
(11) $HEAP0 \supseteq t2$	$(deref_1, 7+9)$

Here there is a positive weight cycle involving *HEAP0*, $t1$ and $t2$. This is caused by the use of a *static heap model*, which you may recall from Section 2.2.4 is where all objects returned by

a particular call to `malloc` are represented by one variable. Thus, *HEAP0* actually represents two distinct heap objects in the program and we have carefully used this to achieve the same effect as the cast in the previous example. So, it seems that any formulation of a field-sensitive analysis for C will necessarily have to deal with positive weight cycles. This is supported by the work of Chandra and Reps, who encounter the same issue with a similar field-sensitive analysis [CR99a, CR99b]. In general, the problem is that cycles describe infinite derivations. To overcome this, we use *end()* information, as with function pointers, so that a variable is only incremented within its enclosing block.

Another problem with weighted edges is that *cycle elimination* is now unsafe, since nodes in a cycle need no longer share the same solution. To tackle this, we observe that a cycle can be collapsed when there is a zero weighted path between all nodes and intra-cycle weighted edges are preserved as self loops. The following example demonstrates this, where unlabelled edges are assumed to have zero weight:

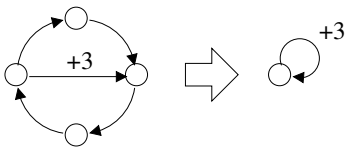

A further source of complication for our system is the difficulty in determining how many fields a heap variable should have. This is especially true if a static heap model is used, as highlighted in the following:

```
typedef struct {double d1; int *f2;} aggr1;
typedef struct {int   *f1; int *f3;} aggr2;

void *f(int s) { return malloc(s); }   f* ⊇ {HEAP0}
void *g(int s) { return malloc(s); }   g* ⊇ {HEAP1}

aggr1 *p = f(sizeof(aggr1));           p ⊇ f*
aggr2 *q = f(sizeof(aggr2));           q ⊇ f*
int *x = f(100);                       x ⊇ f*
int *y = g(100);                       y ⊇ g*
```

The issue is that we cannot, in general, determine which heap variables will be used as aggregates. Indeed, the same variable can be used as both aggregate and scalar (e.g. *HEAP0* above). Thus, we either model heap variables field-insensitively or assume they can be treated as aggregates. Our choice is the latter, raising a further problem: *how many fields should each heap variable have?* A simple solution is to give them the same number as the largest `struct` in the program. Effectively then, each heap variable is modelling the C `union` of all `structs`. So, in the above, *HEAP0* and *HEAP1* both model `aggr1` and `aggr2` and are implemented with two constraint variables: the first representing fields `f1` and `d1`; the second `f2` and `f3`. The observant reader will have noticed something strange here: *the first constraint variable models fields of different sizes*. This seems

	Constraint Variables			
	Total	Addr	Heap	# PWC
uucp	3306 / 5139	199 / 1873	20 / 940	1
make	4773 / 6920	259 / 2396	69 / 1794	0
gawk	7288 / 10125	331 / 3135	96 / 2496	0
147.vortex	11921 / 16011	2201 / 5943	21 / 2310	0
bash	10831 / 13109	696 / 2878	36 / 936	0
sendmail	10218 / 12869	727 / 3270	13 / 949	1
emacs	17961 / 38170	3844 / 23618	172 / 12900	0
126.gcc	27878 / 50637	1113 / 23774	231 / 22407	0
cc1	42822 / 75279	1455 / 33806	258 / 31992	1
named	34649 / 47101	4279 / 15765	24 / 1704	1
gs	63568 / 100209	8579 / 32887	17 / 1887	2

Table 5.1: Data comparing the field-insensitive and -sensitive constraint sets. The breakdown of constraint variables shows the total count, the number of address-taken and the number modelling the heap. In all cases, the two values given apply to the insensitive and sensitive constraint sets (in that order). Note, the data for the insensitive analysis is sourced from Table 4.1.

a problem as, for example, writing to `d1` should invalidate `f1` and `f3`. In practice, however, this cannot be exploited without using undefined C code, since it relies on implementation dependent information regarding type size:

`aggr1 *p = malloc(sizeof(aggr1));`	$idx(\mathit{HEAP0.F0}) = 0$
	$idx(\mathit{HEAP0.F1}) = 1$
`int a,*r;`	$p \supseteq \{\mathit{HEAP0.F0}\}$
`aggr2 *q = (aggr2 *) p;`	$q \supseteq p$
`q->f3 = &a;`	$*(q+1) \supseteq \{a\}$
`p->d1 = 1.0; /* clobbers q->f3 */`	$*(p+0) \supseteq \{?\}$
`r = q->f3;`	$r \supseteq *(q+1)$

Here, our analysis concludes $r \mapsto \{a\}$, which is unsound on platforms where `sizeof(double)` is larger that `sizeof(int)` because the assignment to `p->d1` overwrites part of `q->f3`. Note the special value "?", used to indicate that a pointer may target anything. In general, we are not concerned with this issue as our objective is to model portable C programs only. Finally, nested `structs` are easily dealt with by "inlining" them into their enclosing `struct`, so that each nested field is modelled by a distinct constraint variable.

5.3 Experimental Study

We now present a practical investigation into the effects on performance and precision of field-sensitivity using our benchmark suite. In what follows, the entire experimental setup including host machine, constraint generation, variable substitution, set implementation, timing, metrics and more remains identical to that previously used in Section 4.1.4. Therefore, a direct comparison between the performance and behaviour of all algorithms can be made.

Table 5.1 provides a comparison of some interesting differences between the new constraint sets generated for the field-sensitive analysis and those used previously for the insensitive analysis. In particular, we see that the sensitive analysis always uses more constraint variables, which is expected as each field is now modelled with a separate variable. In fact, there will be more constraints for similar reasons, although these are omitted for brevity as the differences are small and insignificant. Finally, the "# PWC" metric shows the number of positive weight cycles in the final graph. It is important to realise that this count maybe higher during solving, because some cycles could end up being combined in the final graph. Note that, if at least one positive weight cycle is created then "# PWC" will report a count greater than zero. This is because cycle detection cannot eliminate positive weight cycles — it can only reduce them to self loops.

Figure 5.3 looks at the effect of field-sensitivity on solving time. It shows clearly that the field-sensitive analysis is more expensive to compute. Furthermore, with the exception of `emacs`, those benchmarks which have positive weight cycles are significantly more expensive, relatively speaking, than the others.

Comments: Figure 5.4 gives some indication why the field-sensitive analysis is more costly. It shows the field-sensitive analysis always has the higher visit count. Part of the reason for this is that there are more constraint variables (i.e. nodes in the graph) for the sensitive analysis (recall Table 5.1). However, looking at Figure 5.5, we see that in many cases the cost of performing a set union is actually lower. This suggests that the increased precision offered by field-sensitivity could actually lead to improved performance. Indeed, this idea is not new and others have made such observations before (see e.g. [LH03, RMR01, WL02]). An interesting point here is that average set size is always *lower* for benchmarks which don't have positive weight cycles, whilst it is always *higher* on those that do. This strongly suggests that positive weight cycles are a major expense and that eliminating them would be beneficial.

Figure 5.6 looks at the effect on precision of field-sensitivity but, before any discussion, we must first understand exactly what is being shown. The chart reports the number of possible targets for a dereference site, averaged across all dereference sites. This is called the "Average Deref" metric. It gives a more useful measure of precision, compared with the average set size of all pointer variables, since only dereference sites are of interest to client analyses. To facilitate a meaningful comparison (in terms of precision) between the sensitive and insensitive analyses we must normalise the value. To understand why, consider a pointer p targeting the first field of variable "`struct {int f1; int f2;} a`". For the insensitive analysis, we have the solution $p \supseteq \{a\}$, whilst the sensitive analysis gives $p \supseteq \{a.f1\}$. Thus, the two appear to offer the same level of precision, since their solution sets are of equal size. However, this is misleading because the insensitive analysis actually concludes that p may point to *any field* of a. Therefore, we normalise the insensitive solution by counting each aggregate by the number of fields it contains. In other words, we count $p \supseteq \{a\}$ as though it was $p \supseteq \{a.f1, a.f2\}$.

The main observation from Figure 5.6 is that field-sensitivity gives more precise results across the board. However, we again find there are significant differences between those benchmarks

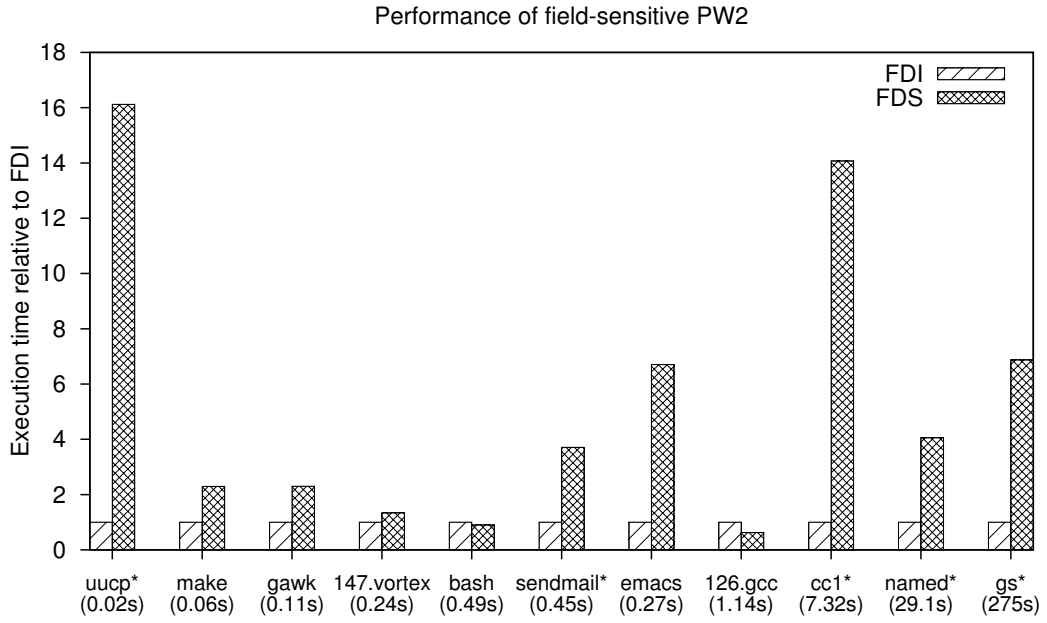

Figure 5.3: A chart of our experimental data investigating the effect of field-sensitivity on the performance of algorithm PW2. This is given relative to the field-insensitive implementation (FDI) to allow data for different benchmarks to be shown on the same chart. Below each benchmark, the exact time taken by FDI is shown for reference. Both implementations employed Tarjan's algorithm for online cycle detection and did not use difference propagation. Benchmarks containing positive weight cycles are marked with an asterisk.

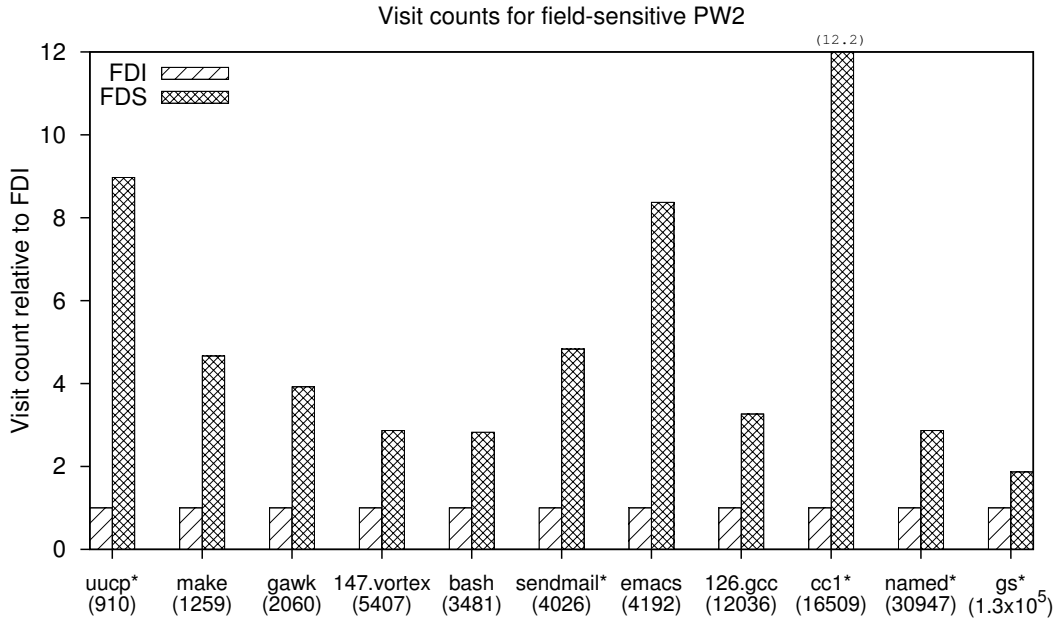

Figure 5.4: A chart of our experimental data investigating the effect of field-sensitivity on visit count for algorithm PW2. It shows the number of nodes visited by PW2 for the field-insensitive (FDI) and -sensitive (FDS) implementations. This is given relative to FDI implementation and, below each benchmark, the exact number of nodes visited by FDI is provided. All experimental parameters are the same as for Figure 5.3 and benchmarks containing positive weight cycles are marked with an asterisk.

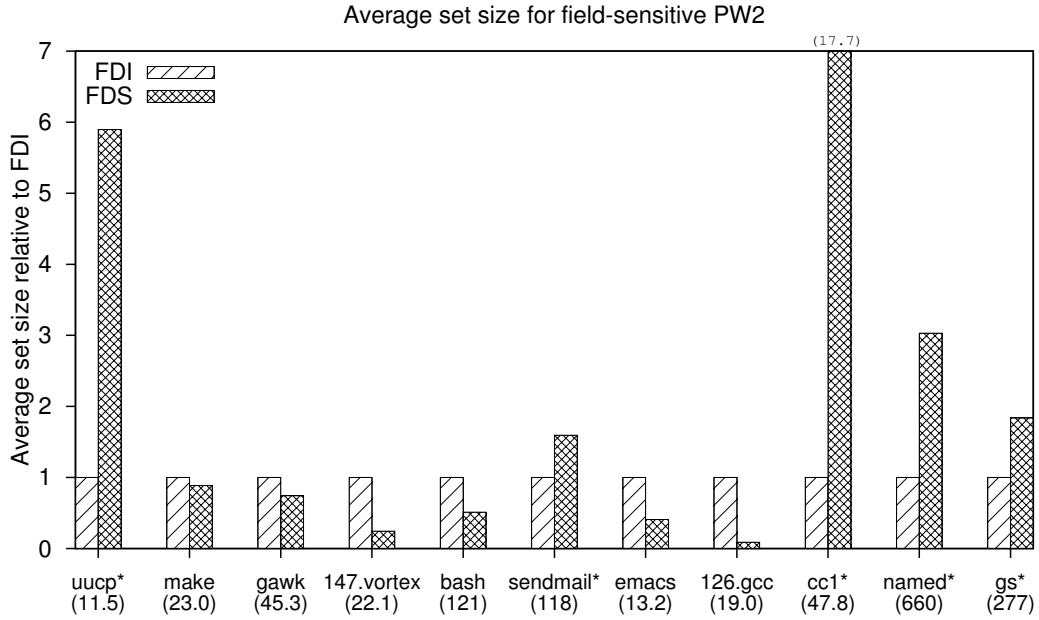

Figure 5.5: A chart of our experimental data investigating the effect of field-sensitivity on average set size for algorithm PW2. It shows the average set size across all set union operations for the field-insensitive (FDI) and -sensitive (FDS) implementations. This is given relative to the FDI implementation and, below each benchmark, the exact values for FDI are provided for reference. All experimental parameters are the same as for Figure 5.3 and benchmarks containing positive weight cycles are marked with an asterisk.

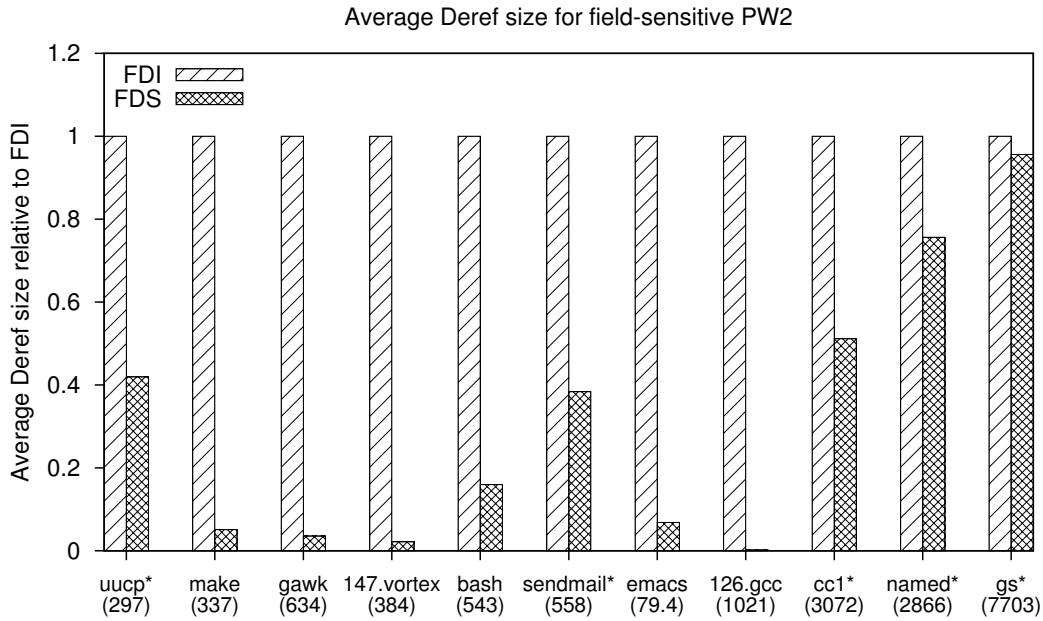

Figure 5.6: A chart of our experimental data investigating the effect of field-sensitivity on the Average Deref metric. This is shown for the field-insensitive (FDI) and -sensitive (FDS) implementations and is given relative to FDI. Below each benchmark, the exact figures for FDI are given for reference. All experimental parameters remain the same as for Figure 5.3 and benchmarks containing positive weight cycles are marked with an asterisk.

which have positive weight cycles and those which do not. In particular, those without always show a significantly greater increase in precision from field-sensitivity. Figures 5.7 and 5.8 break up the Average Deref metric to show its distribution for each benchmark. They concur with our previous findings that field-sensitivity increases precision, as a general shift is seen from right-to-left, indicating that more dereference sites have fewer targets. We also observe that a large proportion of dereference sites for the three largest benchmarks have a thousand elements or more. And yet, the two similar sized benchmarks `emacs` and `126.gcc` (which don't contain positive weight cycles) have much better distributions. From this, we conclude that positive weight cycles are also a major factor affecting the precision of field-sensitive pointer analysis. Finally, zero-sized sets for Average Deref arise from an artifact of our linker, which attempts to mimic the GNU linker as closely as possible. The issue is that, when a given object file is linked with the program, all functions contained therein are included — even if not used. Therefore, most of the unreachable code arises from our GNU C library model, where many functions are spread over a small number of files.

5.4 Related Work

We now return to consider the relationship between our system and the two comparable previous works [YHR99, CR99a]. The most important of these, due to Yong *et al.* [YHR99], is a framework covering a spectrum of analyses from complete field-insensitivity through various levels of field-sensitivity. The main difference from our work is the approach taken to modelling field-addresses where, instead of integer offsets, string concatenation is used. To understand what this means, consider:

```
typedef struct { int *f1; int *f2; } aggr1;

aggr1 a,*b; int *p,c;
a.f2 = &c;                (1) a.f2 ⊇ {c}
b = &a;                   (2) b ⊇ {a}
p = b->f2;                (3) p ⊇ (*b)||f2
```

---

(4) $p \supseteq a.f2$ ($\mathit{fdref}_1, 2+3$)
(5) $p \supseteq \{c\}$ ($\mathit{trans}, 1+4$)

Here, the $||$ operator can be thought of essentially as string concatenation, such that $\{a\}||b \Rightarrow a.b$ and $(*a)||b \Rightarrow c.b$, if $a \supseteq \{c\}$. Hence, the corresponding inference rules are:

$$[\mathit{fdref}_1]\ \frac{q \supseteq (*p)||f \quad p \supseteq \{a\}}{q \supseteq a.f} \qquad [\mathit{fdref}_2]\ \frac{(*p)||f \supseteq q \quad p \supseteq \{a\}}{a.f \supseteq q}$$

Thus, we see that $p \supseteq (*b)||x$ replaces $p \supseteq *(b+k)$ from our system. While this difference appears trivial, there are hidden complications in dealing with certain uses of casting — *even when such*

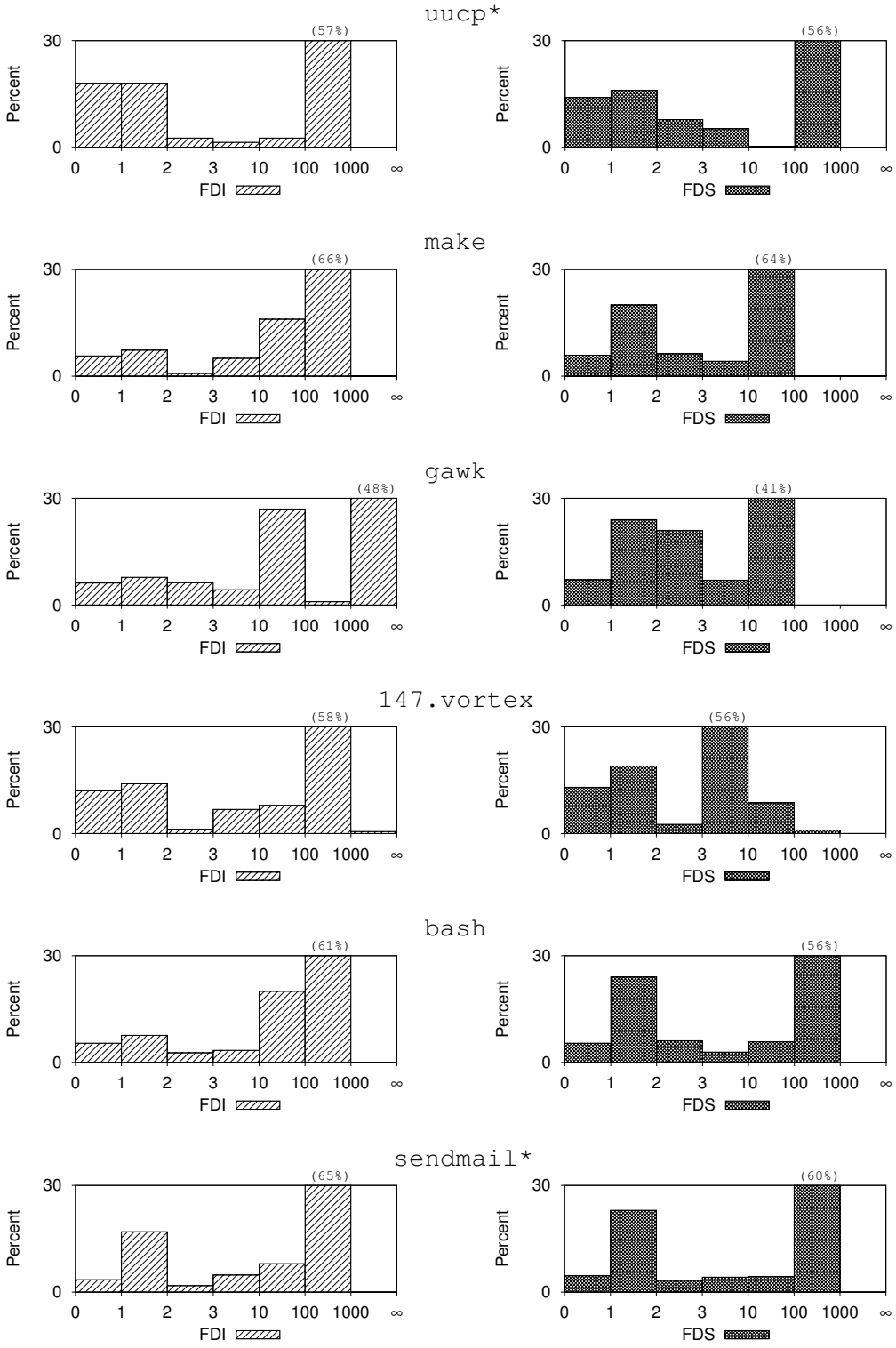

Figure 5.7: Charts of our experimental data showing a breakdown of the average points-to set size at dereference sites for each benchmark. Each bar indicates how many dereference sites (as a percentage of the total) have points-to sets of size X, where X lies between the left boundary and up to, but not including, the right boundary. For example, the second bar in each chart gives the number of dereference sites with points-to sets containing exactly one element. Benchmarks containing positive weight cycles are marked with an asterisk. Note, zero sized sets arise from an artifact of our linker (see the discussion for more on this).

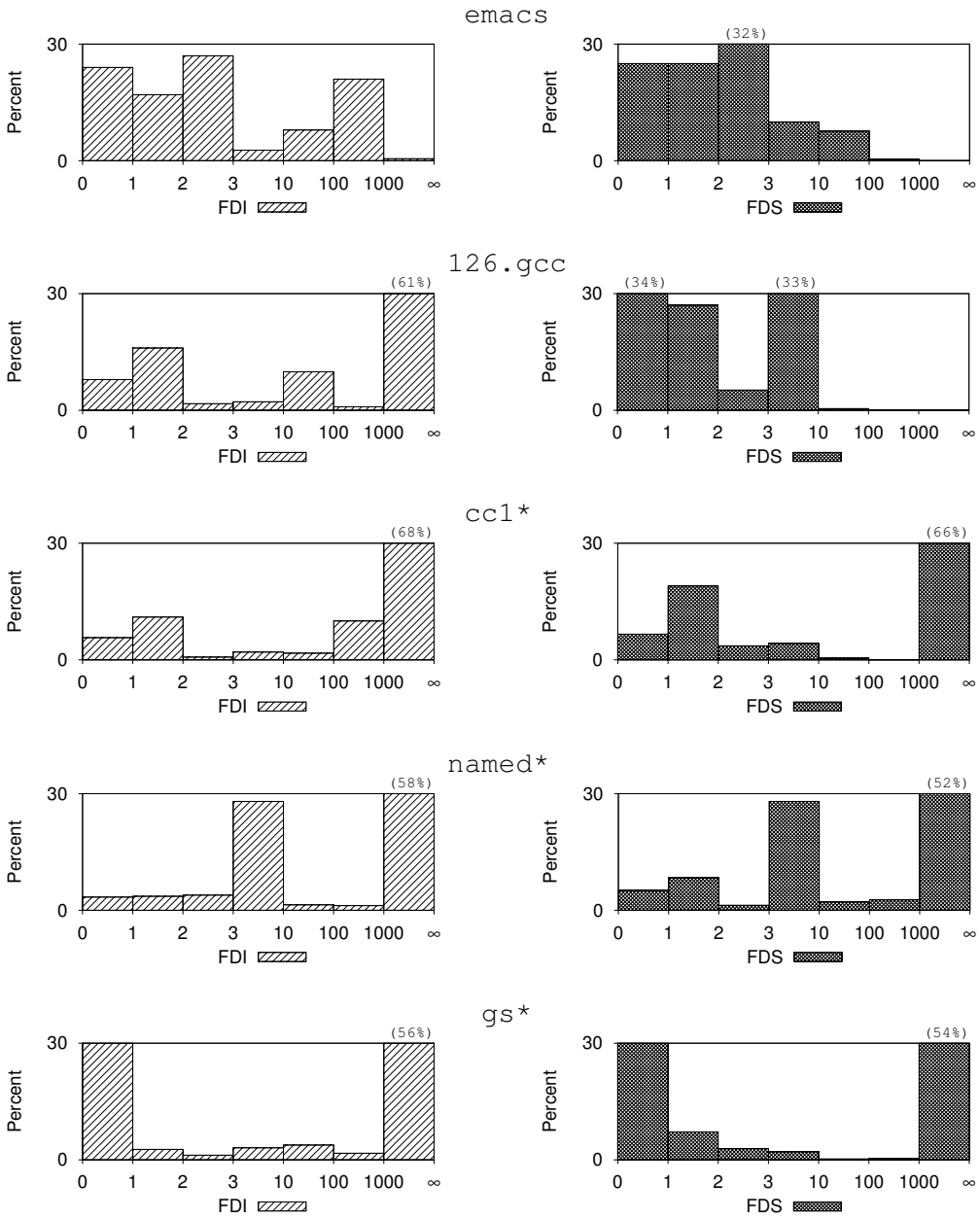

Figure 5.8: More charts of our experimental data showing a breakdown of the average points-to set size at dereference sites for each benchmark. Each bar indicates how many dereference sites (as a percentage of the total) have points-to sets of size X, where X lies between the left boundary and up to, but not including, the right boundary. For example, the second bar in each chart gives the number of dereference sites with points-to sets containing exactly one element. Benchmarks containing positive weight cycles are marked with an asterisk. Note, zero sized sets arise from an artifact of our linker (see the discussion for more on this).

uses are defined as portable within the ISO/ANSI C standard. The relevant points from the standard can be summarised as follows:

1. A pointer to a structure also points to the first field of that structure [ISO90, 6.5.2.1]. As a consequence, the first field of a structure must be at offset 0.

2. Accessing a union member after the last store was to a different member gives implementation-defined behaviour [ISO90, 6.3.2.3]. Suppose we have "`union{int a;float b;} x`". Now, we can safely write and then read `x.a`, but we cannot safely write to `x.b` and then read `x.a`.

3. As an exception to the above, if a `union` contains several structures whose initial members have *compatible types*, then it is permitted to access the common initial sequence of any of them [ISO90, 6.3.2.3]. Note, it is sufficient for us to simply take *compatible types* to mean *identical types*, although the actual definition is more subtle. To understand the meaning of this point, suppose we have "`union {T1 a;T2; b} x`", where T1 and T2 are two `struct`'s whose first N members have identical types. Furthermore, suppose we assign to `x.a`. At this point, we may read any of the first N members of `x.b` and, as expected, they will have the same values as the first N members of `x.a`. This contrasts with the previous rule, which stated we may only read from `x.a`.

The first point above is fairly straightforward and the following example demonstrates that the string concatenation approach cannot model it correctly:

```
typedef struct { int *f1; int *f2; } aggr1;
```

	String Concatenation	Integer Offset
`aggr1 a,*q=&a;`	(1) $q \supseteq \{a\}$	(1) $q \supseteq \{a.f1\}$
`int c,*p;`		
`a.f1 = &c;`	(2) $a.f1 \supseteq \{c\}$	(2) $a.f1 \supseteq \{c\}$
`p = *((int*)q);`	(3) $p \supseteq *q$	(3) $p \supseteq *q$
	(4) $p \supseteq a \quad (deref_1, 1{+}3)$	(4) $p \supseteq a.f1 \quad (deref_1, 1{+}3)$
		(5) $p \supseteq \{c\} \quad (trans, 2{+}5)$

What we see is that the string concatenation system is unable to correctly conclude $p \mapsto \{c\}$, where as our system has no trouble. The issue here arises from the translation of "`&a`" into "a", instead of "$a.f1$". Unfortunately, the obvious solution of using the latter translation to resolve this introduces a further problem:

```
aggr1 a,*q = &a;
int *p,c;
a.f1 = &c;
p = q->f1
```

(1) $q \supseteq \{a.f1\}$

(2) $a.f1 \supseteq \{c\}$

(3) $p \supseteq (*q)||f1$

---

(4) $p \supseteq a.f1.f1 \quad (\mathit{fdref}_1, 1{+}3)$

Again, it is impossible to conclude $p \mapsto \{c\}$ from here. The real problem is that individual locations can have multiple names (e.g. `&a` and `&a.f1` above) and a system based solely on unique strings cannot easily deal with this. Another example where this issue arises is given in Figure 5.9, where a different aspect of the ISO/ANSI standard is exploited (points 2 + 3 from the above summary). In this case, it is the ability to access the common initial sequence of two structures interchangeably which causes the trouble.

To overcome the issues involved with string concatenation, Yong *et al.* introduce three functions, *normalise, lookup* and *resolve*, whose purpose is to bridge the gap between different names representing the same location. This makes their system significantly more complicated and less elegant than our approach, which avoids these issues entirely. However, an important feature of their framework is the ability to describe both portable and non-portable analyses. The latter can be used to support commonly found, but undefined C coding practices which rely on implementation-specific information, such as type size and alignment. In contrast, our system as described cannot safely handle such practices. However, this could be done with only minor modification (i.e. using actual offsets instead of field numbers) and, in fact, Nystrom *et al.* claim to have done just this, although they do not discuss exact details [NKH04b].

Yong *et al.* also examine the precision obtainable with field-sensitivity and their findings concur with ours in suggesting that Average Deref size can be reduced by half. Finally, they do not discuss the positive weight cycle problem, perhaps because it is only relevant to particular instances of their framework. Nevertheless, to obtain an equivalent analysis to ours, this issue must be addressed. Indeed, as we have mentioned, Chandra and Reps do so in their analysis, which they describe as an instance of the Yong *et al.* framework [CR99a, CR99b]. Their solution is to adopt a worse-case assumption about pointers in positive weight cycles (i.e. they point to every field of each target). Unfortunately, they do not provide any experimental data which could be used as the basis of a comparison with our system.

5.4.1 Field-Based Pointer Analysis

At this point, we return to discuss the third technique for modelling aggregate variables, known as the field-based approach. The reader may have found it strange that this was omitted from our experimental study and the reason was simply that we have some concerns over its soundness. Note, these relate specifically to the analysis of C and previous works have failed to mentioned them before (see [HT01, And94]).

Recall from Section 2.2.3, that under the field-based method, only one constraint variable is

```
typedef struct { int *f1; int *f2; } aggr1;
typedef struct { int *f3; int *f4; } aggr2;
```

	String Concatenation	Integer Offset
`aggr1 a;`		(1) $idx(a.f1) = 0$
		(2) $idx(a.f2) = 1$
`aggr2 b;`		(3) $idx(b.f3) = 2$
		(4) $idx(b.f4) = 3$
`void *c;`		(5) $idx(c) = 4$
`int d;`		(6) $idx(d) = 5$
`b.f3 = &d`	(1) $b.f3 \supseteq \{d\}$	(7) $b.f3 \supseteq \{d\}$
`c = &b;`	(2) $c \supseteq \{b\}$	(8) $c \supseteq \{b.f3\}$
`a = (aggr1) *c;`	(3) $a.f1 \supseteq (*c)\|\|f1$	(9) $a.f1 \supseteq *(c+0)$
	(4) $a.f2 \supseteq (*c)\|\|f2$	(10) $a.f2 \supseteq *(c+1)$
	(5) $a.f1 \supseteq b.f1$ ($\mathit{fderef}_1, 2+3$)	(11) $a.f1 \supseteq b.f3$ ($\mathit{deref}_4, 3+8+9$)
	(6) $a.f2 \supseteq b.f2$ ($\mathit{fderef}_1, 2+4$)	(12) $a.f2 \supseteq b.f4$ ($\mathit{deref}_4, 3+4+8+10$)
		(13) $a.f2 \supseteq \{d\}$ ($\mathit{trans}, 7+11$)

Figure 5.9: This example illustrates an issue with the string concatenation approach to field-sensitivity. The problem arises because the type of "a" determines which field names are used in the concatenation, leading to constraints involving non-existing variables $b.f1$ and $b.f2$. An interesting point here is that, strictly speaking, this code has implementation-defined behaviour under the ISO/ANSI C standard. This is because the two `struct`'s must be wrapped in a union in order to be well-defined under the standard (see summary point 3 in Section 5.4). We have not done this purely to simplify the example.

provided to represent every instance of a particular field of an aggregate type. To implement this type of analysis, we need only our original inference system from Figure 2.1. The key difference, then, lies in the translation of C into the constraint language. The following illustrates this:

```
typedef struct { int *f1; int *f2; } aggr1;
```

`aggr1 a,b;`	Field-based	Field-insensitive
`int c,d,*p;`		
`a.f1 = &c;`	$aggr1.f1 \supseteq \{c\}$	$a \supseteq \{c\}$
`b.f1 = &d;`	$aggr1.f1 \supseteq \{d\}$	$b \supseteq \{d\}$
`p = a.f1;`	$p \supseteq aggr1.f1$	$p \supseteq a$

Note here, that the `aggr1` variable is provided to model every instance of the corresponding type. Hopefully, it is easy enough to see that the field-based analysis will conclude $p \mapsto \{c, d\}$, whilst the other gives the more precise $p \mapsto \{c\}$. In general, the relative precision of the two approaches is very much dependent upon the program in question. Now, the following C code, whilst completely portable under the ISO/ANSI standard, appears to be handled incorrectly by the field-based approach:

`aggr1 *p; int **q,*s,a;`	
`void *r = malloc(sizeof(aggr1));`	$r \supseteq \{\textit{HEAP0}\}$
`q = r;`	$q \supseteq r$
`p = r;`	$p \supseteq r$
`*q = &a;`	$*q \supseteq \{a\}$
`s = p->f1;`	$s \supseteq aggr1.f1$

The problem then, is that under the ISO/ANSI standard a pointer to a `struct` can be used interchangeably with a pointer to its first field. Therefore, we have carefully constructed this example to be difficult (if not impossible) for an inference system to conclude that `q` points to an instance of `aggr1` when it is dereferenced. The result is that, under our original inference system, `&a` is written to variable *HEAP0* and not *aggr1.f1*, leading to the unsound conclusion that $s \not\mapsto \{a\}$. At this point, a number of possible solutions present themselves and, although we have not explored them in any detail, it seems likely that they will all impact upon the precision and cost of the analysis.

5.5 Concluding Remarks

In this chapter, we have presented a novel approach to indirect function calls and field-sensitivity. We have shown, through experimental study, how the latter offers a significant improvement in precision, albeit at some computational cost. Furthermore, although our approach is not the first solution to the problem of field-sensitivity in C, we argue it is the simplest and most elegant and have provided numerous examples to support this.

While the overall conclusions of our experiments are positive, they also highlight a significant issue — namely that positive weight cycles are a major hindrance to efficient and precise field-sensitive analysis. Therefore, we feel that future work should consider this issue further and, hopefully, a satisfactory solution will be found. Another area of interest would be to investigate the effect on solving time of using the difference propagation technique with the field-sensitive analysis, which due to time constraints we have been unable to do.

Chapter 6

Conclusions and Future Work

In this chapter, we review the contributions of this thesis in light of a greater understanding of their meaning. We also make suggestions for future work, covering both improvements to the current work as well as completely new directions which have opened up. Having done this, we draw our final conclusions.

6.1 Review of Contributions

- We presented a fully dynamic, unit change algorithm called POTO1 for maintaining the topological order of a directed acyclic graph. While this has marginally inferior time complexity compared with AHRSZ, it is far simpler to implement, has smaller storage requirements and fewer restrictions (i.e. 2^{32} nodes can be used with 32-bit integers). We also provided an experimental study over random DAGs comparing POTO1 against the two previously known works (MNR and AHRSZ), which concluded that it was the most efficient overall. Specifically, MNR was seen to be marginally more efficient than POTO1 on dense graphs, but significantly worse on sparse graphs. Furthermore, AHRSZ was always a constant factor slower than POTO1.

- We presented a fully dynamic, batch algorithm for maintaining the topological order of a DAG, referred to as POTO2. For a batch of b edge insertions, this has an optimal $O(b+v+e)$ bound on its runtime — a significant improvement over the $O(b(v+e))$ bound obtained for the three unit change algorithms. We also experimentally evaluated the algorithm against MNR, POTO1, AHRSZ and SOTO, which the reader may recall from Figure 3.1 is based upon the standard (offline) topological sort. This showed that POTO2 was largely inferior to POTO1 on sparse graphs, but that on dense graphs with reasonable batch sizes it was the more efficient.

- We presented an extension to the above algorithms for dynamically identifying strongly connected components (cycles) in digraphs. Thus, we obtain the first solutions which do not traverse the entire graph for half of all edge insertions in the worst case.

- We presented a theoretical and practical investigation into a technique called *difference propagation*. In particular, we showed how this technique permits a practical, cubic time solving algorithm. Furthermore, we provided an experimental evaluation of difference propagation on 11 common C programs, ranging in size from 15,000 to 200,000 lines of code. This concluded that difference propagation offered consistently better performance than a standard worklist approach. However, the improvements obtained were perhaps somewhat disappointing, although they indicate that larger benchmarks may show better results.

- We presented a theoretical and practical investigation into the effects of cycle detection and iteration strategy on performance. Our experimental results confirmed that a previously known iteration strategy, called *Least Recently Fired*, was significantly faster than two simple approaches. Furthermore, the results demonstrated that using a topological iteration strategy was even better. Here, algorithm POSCC2 was found to give better performance than either POSCC1 or Tarjan's algorithm, although the gain was not always significant.

- We presented an extension to the language of set constraints supporting function pointers and field-sensitive pointer analysis of C. We showed, in some detail, how this provides a simpler and more elegant solution than the previously known approaches and also addressed some issues (e.g. the PWC problem) which had not received adequate attention. Furthermore, we provided the largest experimental evaluation to date of field-sensitive pointer analysis for C. The conclusions from this were that field-sensitivity offers significantly greater precision at the price of, in some cases, much longer solving times. The results also showed a correlation between the presence of positive weight cycles and reduced gains in precision as well as greater solving times.

6.2 Future Work for the Online Topological Order Problem

Contained in this thesis is the most detailed and thorough examination to date of solutions to the problem of maintaining a topological order online. And yet, there are many ways in which this work could be taken forward. In particular, our motivation stems from an obvious and well-known application of these algorithms to pointer analysis. However, our developments are certainly not limited to this domain and, while we have yet to take this further, it seems likely that many different areas stand to benefit from them.

For example, whilst researching Chapter 3, we came across a Markov-Chain approach to generating random DAGs [MBMD01]. The algorithm described relies upon the use of an online cycle detector, for which the authors are only able to suggest a rather crude algorithm (in fact, that from [IR78]). Thus, it seems likely either POSCC1 or POSCC2 would improve the practical performance of the overall algorithm. Another interesting area which could be explored is that of online transitive closure. Although many existing algorithms for this problem are known (e.g. [KS99, BHS02, DI00, RZ02]), they all employ some form of matrix multiplication. However, solutions based upon graph traversal (i.e. Tarjan's algorithm for identifying SCCs) would likely offer much better performance in practice. Indeed, for the offline problem, it is well known that those

using graph traversal (e.g. [IRW93, Nuu95]) are a better choice in practice, in spite of their worse theoretical time complexity. Hence, we suspect the lack of efficient algorithms for online cycle detection is the main reason that graph traversal methods have yet to be used for online transitive closure.

In addition to exploring other domains for applications of POTO1 or POTO2, there remain several other specific ways in which this work could be taken forward and we briefly discuss them now.

6.2.1 Experiments on Real-World Graphs

In general, it is well known that uniformly generated random graphs do not often reflect real-life structures. Thus, there is some uncertainty as to whether the conclusions from our experimental analysis into the performance of algorithms for the OTO problem will apply in practice. To address this issue, it would be interesting to experiment with real-world graphs. Of course, one problem here is in finding sufficient graphs to make any comparison meaningful.

In fact, exploring alternative approaches to generating random DAGs would also be valuable. For example, Ioannidis *et al.* use a parameter, called the *locality factor*, to restrict the maximum number of nodes which may come between the head and tail of an edge in the order [IRW93]. Thus, looking at the behaviour of our algorithms at different locality factors might prove fruitful.

6.2.2 A Bounded Complexity Result for POTO2

As already noted, the theoretical analysis of algorithm POTO2 in Section 3.3 does not provide a result in terms of $|\delta_{xy}|$ and $|AR_{xy}|$. This was not because we could not find one, but that we simply did not have time to try. Furthermore, while the $O(b + v + e)$ bound given does improve upon that of MNR, AHRSZ and POTO1 it does not, in fact, improve upon that of SOTO. Recall from Figure 3.1 that this algorithm uses a standard offline topological sort and achieves the same bound as POTO2. Nevertheless, we are confident that a result distinguishing POTO2 from SOTO can be found and, most likely, without significant effort.

6.2.3 A Batch Variant of POTO1

Since we were able to develop a batch variant of the MNR algorithm, it seems plausible that a batch variant of algorithm POTO1 might also exist. In fact, while we have not yet obtained a complete algorithm, some progress has been made in this direction and we now briefly discuss this.

A key invariant enforced by algorithm POTO1 is that nodes discovered during the forward search can only move forward (i.e. up) in the order, whilst those found during the backward search can only move backward. To aid our discussion, we refer to these node types as *F-nodes* and *B-nodes* respectively. In fact, the batch update problem exposes a third class of node, referred to as primary or *P-nodes*, which were not encountered before. The primary nodes have the interesting

property that they can be moved in *either direction* within the order. The following aims to clarify the three node types:

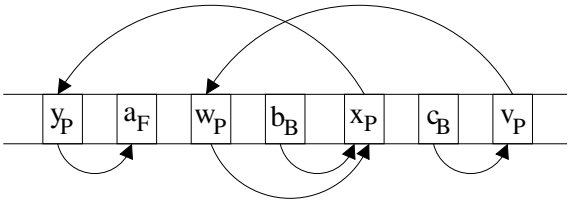

Here we have marked the class of each node using a subscript. The general procedure for determining node type is as follows: firstly, all nodes visited by a reverse search from y are marked as *B-nodes*; secondly, all those visited by a forward search from v are marked as *F-nodes*; finally, those which are both an *F-node* and a *B-node* are marked as *P-nodes*. At this point, we can rearrange the ordering by allocating *B-nodes* to the leftmost slots, *F-nodes* to the rightmost slots and *P-nodes* to the remainder, giving:

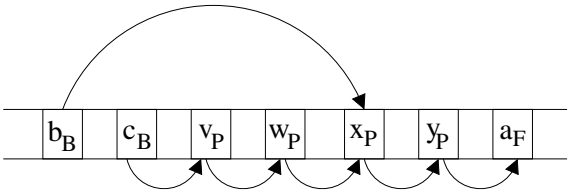

Notice that the *B-nodes* retain their original (relative) ordering, whilst the *P-nodes* are now laid out in topological order. Generally speaking, this procedure works rather well but, unfortunately, there are some problem cases. For example:

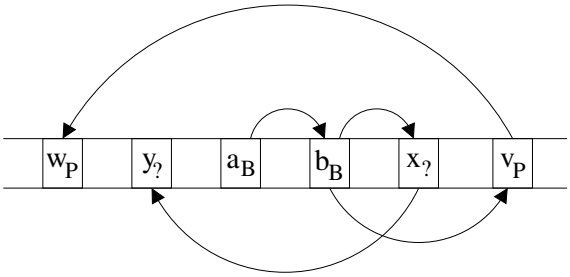

Here, nodes x and y do not get marked under the procedure as described. The problem is that we must position a and b into the two leftmost slots and, hence, y must be moved. Therefore, our procedure must be extended to mark x and y appropriately and, furthermore, to allocate nodes correctly. While this latter point may seem trivial, it is unfortunately somewhat more complicated than it first appears. Nevertheless, we strongly believe that our procedure can be extended to cover these problem cases and we hope to complete this in the near future.

6.2.4 Improving POTO1

As noted at the end of Chapter 3, there are some possibilities for improving algorithm POTO1 further. The ultimate objective, of course, would be to obtain a worse-case time bound comparable with AHRSZ, although it remains wholly unclear whether this is possible. Nevertheless, we have identified one small stepping stone in this process, exemplified by the following graph:

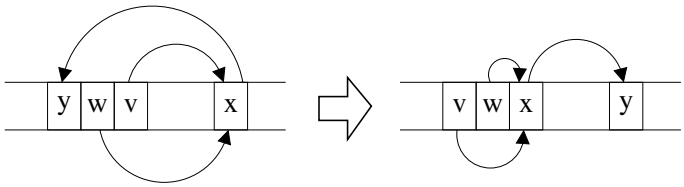

The key point about this example is that we can obtain a valid ordering without repositioning w. Algorithm POTO1, however, would have visited w and generated a slightly different solution (the above, but with v and w swapped). Of course, a saving of one node is insignificant, but it is easy enough to see that we can construct examples where the number is arbitrarily large. To address this issue in POTO1, we believe that breadth-first (not depth-first) searches should be used to identify nodes during discovery. This would work in a similar way to the frontiers approach of AHRSZ, in that discovery now stops when the forward and backward searches meet.

6.3 Future Work on Pointer Analysis

Work on pointer analysis is continuing at a fast pace, with new algorithms developed all the time. For example, the use of *Binary Decision Diagrams (BDD)* has been recently embraced by the community as a way of substantially reducing storage requirements [WL04, ZC04, Zhu02, LH04, BLQ$^+$03]. Thus, it appears there is scope in looking at whether such emerging techniques can be integrated with those developed in this thesis — especially the algorithms for online cycle detection and topological order.

Of course, the hunger for greater precision at less cost has not abated and, recently, algorithms have begun to tackle the problem of providing efficient, context-sensitive pointer analysis [WL04, NKH04b]. However, this comes at some cost with solving times being increased by many orders of magnitude on medium to large benchmarks. Thus, it seems that the value of increased scalability offered by difference propagation and our advanced cycle detectors may be greater for analyses requiring high precision and future work should certainly explore this direction.

Finally, there are numerous and, perhaps more immediate, improvements which could be made to the current work and we briefly elaborate on each now.

6.3.1 Eliminating Positive Weight Cycles

One interesting conclusion from Chapter 5, was that positive weight cycles are a major hindrance to efficient and precise field-sensitive pointer analysis. Thus, it would be beneficial if they could

somehow be circumnavigated. One approach might be to argue that, since positive weight cycles can only arise from imprecision in the analysis itself, they do not in fact affect soundness of the solution. This would lead to a conclusion that positive weight cycles could be identified and safely broken during the analysis. However, we caution that our reasoning along these lines remains immature and requires further development.

Another approach to the problem might be to adopt a technique often used in program analysis, known as widening (e.g. [Bou93b, CC91, NNH99]). The idea would be to identify positive weight cycles during the analysis and, upon finding one, to immediately maximise the solution sets of its members. However, while this approach could certainly help improve runtime, it would not improve precision and this could be an issue. Regardless, it remains interesting to see what could be done here.

6.3.2 Developing the Heintze-Tardieu Algorithm

The results of the experimental study conducted in Chapter 4 suggest that the Heintze-Tardieu solver is efficient and robust, compared with the fastest worklist solvers we have developed. This was in spite of having an inferior, worse-case time bound of $O(v^4)$. Of course, some strange anomaly of our experimental setup could be to blame here, but we feel the consistent performance indicates something more interesting. As mentioned in the conclusion of Chapter 4, although we have made some considerable effort to understand HT, we have so far failed to unlock the key to its mystery. In addition, we believe the ideas from difference propagation could be combined with this algorithm to obtain an optimal $O(v^3)$ time bound.

6.3.3 Transitive Edges

The ability to remove transitive edges from the constraint graph would offer clear and immediate benefits for pointer analysis algorithms. To see why, consider the following:

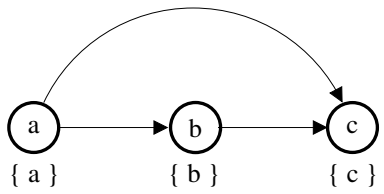

In the above, there is a single transitive edge — namely $x \rightarrow z$. Removing this edge cannot affect the final solution and would offer a performance improvement. This benefit comes because, by not propagating along the edge, we are performing fewer (potentially expensive) set union operations. In general, there has been little work done on transitive reduction (see [PvL88, Sim90, KRY94, Hsu75]), the most significant being that by Aho, Garey and Ullman [AGU72]. They showed that an $O(n^2)$ transitive reduction algorithm reduction would imply an $O(n^2)$ transitive closure algorithm. Thus, it seems unlikely that a fast reduction algorithm will be found. Nevertheless, a fast algorithm that identified *some* transitive edges would still be useful. In fact, this is exactly

what *inductive form* (see Appendix A) aims to do. Unfortunately, there has been little or no work evaluating the effectiveness of this method in reducing the number of transitive edges. Therefore, we feel it remains to be seen whether the goal of inductive form is achieved and useful work remains to be done here.

6.4 Conclusions

This chapter concludes the thesis with a summary of the main points and a discussion of interesting directions for future work. The main goal of the thesis was to develop increasingly efficient techniques for pointer analysis and, while this has certainly been achieved, the results are slightly disappointing. Nevertheless, much has been achieved and, in particular, we feel that the directed graph algorithms which were developed have an exciting future. Finally, we thank the reader for their attention and hope they have found this work stimulating and enjoyable.

Appendix A

Relating to Heintze-Aiken Systems

The purpose of this appendix is to formally relate the language of set constraints used in this thesis with the more standard system used by Heintze, Aiken and others. Having done this, we provide a discussion of *inductive form*.

The standard system of set constraints, such as those found in [AW93, MR97, FFA97, FFSA98, SFA00, FFA00, Aik99, KA04], is based around the following language:

$$X \supseteq Y \mid X \supseteq c(X_1, \ldots, X_n) \mid proj(c, i, X) \supseteq X$$

Here, X and Y are constraint variables as before, $c(\ldots)$ is a *constructor* and $proj$ is the *projection operator*. Conceptually, constructors define different element types to be used in the analysis. In our system, we had no use for constructors because there was only one element type — the address of a variable. However, more complex analyses may need several element types to co-exist and constructors enable this. The projection operator is harder to understand. Essentially, it introduces new constraints into the system, much like the dereference operator in our complex constraints does. A subtle difference, the reason for which will only be apparent later, is that the projection operator can only appear on the left-hand side of a constraint (recall our dereference operator can be on either side). The following inference rules are used to evaluate projections:

$$[proj_1] \quad \frac{proj(c, k, Y) \supseteq c(X_1, \ldots, X_k, \ldots, X_n)}{Y \supseteq X_k}$$

$$[proj_2] \quad \frac{proj(c, k, Y) \supseteq c(X_1, \ldots, \overline{X_k}, \ldots, X_n)}{Y \subseteq X_k}$$

Looking at these rules, we see the projection operator introduces a constraint between the k^{th} argument of the constructor and that defined inside the projection itself. The difference between the rules is simply the direction given to the subset operator. This distinction is subtle, but crucial to understanding how the projection operator relates to the dereference operator from our language. The key point is that the argument positions for a given constructor type must be predefined as either *covariant* or *contravariant* and this choice determines which direction is taken. Thus, to aid clarity, it is common to see *contravariant* arguments marked by an overbar and, hence, the second rule applies to them. At this point, the reader may be slightly confused as to what contravariance is

$$[trans] \quad \frac{X \supseteq c(Z_1, \ldots, Z_n) \quad Y \supseteq X}{Y \supseteq c(Z_1, \ldots, Z_n)}$$

Figure A.1: Illustrating the closure rule used in conjunction with standard form

for and how it relates to our constraint language. As mentioned already, projection can only occur on the left-hand side of a constraint. Thus, if we regard projection as performing the same role of our dereference operator, then this restriction appears to prevent us from modelling languages which allow dereferences on the right-hand side. In fact, this is supported through contravariance and, following this discussion, we provide an example demonstrating how. Hopefully, it is becoming clear that we do not need this notion of contravariance as our dereference operator can be on either side and, hence, we avoid this complicated issue.

At this point, we have mostly completed our discussion of traditional set constraints. All that remains is to provide an example clarifying what we have said. Therefore, we now present the common approach to performing pointer analysis with set constraints, such as that used in [FFA97, FFSA98, SFA00, FFA00]. The main idea is to model the address of an object with a special constructor, $ref(a, \overline{a})$, which is covariant in its first argument and contravariant in its second. Thus, the following demonstrates how a simple program is translated and solved using the projection rules and the closure rule of Figure A.1:

```
int *r,*s,*t;
int **p,**q;
int a;
```

	Traditional system		Our system	
`s = &a`	(1) $s \supseteq ref(a, \overline{a})$		(1) $s \supseteq \{a\}$	
`p = &r`	(2) $p \supseteq ref(r, \overline{r})$		(2) $p \supseteq \{r\}$	
`q = p`	(3) $q \supseteq p$		(3) $q \supseteq p$	
`*q = s`	(4) $proj(ref, 2, s) \supseteq q$		(4) $*q \supseteq s$	
`t = *q`	(5) $proj(ref, 1, t) \supseteq q$		(5) $t \supseteq *q$	
	(6) $q \supseteq ref(r, \overline{r})$	$(trans, 2{+}3)$	(6) $q \supseteq \{r\}$	$(trans, 2{+}3)$
	(7) $proj(ref, 2, s) \supseteq ref(r, \overline{r})$	$(trans, 4{+}6)$		
	(8) $r \supseteq s$	$(proj_2, 7)$	(7) $r \supseteq s$	$(deref_2, 4{+}6)$
	(9) $r \supseteq ref(a, \overline{a})$	$(trans, 1{+}8)$	(8) $r \supseteq \{a\}$	$(trans, 1{+}7)$
	(10) $proj(ref, 1, t) \supseteq ref(r, \overline{r})$	$(trans, 5{+}6)$		
	(11) $t \supseteq r$	$(proj_1, 10)$	(9) $t \supseteq r$	$(deref_1, 5{+}6)$
	(12) $t \supseteq ref(a, \overline{a})$	$(trans, 9{+}11)$	(10) $t \supseteq \{a\}$	$(trans, 8{+}9)$

A.1 Inductive Form

The approach to solving set constraints presented above and throughout this thesis is called *Standard Form* [AW93]. An alternative, *Inductive Form*, is often described as a sparse and efficient representation [SFA00, RMR01]. In this section, we investigate this further.

To understand how inductive form works, we must first consider standard form in terms of *predecessor* and *successor* edges. Here, successor edges correspond to the edges used in all previous examples, while predecessor edges represent the solution sets themselves. The following aims to clarify this, where dotted edges are predecessor edges:

$X \supseteq ref(a, \overline{a})$
$X \supseteq ref(b, \overline{b})$
$Y \supseteq ref(c, \overline{c})$
$Y \supseteq X$
$Z \supseteq Y$
$proj(ref, 1, U) \supseteq Z$

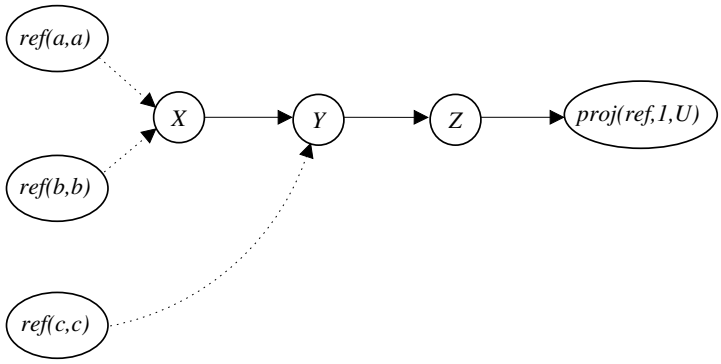

This shows a constraint set and the corresponding graph in standard form and, as expected, we can solve it to obtain the following:

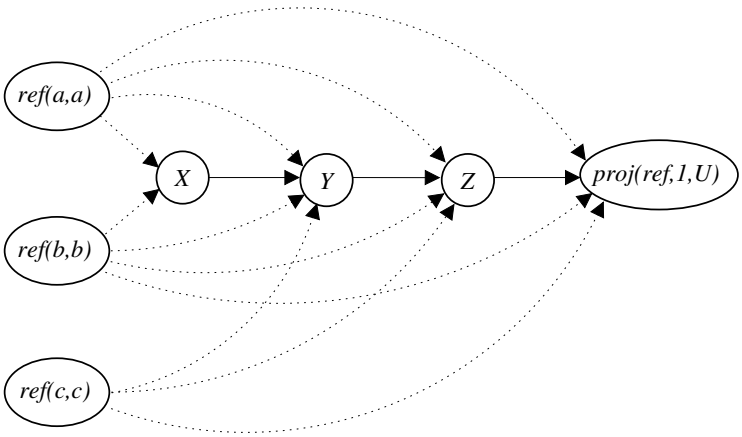

Note, we are not concerned with evaluating the projection as it is not relevant to the discussion. The point is that there are 14 edges involved in this graph. Now, the general idea behind inductive form is to reduce the number of edges by maintaining the graph in a partially completed form. This is achieved by allowing both edge types to represent variable-variable constraints such as $X \supseteq Y$, which constitutes a significant departure from standard form. Furthermore, it raises the issue of deciding when to use a predecessor edge and when to use a successor edge and, to resolve this, a fixed total order of nodes, denoted by $o(\cdot)$, is employed. Thus, if $o(X) < o(Y)$ then a predecessor edge is chosen to represent $X \supseteq Y$, otherwise a successor edge is used. The choice of ordering dramatically affects efficiency and finding an optimal order is hard [SFA00, FFSA98], although we remain unsure whether it is actually NP-hard or not. So, assuming an ordering of $o(X) < o(Z) < o(Y)$ the inductive form of our above example initially looks like:

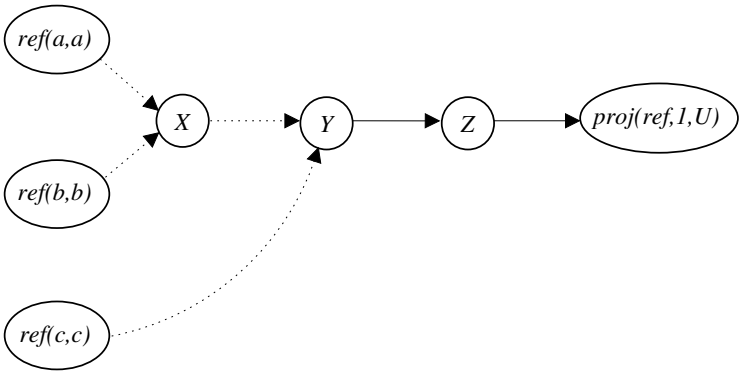

Here, we see the graph looks much the same to that of standard form, except that $X \rightarrow Y$ is now a predecessor edge. Following the usual terminology, we refer to constructor nodes as *sources* and projection nodes as *sinks*. Now, an important point, without which the system could not work, is that edges from source nodes are always predecessors, while those to sinks are always successors. In fact, this is the primary reason why projection is only permitted on the left-hand side of a constraint — because otherwise sources might not connect to sinks [SFA00]. So, to solve the graph, the following closure rule is used in place of that in Figure A.1:

$$L \dashrightarrow X \longrightarrow R \Rightarrow L \subseteq R$$

Here, L is either a source or a variable node, while R may be either a sink or variable node. Note, to evaluate projections, the same rules as before (i.e. $proj_1$ and $proj_2$) are employed. Thus, we can solve the graph through repeated application of the new closure rule, which gives:

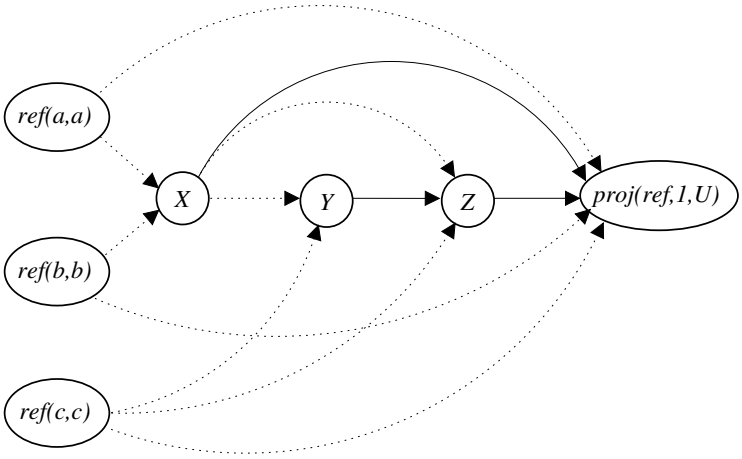

Notice that source-sink edges are always resolved as predecessors. From this it should be clear that the inductive form solution has fewer edges (12 compared with 14) and, although the difference seems small, we can construct examples where it is larger. One issue is that, unlike standard form, the solution is no longer explicit, meaning we must traverse the graph to obtain the points-to set for a given node. However, this only needs to be done once at the end and, thus, should not impose any significant overheads.

Appendix B

Strongly Connected Components

One algorithm is frequently referenced in this thesis and, indeed, underpins much of the work contained herein. This is Tarjan's algorithm for detecting *strongly connected components* (i.e. cycles) in digraphs [Tar72]. The power of this algorithm is the ability to identify all cycles in linear (i.e. $O(v+e)$) time. In this section, we examine it and briefly discuss some recent improvements.

Definition 10. For a digraph, $G = (V, E)$, a node x *reaches* a node y, written $x \overset{G}{\rightsquigarrow} y$, if $x = y$ or $x \rightarrow y \in E$ or $\exists z.[x \rightarrow z \in E \ \wedge \ z \overset{G}{\rightsquigarrow} y]$. The G is often omitted from $\overset{G}{\rightsquigarrow}$, when it is clear from the context. We also say that y is reachable from x and that x is an *ancestor* of y.

Definition 11. A strongly connected component (SCC) of a digraph, $G = (V, E)$, is a subgraph $S = (V_s, E_S)$, where $V_s \subseteq V, E_s \subseteq E$ and $\forall x, y \in V_s.[x \overset{S}{\rightsquigarrow} y \wedge y \overset{S}{\rightsquigarrow} x]$.

Tarjan's algorithm operates using a single *depth-first traversal* of the graph. To be clear in our meaning of this, a traversal algorithm is provided in Figure B.1. Note, the $index$ counter, while unnecessary, aids our discussion. We define the *visitation index* or $vindex$ of a node x as the $index$ value when $visit(x)$ is called. An edge $x \rightarrow y$ is referred to as being *traversed* if $visit(y)$ is invoked from $visit(x)$. We now illustrate a traversal by labelling each node with its $vindex$:

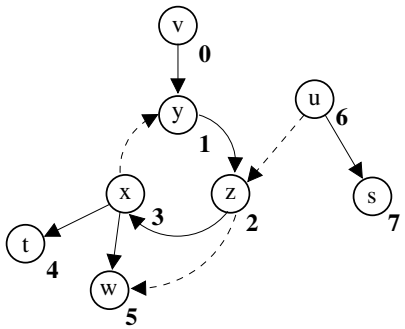

Here, the dashed edges are those not traversed by the algorithm. From this example, hopefully one thing is clear: *any cycle must be broken by an untraversed edge*. This holds as a path is traversed as soon as the first node x of a cycle is visited to the others. By definition, this traversal will eventually reach a node y with an edge back to x. By classifying the untraversed edges, we can identify those breaking cycles and, from this, the cycles themselves. One way of achieving this is by viewing the traversal as a set of *trees* whose edges are those actually traversed:

```
procedure traverse()
  index = 0;
  foreach v ∈ V do
    if v not visited then visit(v);

procedure visit(n)
  mark n as visited;
  index = index + 1;
  foreach n → w ∈ E do
    if w not visited then visit(w);
```

Figure B.1: A procedure for depth-first traversal of a directed graph

Definition 12. A traversal tree, for a digraph $G = (V, E)$ is a tree defined as $G_T = (r, V_T, E_T)$, where $V_T \subseteq V$, $E_T = \{x \rightarrow y \in E \mid visit(x)\ invoked\ visit(y)\}$ and r is the distinguished root node having no predecessors. Furthermore, there is exactly one path between r and every node in the tree.

Thus, if $visit(x)$ is called from `traverse`, then x will be the root of a traversal tree constructed by the ensuing calls to $visit$. For our previous example, there are two traversal trees:

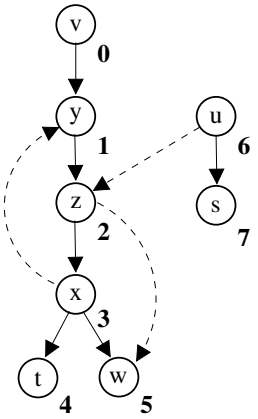

Note, the dashed edges are those untraversed (as before) and are not part of any traversal tree. In the literature, it is common to see these edges being referred to as *non-tree* edges, with traversed edges being called *tree edges* (for obvious reasons). We can make a few useful observations about these traversal trees. Firstly, it turns out that non-tree edges can be categorised as *forward-, backward-* or *cross-edges*. The forward edges are those which go "down" a path of the tree (e.g. $z \rightarrow w$), while back edges go "up" a tree path (e.g $x \rightarrow y$). Thus, forward edges are always *transitive*. Formally:

Definition 13. For a digraph $G = (V, E)$, an edge $x \rightarrow y \in E$ is a forward-edge, with respect to some traversal tree $T = (r, V_T, E_T)$, if $x \rightarrow y \notin E_T \wedge x \overset{T}{\rightsquigarrow} y$.

Definition 14. For a digraph $G = (V, E)$, an edge $x \rightarrow y \in E$ is a back-edge, with respect to some traversal tree $T = (r, V_T, E_T)$, if $x \rightarrow y \notin E_T \wedge y \overset{T}{\rightsquigarrow} x$.

The *cross-edges* constitute the remaining non-tree edges (e.g. $u \rightarrow z$), which connect disjoint trees and sub-trees. The second interesting point about traversal trees is that the path from the root to some node x corresponds to the call stack when $visit(x)$ is invoked. For example, when $visit(w)$ is entered, the call stack looks like:

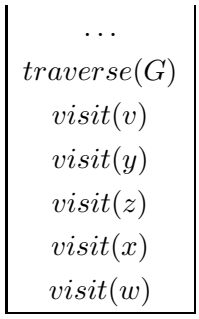

The key observation here is that, all ancestors in the tree of a node x will be on the call stack during $visit(x)$. Therefore, a back edge $x \rightarrow y$ can be identified inside $visit(x)$ by looking for $visit(y)$ on the call stack. Furthermore, it holds from Definition 14, that the head and tail of a back-edge must be part of some cycle. Thus, we have the rough outline of an algorithm: *traverse the graph, using back-edges to identify cycles*. Tarjan exploits all of these facts in his algorithm, presented in Figure B.2 and there is one point which must be understood: the algorithm actually finds *maximal strongly connected components*, meaning that two cycles with common nodes are always identified as one.

The algorithm operates by maintaining, in $root[x]$, the earliest node which has been visited and is reachable from x via a back-edge. Thus, as $root[x] = x$ initially, we know that all nodes between $root[x]$ and x in the traversal tree are part of the same cycle. The purpose of $stack$ is to mirror the current traversal path so these nodes can be identified. Another important piece is the array $in\_component$, which can be thought of as maintaining the following invariant: if, for some node x, $in\_component(x) = false$ then either $visit(x)$ is on the call stack or x reaches (via a back-edge) some node y, for which $visit(y)$ is on the call stack. Note that, in both cases, $root(x)$ identifies the node whose $visit$ invocation is on the call stack. The algorithm back-propagates this $in\_component$ information to determine which nodes are in the component currently being explored. This is similar to the way *component* information is back-propagated to identify members of a cycle in our extensions to MNR and POTO1 for identifying SCCs (see Section 3.5).

As mentioned already, the algorithm requires $O(v+e)$ time to operate and uses $O(v)$ space in addition to that required for the graph itself. In fact, we can be more precise about the additional storage requirements as the algorithm requires at most $v(2+3w)$ bits, where w is the word size. This is because two bits per node are needed for the $in\_component$ and $visited$ flags, while two words are needed for $vindex$ and $root$. Furthermore, the $stack$ can hold at most v elements and, thus, one extra word is needed per node in the worse case..

Since the original publication of Tarjan's algorithm, there have been some minor improvements. The first of these was by Nuutila, who realised it was unnecessary to put each visited node onto $stack$ [NSS94, Nuu95]. In fact, only those identified as members of a cycle need to be and,

```
procedure Tarjan_SCC()
  index = 0;
  stack = ∅;
  foreach v ∈ V do
    if v not visited then visit(v);

procedure visit(n)
  mark n as visited;
  root[n] = n;
  push(n, stack)
  in_component[n] = false;
  vindex[n] = index;
  index = index + 1;

  foreach n → w ∈ E do
    if w ∉ visited then visit(w);
    if ¬in_component(w) then
      if vindex[root[w]] < vindex[root[n]] then
        root[n] = root[w];

  if root[n] = n then
    do
      w =pop(stack);
      in_component[w] = true;
      root[w] = n;
    while w ≠ n;
```

Figure B.2: Tarjan's algorithm for detecting the strongly connected components of a digraph

thus, a reduced space requirement can be achieved. Note that, in the worse case, nothing is saved as each node is part of a cycle. The second improvement was by Gabow [Gab00], who managed to further reduce the storage requirements by replacing the *vindex* array with a stack. However, this doesn't allow us to reduce the maximum storage requirement from $v(2 + 3w)$ bits, as the new stack can still hold v elements in the worse case. The point is that it is unlikely to do so in practice, whereas the array must always.

One final point about Tarjan's algorithm is that it is an *offline* algorithm. That is to say, updating the solution after an edge has been inserted or removed requires recomputing it from scratch. This is somewhat inefficient and, in Chapter 3, we present new algorithms which do much better.

Bibliography

[ACL00] William Aiello, Fan Chung, and Linyuan Lu. A random graph model for power law graphs. In *Proceedings of the ACM Symposium on the Theory of Computing (STOC)*, pages 171–180, May 2000.

[AGU72] Alred V. Aho, Michael R. Garey, and Jeffrey D. Ullman. The transitive reduction of a directed graph. *SIAM Journal on Computing*, 1(2):131–137, June 1972.

[AHM+98] Rajeev Alur, Thomas A. Henzinger, Freddy Y. C. Mang, Shaz Qadeer, Sriram K. Rajamani, and Serdar Tasiran. MOCHA: Modularity in model checking. In *Proceedings of the conference on Computer Aided Verification (CAV)*, volume 1427 of *Lecture Notes in Computer Science*, pages 521–525. Springer-Verlag, June 1998.

[AHR+90] Bowen Alpern, Roger Hoover, Barry K. Rosen, Peter F. Sweeney, and F. Kenneth Zadeck. Incremental evaluation of computational circuits. In *Proceedings of the ACM-SIAM Symposium on Discrete Algorithms (SODA)*, pages 32–42. ACM Press, January 1990.

[Aik94] Alexander Aiken. Set constraints: Results, applications, and future directions. In *Proceedings of the workshop on Principles and Practice of Constraint Programming (PPCP)*, volume 874 of *LNCS*, pages 326–335. Springer-Verlag, May 1994.

[Aik99] Alexander Aiken. Introduction to set constraint-based program analysis. *Science of Computer Programming*, 35(2–3):79–111, 1999.

[AK87] Randy Allen and Ken Kennedy. Automatic translation of Fortran programs to vector form. *ACM Transactions on Programming Languages and Systems (TOPLAS)*, 9(4):491–542, 1987.

[And94] Lars O. Andersen. *Program Analysis and Specialization for the C Programming Language*. PhD thesis, DIKU, University of Copenhagen, May 1994.

[AW92] Alexander Aiken and Edward L. Wimmers. Solving systems of set constraints. In *Proceedings of the IEEE symposium on Logic in Computer Science (LICS)*, pages 329–340. IEEE Computer Society Press, June 1992.

[AW93] Alexander Aiken and Edward L. Wimmers. Type inclusion constraints and type inference. In *Proceedings of the ACM conference on Functional Programming Languages and Computer Architecture (FPCA)*, pages 31–41. ACM Press, June 1993.

[BCC+02] Bruno Blanchet, Patrik Cousot, Radhia Cousot, Jérôme Feret, Laurent Mauborgne, Antoine Miné, David Monniaux, and Xavier Rival. Design and implementation of a special-purpose static program analyzer for safety-critical real-time embedded software. In *The Essence of Computation: Complexity, Analysis, Transformation*, volume 2566 of *Lecture Notes in Computer Science*, pages 85–108. Springer-Verlag, 2002.

[BCC+03] Bruno Blanchet, Patrik Cousot, Radhia Cousot, Jérôme Feret, Laurent Mauborgne, Antoine Miné, David Monniaux, and Xavier Rival. A static analyzer for large safety-critical software. In *Proceedings of the ACM conference on Programming Language Design and Implementation (PLDI)*, pages 196–207. ACM Press, June 2003.

[BCD+02] Michael A. Bender, Richard Cole, Erik D. Demaine, Martin Farach-Colton, and Jack Zito. Two simplified algorithms for maintaining order in a list. In *Proceedings of the European Symposium on Algorithms (ESA)*, volume 2461 of *Lecture Notes in Computer Science*, pages 152–164. Springer-Verlag, September 2002.

[BE84] Amnon Barak and Paul Erdös. On the maximal number of strongly independent vertices in a random acyclic directed graph. 5(4):508–514, 1984.

[Ber92] Arthur M. Berman. *Lower And Upper Bounds For Incremental Algorithms*. PhD thesis, Rutgers University, New Brunswick, New Jersey, October 1992.

[BH93] Thomas Ball and Susan Horwitz. Slicing programs with arbitrary control-flow. In *Proceedings of the Workshop on Automated and Algorithmic Debugging (AADEBUG)*, volume 749 of *Lecture Notes in Computer Science*, pages 206–222. Springer-Verlag, May 1993.

[BHA85] Geoffrey L. Burn, Chris Hankin, and Samson Abramsky. The theory of strictness analysis for higher order functions. In *On Programs as data objects*, pages 42–62. Springer-Verlag, 1985.

[BHS02] Surender Baswana, Ramesh Hariharan, and Sandeep Sen. Improved decremental algorithms for maintaining transitive closure and all-pairs shortest paths in digraphs under edge deletions. In *Proceedings of the ACM Symposium on Theory of Computing (STOC)*, pages 117–123. ACM Press, May 2002.

[Bin98] David Binkley. The application of program slicing to regression testing. *Information and Software Technology*, 40(11-12):583–594, 1998.

[BJCD87] Maurice Bruynooghe, Gerda Janssens, Alain Callebaut, and Bart Demoen. Abstract interpretation: Towards the global optimization of Prolog programs. In *Proceedings of the IEEE Symposium on Logic Programming (SLP)*, pages 192–204. IEEE Computer Society Press, August 1987.

[BLQ+03] Marc Berndl, Ondřej Lhoták, Fneg Qian, Laurie J. Hendren, and Navindra Umanee. Points-to analysis using BDDs. In *Proceedings of the ACM conference on Programming Language Design and Implementation (PLDI)*, pages 196–207. ACM Press, June 2003.

[Bou93a] François Bourdoncle. Abstract debugging of higher-order imperative languages. *ACM SIGPLAN Notices*, 28(6):46–55, 1993.

[Bou93b] François Bourdoncle. Efficient chaotic iteration strategies with widenings. In *Proceedings of the conference on Formal Methods in Programming and their Applications*, volume 735 of *Lecture Notes in Computer Science*, pages 128–141. Springer-Verlag, June 1993.

[BR01] Thomas Ball and Sriram K. Rajamani. Bebop: a path-sensitive interprocedural dataflow engine. In *Proceedings of the ACM workshop on Program Analysis for Software Tools and Engineering (PASTE)*, pages 97–103. ACM Press, June 2001.

[Bru91] Maurice Bruynooghe. A Practical Framework for the Abstract Interpretation of Logic Programs. *Journal of Logic Programming*, 10(2):91–124, 1991.

[Bry86] Randal E. Bryant. Graph-based algorithms for Boolean function manipulation. *IEEE Transactions on Computers (TC)*, C-35(8):677–691, August 1986.

[Bur90] Michael Burke. An interval-based approach to exhaustive and incremental interprocedural data-flow analysis. *ACM Transactions on Programming Language Systems (TOPLAS)*, 12(3):341–395, 1990.

[BW96] Beate Bollig and Ingo Wegener. Improving the variable ordering of OBDDs is NP-complete. *IEEE Transactions on Computers (TC)*, 45(9):993–1002, 1996.

[CBC93] Jong-Deok Choi, Michael Burke, and Paul Carini. Efficient flow-sensitive interprocedural computation of pointer-induced aliases and side effects. In *Proceedings of the ACM symposium on Principles of Programming Languages (POPL)*, pages 232–245. ACM Press, January 1993.

[CBL01] Nitin Chandrachoodan, Shuvra S. Bhattacharyya, and K. J. Ray Liu. Adaptive negative cycle detection in dynamic graphs. In *Proceedings of the International Symposium on Circuits and Systems (ISCAS)*, pages 163–166. IEEE Computer Society Press, May 2001.

[CC77] Patrick Cousot and Radhia Cousot. Abstract interpretation: a unified lattice model for static analysis of programs by construction or approximation of fixpoints. In *Proceedings of the ACM Symposium on Principles of Programming Languages (POPL)*, pages 238–252. ACM Press, January 1977.

[CC79] Patrick Cousot and Radhia Cousot. Systematic design of program analysis frameworks. In *Proceedings of the ACM Symposium on Principles of Programming Languages (POPL)*, pages 269–282. ACM Press, January 1979.

[CC91] Patrick Cousot and Radhia Cousot. Comparison of the Galois connection and widening/narrowing approaches to abstract interpretation. *BIGRE*, 74:107–110, October 1991.

[CC92a] Patrick Cousot and Radhia Cousot. Abstract Interpretation and Application to Logic Programs. *Journal of Logic Programming*, 13(2 and 3):103–179, July 1992.

[CC92b] Patrick Cousot and Radhia Cousot. Inductive definitions, semantics and abstract interpretations. In *Proceedings of the ACM Symposium on the Principles of Programming Languages*, pages 83–94. ACM Press, January 1992.

[CCL+96] Fred C. Chow, Sun Chan, Shin-Ming Liu, Raymond Lo, and Mark Streich. Effective representation of aliases and indirect memory operations in SSA form. In *Proceedings of the conference on Compiler Construction (CC)*, volume 1060 of *Lecture Notes in Computer Science*, pages 253–267. Springer-Verlag, 1996.

[CDL88] David Callahan, Jack Dongarra, and D. Levine. Vectorizing compilers: a test suite and results. In *Proceedings of the ACM/IEEE Supercomputing Conference (SC)*, pages 98–105. IEEE Computer Society Press, November 1988.

[CFR+89] Ron Cytron, Jeanne Ferrante, Barry K. Rosen, Mark K. Wegman, and F. Kenneth Zadeck. An efficient method of computing static single assignment form. In *Proceedings of the ACM Symposium on Principles of Programming Languages (POPL)*, pages 25–35. ACM Press, January 1989.

[CFR+91] Ron Cytron, Jeanne Ferrante, Barry K. Rosen, Mark N. Wegman, and F. Kenneth Zadeck. Efficiently computing static single assignment form and the control dependence graph. *ACM Transactions on Programming Languages and Systems (TOPLAS)*, 13(4):451–490, 1991.

[CG93] Ron Cytron and Reid Gershbein. Efficient accommodation of may-alias information in SSA form. In *Proceedings of the ACM conference on Programming Language Design and Implementation (PLDI)*, pages 36–45. ACM Press, June 1993.

[CH94] Li-Ling Chen and Williams L. Harrison. An efficient approach to computing fixpoints for complex program analysis. In *Proceedings of the ACM Supercomputing Conference (SC)*, pages 98–106. ACM Press, November 1994.

[CH00] Ben-Chung Cheng and Wen-Mei W. Hwu. Modular interprocedural pointer analysis using access paths: design, implementation, and evaluation. In *Proceedings of the ACM conference on Programming Language Design and Implementation (PLDI)*, pages 57–69. ACM Press, June 2000.

[Cha03] Venkatesan T. Chakaravarthy. New results on the computability and complexity of points–to analysis. In *Proceedings of the ACM symposium on Principles of Programming Languages (POPL)*, pages 115–125. ACM Press, January 2003.

[CLRS01] Thomas H. Cormen, Charles E. Leiserson, Ronald L. Rivest, and Clifford Stein. *Introduction to Algorithms*. MIT Press, 2001.

[Cou78] Patrick Cousot. *Méthodes itératives de construction et d'approximation de point fixes d'opérateurs monotone sur un treillis, analyse sémantique des programmes*. Ph.D. thesis, University of Grenoble, France, 1978.

[CR99a] Satish Chandra and Thomas Reps. Physical type checking for C. In *Proceedings of the ACM workshop on Program Analysis for Software Tools and Engineering (PASTE)*, pages 66–75. ACM Press, September 1999.

[CR99b] Satish Chandra and Thomas Reps. Physical type checking for C. Technical Report BL0113590-990302-04, Lucent Technologies, Bell Laboiatories, 1999.

[CRL99] Ramkrishna Chatterjee, Barbara G. Ryder, and William A. Landi. Relevant context inference. In *Proceedings of the ACM symposium on Principles of Programming Languages (POPL)*, pages 133–146. ACM Press, June 1999.

[CSS96] Jong-Deok Choi, Vivek Sarkar, and Edith Schonberg. Incremental computation of static single assignment form. In *Proceedings of the conference on Compiler Construction (CC)*, volume 1060 of *Lecture Notes in Computer Science*, pages 223–237. Springer-Verlag, April 1996.

[Das00] Manuvir Das. Unification-based pointer analysis with directional assignments. In *Proceedings of the ACM conference on Programming Language Design and Implementation (PLDI)*, pages 35–46. ACM Press, June 2000.

[DFHH00] Sebastian Danicic, Chris Fox, Mark Harman, and Rob Hierons. ConSIT: A conditioned program slicer. In *Proceedings of the IEEE conference on Software Maintenance (ICSM)*, pages 216–226. IEEE Computer Society, October 2000.

[DFMSN00] Camil Demetrescu, Daniele Frigioni, Alberto Marchetti-Spaccamela, and Umberto Nanni. Maintaining shortest paths in digraphs with arbitrary arc weights: An experimental study. In *Proceedings of the Workshop on Algorithm Engineering (WAE)*, volume 1982 of *Lecture Notes in Computer Science*, pages 218–229. Springer-Verlag, September 2000.

[DI00] Camil Demetrescu and Guiseppe F. Italiano. Fully dynamic transitive closure: breaking through the $O(n^2)$ barrier. In *Proceedings of the IEEE Symposium on Foundations of Computer Science (FOCS)*, pages 381–389. IEEE Computer Society Press, November 2000.

[DLFR01] Manuvir Das, Ben Liblit, Manuel Fähndrich, and Jakob Rehof. Estimating the impact of scalable pointer analysis on optimization. In *Proceedings of the Static Analysis Symposium (SAS)*, volume 2126 of *Lecture Notes in Computer Science*, pages 260–278. Springer-Verlag, July 2001.

[DMM98] Amer Diwan, Kathryn S. McKinley, and J. Eliot B. Moss. Type-based alias analysis. In *Proceedings of the ACM conference on Programming Language Design and Implementation (PLDI)*, pages 106–117. ACM Press, June 1998.

[DPZ00] Hristo Djidjev, Grammati E. Pantziou, and Christos D. Zaroliagis. Improved algorithms for dynamic shortest paths. *Algorithmica*, 28(4):367–389, 2000.

[DRS03] Nurit Dor, Michael Rodeh, and Mooly Sagiv. CSSV: Towards a realistic tool for statically detecting all buffer overflows in C. In *Proceedings of the ACM conference on Programming Language Design and Implementation (PLDI)*, pages 155–167. ACM Press, June 2003.

[DS87] Paul F. Dietz and Daniel D. Sleator. Two algorithms for maintaining order in a list. In *Proceedings of the ACM Symposium on Theory of Computing (STOC)*, pages 365–372. ACM Press, May 1987.

[EGH94] Maryam Emami, Rakesh Ghiya, and Laurie J. Hendren. Context-sensitive interprocedural points-to analysis in the presence of function pointers. In *Proceedings of the ACM conference on Programming Language Design and Implementation (PLDI)*, pages 242–256. ACM Press, June 1994.

[ER60] Paul Erdös and Alfred Rényi. On the evolution of random graphs. *Mathematical Institute of the Hungarian Academy of Sciences*, 5:17–61, 1960.

[ER89] Mark W. Eichin and Jon A. Rochlis. With microscope and tweezers: An analysis of the internet virus of November 1988. In *Proceedings of the IEEE Symposium on Research in Security and Privacy*, pages 326–343, 1989.

[FFA97] Jeffrey S. Foster, Manuel Fähndrich, and Alexander Aiken. Flow-insensitive points-to analysis with term and set constraints. Technical Report CSD-97-964, University of California, Berkeley, 1997.

[FFA00] Jeffrey S. Foster, Manuel Fähndrich, and Alexander Aiken. Polymorphic versus monomorphic flow-insensitive points-to analysis for C. In *Proceedings of the Static Analysis Symposium (SAS)*, volume 1824 of *Lecture Notes in Computer Science*, pages 175–198. Springer-Verlag, July 2000.

[FFSA98] Manuel Fähndrich, Jeffrey S. Foster, Zhendong Su, and Alexander Aiken. Partial online cycle elimination in inclusion constraint graphs. In *Proceedings of the ACM conference on Programming Language Design and Implementation (PLDI)*, pages 85–96. ACM Press, June 1998.

[Fla97] Cormac Flanagan. *Effective Static Debugging via Componential Set-Based Analysis*. PhD thesis, Rice University, 1997.

[FLL+02] Cormac Flanagan, K. Rustan M. Leino, Mark Lillibridge, Greg Nelson, James B. Saxe, and Raymie Stata. Extended static checking for Java. In *Proceedings of the ACM conference on Programming Language Design and Implementation (PLDI)*, pages 234–245. ACM Press, June 2002.

[FMSN94] Daniele Frigioni, Alberto Marchetti-Spaccamela, and Umberto Nanni. Incremental algorithms for the single-source shortest path problem. In *Proceedings of the conference on Foundations of Software Technology and Theoretical Computer Science (FSTTCS)*, volume 880 of *Lecture Notes in Computer Science*, pages 113–124. Springer-Verlag, December 1994.

[FMSN98] Daniele Frigioni, Alberto Marchetti-Spaccamela, and Umberto Nanni. Fully dynamic shortest paths and negative cycles detection on digraphs with arbitrary arc weights. In *Proceedings of the European Symposium on Algorithms (ESA)*, volume 1461 of *Lecture Notes in Computer Science*, pages 320–331. Springer-Verlag, August 1998.

[FRD00] Manuel Fähndrich, Jakob Rehof, and Manuvir Das. Scalable context-sensitive flow analysis using instantiation constraints. In *Proceedings of the ACM conference on Programming Language Design and Implementation (PLDI)*, pages 253–263. ACM Press, June 2000.

[FS96] Christian Fecht and Helmut Seidl. An even faster solver for general systems of equations. In *Proceedings of the Static Analysis Symposium (SAS)*, volume 1145 of *Lecture Notes in Computer Science*, pages 189–204. Springer-Verlag, September 1996.

[FS98] Christian Fecht and Helmut Seidl. Propagating differences: An efficient new fixpoint algorithm for distributive constraint systems. In *Proceedings of the European Symposium on Programming (ESOP)*, volume 1381 of *Lecture Notes in Computer Science*, pages 90–104. Springer-Verlag, April 1998.

[Gab00] Harold N. Gabow. Path-based depth-first search for strong and biconnected components. *Information Processing Letters*, 74(3–4):107–114, May 2000.

[GKT91] Gina Goff, Ken Kennedy, and Chau-Wen Tseng. Practical dependence testing. In *Proceedings of the ACM conference on Programming Language Design and Implementation (PLDI)*, pages 15–29. ACM Press, June 1991.

[GL03] Samuel Z. Guyer and Calvin Lin. Client-driven pointer analysis. In *Proceedings of the Static Analysis Symposium (SAS)*, volume 2694 of *Lecture Notes in Computer Science*, pages 214–236. Springer-Verlag, June 2003.

[GLS01] Rakesh Ghiya, Daniel Lavery, and David Sehr. On the importance of points-to analysis and other memory disambiguation methods for C programs. In *Proceedings of the ACM conference on Programming Language Design and Implementation (PLDI)*, pages 47–58. ACM Press, June 2001.

[God97] Patrice Godefroid. VeriSoft: A tool for the automatic analysis of concurrent reactive software. In *Proceedings of the conference on Computer Aided Verification (CAV)*, volume 1254 of *Lecture Notes in Computer Science*, pages 476–479. Springer-Verlag, June 1997.

[Goy99] Deepak Goyal. An improved inter-procedural may-alias analysis algorithm. Technical Report 1999-777, New York University, 1999.

[Guy03] Samuel Z. Guyer. *Incorporating Domain-Specific Information into the Compilation Process*. PhD thesis, Department of Computer Science, University of Texas at Austin, 2003.

[HAM+95] Mary H. Hall, Saman P. Amarasinghe, Brian R. Murphy, Shih-Wei Liao, and Monica S. Lam. Detecting coarse-grain parallelism using an interprocedural parallelizing compiler. In *Proceedings of the ACM/IEEE Supercomputing Conference (SC)*, pages 1–26. ACM Press, December 1995.

[HBCC99] Michael Hind, Michael Burke, Paul Carini, and Jong-Deok Choi. Interprocedural pointer alias analysis. *ACM Transactions on Programming Languages and Systems (TOPLAS)*, 21(4):848–894, 1999.

[HBD03] Mark Harman, David Binkley, and Sebastian Danicic. Amorphous program slicing. *The Journal of Systems and Software (JSS)*, 68(1):45–64, 2003.

[HDT87] Susan Horwitz, Alan J. Demers, and Tim Teitelbaum. An efficient general iterative algorithm for dataflow analysis. *Acta Informatica*, 24(6):679–694, 1987.

[Hec77] Matthew S. Hecht. *Flow Analysis of Computer Programs*. Elsevier North-Holland, New York, 1st edition, 1977.

[Hei94] Nevin Heintze. Set-based analysis of ML programs. In *Proceedings of the ACM conference on Lisp and Functional Programming (LFP)*, pages 306–317. ACM Press, June 1994.

[HH98] Rebecca Hasti and Susan Horwitz. Using static single assignment form to improve flow-insensitive pointer analysis. In *Proceedings of the ACM conference on Programming Language Design and Implementation (PLDI)*, pages 97–105. ACM Press, June 1998.

[HHWT97] Thomas A. Henzinger, Pei-Hsin Ho, and Howard Wong-Toi. HYTECH: A model checker for hybrid systems. In *Proceedings of the conference on Computer Aided Verification (CAV)*, volume 1254 of *Lecture Notes in Computer Science*, pages 460–463. Springer-Verlag, June 1997.

[HJMS03] Thomas A. Henzinger, Ranjit Jhala, Rupak Majumdar, and Gregoire Sutre. Software verification with Blast. In *Proceedings of the Workshop on Model Checking Software*, volume 2648 of *Lecture Notes in Computer Science*, pages 235–239. Springer-Verlag, July 2003.

[HM94] Chris Hankin and Daniel Le Métayer. Deriving algorithms from type inference systems: Application to strictness analysis. In *Proceedings of the ACM symposium on Principles of Programming Languages (POPL)*, pages 202–212. ACM Press, January 1994.

[HM97a] Nevin Heintze and David McAllester. Linear-time subtransitive control flow analysis. In *Proceedings of the ACM conference on Programming Language Design and Implementation (PLDI)*, pages 261–272. ACM Press, June 1997.

[HM97b] Nevin Heintze and David A. McAllester. On the cubic bottleneck in subtyping and flow analysis. In *Proceedings of the IEEE Symposium on Logic in Computer Science (LICS)*, pages 342–351. IEEE Computer Society Press, June 1997.

[Hol97] Gerard J. Holzmann. The Spin model checker. *IEEE Transactions on Software Engineering*, 23(5):279–95, 1997.

[Hoo87] Roger Hoover. *Incremental Graph Evaluation*. Ph.D. thesis, Department of Computer Science, Cornell University, Ithaca, New York, United States, May 1987.

[Hor97] Susan Horwitz. Precise flow-insensitive may-alias analysis is NP-Hard. *ACM Transactions on Programming Languages and Systems (TOPLAS)*, 19(1):1–6, January 1997.

[HP97] Michael Hind and Anthony Pioli. An empirical comparison of interprocedural pointer alias analyses. Technical Report RC 21058, IBM T.J. Watson Research Center, 1997.

[HP98] Michael Hind and Anthony Pioli. Assessing the effects of flow-sensitivity on pointer alias analyses. In *Proceedings of the Static Analysis Symposium (SAS)*, volume 1503 of *Lecture Notes in Computer Science*, pages 57–81, June 1998.

[HP00] Michael Hind and Anthony Pioli. Which pointer analysis should I use? In *Proceedings of the ACM International Symposium on Software Testing and Analysis (ISSTA)*, pages 113–123. ACM Press, August 2000.

[HRB88] Susan Horwitz, Thomas Reps, and David Binkley. Interprocedural slicing using dependence graphs. *ACM SIGPLAN Notices*, 23(7):35–46, 1988.

[Hsu75] Harry T. Hsu. An algorithm for finding a minimal equivalent graph of a digraph. *Journal of the ACM*, 22(1):11–16, 1975.

[HT01] Nevin Heintze and Olivier Tardieu. Ultra-fast aliasing analysis using CLA: A million lines of C code in a second. In *Proceedings of the ACM conference on Programming Language Design and Implementation (PLDI)*, pages 254–263. ACM Press, June 2001.

[HU75] Matthew S. Hecht and Jeffrey D. Ullman. A simple algorithm for global data flow analysis problems. *SIAM Journal on Computing*, 4(4):519–532, December 1975.

[IC02] Jaime S. Ide and Fabio Gagliardi Cozman. Random generation of bayesian networks. In *Proceedings of the Brazillian Symposium on Artificial Intelligence (SBIA)*, volume 2507, pages 366–375. Springer-Verlag, 2002.

[IEG99] Guiseppe F. Italiano, David Eppstein, and Zvi Galil. Dynamic graph algorithms. In *Handbook of Algorithms and Theory of Computation, Chapter 22*. CRC Press, 1999.

[IR78] Alon Itai and Michael Rodeh. Finding a minimum circuit in a graph. *SIAM Journal on Computing*, 7:413–423, 1978.

[IRW93] Yannis Ioannidis, Raghu Ramakrishnan, and Linda Winger. Transitive closure algorithms based on graph traversal. *ACM Transactions on Database Systems*, 18(3):512–576, 1993.

[ISO90] *ISO/IEC. International Standard ISO/IEC 9899, Programming Languages — C*. 1990.

[JEKL90] Jerry R. Burch, Edmund M. Clarke, Kenneth L. MacMillan, and L.J. Hwang. Symbolic Model Checking: 10^{20} States and Beyond. In *Proceedings of the IEEE Symposium on Logic in Computer Science (LICS)*, pages 1–33. IEEE Computer Society Press, June 1990.

[JHS02] James A. Jones, Mary Jean Harrold, and John Stasko. Visualization of test information to assist fault localization. In *Proceedings of the International Conference on Software Engineering (ICSE)*, pages 467–477. ACM Press, May 2002.

[JLR00] Svante Janson, Tomasz Luczak, and Andrzej Rucinski. *Random Graphs*. Wiley, New York, 2000.

[JM81] Neil D. Jones and Steven S. Muchnick. Flow analysis and optimization of lisp-like structures. In Steven S. Muchnick and Neil D. Jones, editors, *Program Flow Analysis: Theory and Applications*, pages 102–131. Prentice-Hall, 1981.

[JS87] Neil D. Jones and Harald Søndergaard. A semantics-based framework for the abstract interpretation of Prolog. In S. Abramsky and Chris Hankin, editors, *Abstract Interpretation of Declarative Languages*, pages 123–142, Chichester, England, 1987. Ellis Horwood.

[KA04] John Kodumal and Alex Aiken. The set constraint/CFL reachability connection in practice. In *Proceedings of the ACM conference on Programming Language Design and Implementation (PLDI)*, pages 207–218. ACM Press, June 2004.

[Kat04a] Irit Katriel. Online topological ordering and sorting. Technical report, Max-Planck-Institut für Informatik, 2004.

[Kat04b] Irit Katriel. Private communication. Technical report, Max-Planck-Institut für Informatik, 2004.

[KB05] Irit Katriel and Hans L. Bodlaender. Online topological ordering. In *Proceedings of the ACM Symposium on Discrete Algorithms (SODA)*, page (to appear). ACM Press, 2005.

[Ken81] Ken Kennedy. A survey of data flow analysis techniques. In Steven S Muchnick and Neil D Jones, editors, *Program Flow Analysis: Theory and Applications*, chapter 1, pages 5–54. Prentice-Hall, 1981.

[KRY94] Samir Khuller, Balaji Raghavachari, and Neal E. Young. Approximating the minimum equivalent digraph. In *Proceedings of the ACM-SIAM Symposium on Discrete Algorithms (SODA)*, pages 177–186. Society for Industrial and Applied Mathematics, January 1994.

[KS99] Valerie King and Garry Sagert. A fully dynamic algorithm for maintaining the transitive closure. In *Proceedings of the ACM Symposium on Theory of Computing (STOC)*, pages 492–498. ACM Press, May 1999.

[KU76] John B. Kam and Jeffrey D. Ullman. Global data flow analysis and iterative algorithms. *Journal of the ACM*, 23(1):158–171, January 1976.

[KU77] John B. Kam and Jeffrey D. Ullman. Monotone data flow analysis frameworks. *Acta Informatica*, 7:305–317, January 1977.

[KW94] Atsushi Kanamori and Daniel Weise. Worklist management strategies. Technical Report MSR-TR-94-12, Microsoft Research, 1994.

[Kwi03] Marta Kwiatkowska. Model checking for probability and time: From theory to practice. In *Proceedings of the IEEE Symposium on Logic in Computer Science (LICS)*, pages 351–360. IEEE Computer Society Press, June 2003.

[Lan92a] William Landi. *Interprocedural Aliasing in the presence of Pointers*. PhD thesis, Rutgers Univsersity, New Jersey, United States, 1992.

[Lan92b] William Landi. Undecidability of static analysis. *ACM Letters on Programming Languages and Systems*, 1(4):323–337, 1992.

[LH98] Christopher Lapkowski and Laurie J. Hendren. Extended SSA numbering: Introducing SSA properties to languages with multi-level pointers. In *Proceedings of the conference on Compiler Construction (CC)*, volume 1383 of *Lecture Notes in Computer Science*, pages 128–143. Springer-Verlag, April 1998.

[LH99] Donglin Liang and Mary Jean Harrold. Efficient points-to analysis for whole-program analysis. In *Proceedings of the European Software Engineering Confrence (ESEC) and ACM Foundations of Software Engineering (FSE)*, volume 1687 of *Lecture Notes in Computer Science*, pages 199–215. Springer-Verlag / ACM Press, 1999.

[LH01] Donglin Liang and Mary Jean Harrold. Efficient computation of parameterized pointer information for interprocedural analyses. In *Proceedings of the Static Analysis Symposium (SAS)*, volume 2126 of *Lecture Notes in Computer Science*, pages 279–298. Springer-Verlag, July 2001.

[LH03] Ondřej Lhoták and Laurie J. Hendren. Scaling Java points-to analysis using SPARK. In *Proceedings of the conference on Compiler Construction (CC)*, volume 2622 of *Lecture Notes in Computer Science*, pages 153–169. Springer-Verlag, April 2003.

[LH04] Ondřej Lhoták and Laurie J. Hendren. Jedd: a BDD-based relational extension of Java. In *Proceedings of the ACM conference on Programming Language Design and Implementation (PLDI)*, pages 158–169. ACM Press, June 2004.

[LPH01] Donglin Liang, Maikel Pennings, and Mary Jean Harrold. Extending and evaluating flow-insensitive and context-insensitive points-to analyses for Java. In *Proceedings of the ACM Workshop on Program Analyses for Software Tools and Engineering (PASTE)*, pages 73–79. ACM Press, June 2001.

[Luc01] Andrea De Lucia. Program slicing: Methods and applications. In *Proceedings of the IEEE workshop on Source Code Analysis and Manipulation (SCAM)*, pages 142–149. IEEE Computer Society Press, November 2001.

[MBMD01] G Melaçon, Mireille Bousquet-Melou, and I. Dutor. Random generation of directed acyclic graphs. In *Proceedings of the Euroconference on Combinatorics, Graph Theory and Applications (COMB)*, pages 12–15. Elsevier Science Publishers, September 2001.

[McK94] Kathryn S. McKinley. Evaluating automatic parallelization for efficient execution on shared-memory multiprocessors. In *Proceedings of the IEEE/ACM Supercomputing Conference (SC)*, pages 54–63. ACM Press, November 1994.

[Mel87] Chris Mellish. Abstract interpretation of PROLOG programs. In Samson Abramsky and Chris Hankin, editors, *Abstract Interpretation of Declarative Languages*, pages 181–198. Ellis Horwood, 1987.

[MH87] Chris Martin and Chris Hankin. Finding fixed points in finite lattices. In *Proceedings of the conference on Functional Programming Languages and Computer Architecture (FPCA)*, volume 274 of *Lecture Notes in Computer Science*, pages 426–445. Springer-Verlag, September 1987.

[MJ86] Alan Mycroft and Neil D. Jones. A relational framework for abstract interpretation. In *Proceedings of the Workshop on Programs as Data Objects*, volume 217 of *Lecture Notes in Computer Science*, pages 156–171. Springer-Verlag, October 1986.

[MR97] David Melski and Thomas Reps. Interconvertibility of set constraints and context-free language reachability. In *Proceedings of the ACM workshop on Partial Evaluation and Program Manipulation (PEPM)*, pages 74–88. ACM Press, June 1997.

[MRF+02] Roman Manevich, Ganesan Ramalingam, John Field, Deepak Goyal, and Mooly Sagiv. Compactly representing first-order structures for static analysis. In *Proceedings of the Static Analysis Symposium (SAS)*, volume 2477 of *Lecture Notes in Computer Science*, pages 196–212, September 2002.

[MRR02] Ana Milanova, Atanas Rountev, and Barbara Ryder. Parameterized object sensitivity for points-to and side-effect analyses for Java. In *Proceedings of the ACM International Symposium on Software Testing and Analysis (ISSTA)*, pages 1–11. ACM Press, July 2002.

[MSNR96] Alberto Marchetti-Spaccamela, Umberto Nanni, and Hans Rohnert. Maintaining a topological order under edge insertions. *Information Processing Letters*, 59(1):53–58, 1996.

[Myc81] Alan Mycroft. *Abstract Interpretation and Optimizing Transformations for Applicative Programs*. PhD thesis, Unversity of Edinburgh, Scotland, December 1981.

[Mye86] Brad A. Myers. Visual programming, programming by example, and program visualization; A taxonomy. In *Proceedings of the ACM conference on Human Factors in Computing Systems (CHI)*, pages 59–66. ACM Press, 1986.

[NKH04a] Erik M. Nystrom, Hong-Seok Kim, and Wen-Mei W. Hwu. Bottom-up and top-down context-sensitive summary-based pointer analysis. In *Proceedings of the Static Analysis Symposium (SAS)*, volume 3148 of *Lecture Notes in Computer Science*, pages 165–180. Springer-Verlag, 2004.

[NKH04b] Erik M. Nystrom, Hong-Seok Kim, and Wen-Mei W. Hwu. Importance of heap specialization in pointer analysis. In *Proceedings of the ACM workshop on Program*

analysis for Software Tools and Engineering (PASTE), pages 43–48. ACM Press, June 2004.

[NNH99] Flemming Nielson, Hanne R. Nielson, and Chris L. Hankin. *Principles of Program Analysis*. Springer-Verlag, 1999.

[NSS94] Esko Nuutila and Eljas Soisalon-Soininen. On finding the strongly connected components in a directed graph. *Information Processing Letters*, 49(1):9–14, January 1994.

[Nuu95] Esko Nuutila. *Efficient Transitive Closure Computation on Large Digraphs*. PhD thesis, Helsinki University of Technology, Finland, 1995.

[Pio99] Anthony Pioli. Conditional pointer aliasing and constant propagation. Master's thesis, SUNY at New Paltz, New York, United States, 1999.

[PK04] David J. Pearce and Paul H. J. Kelly. A dynamic algorithm for topologically sorting directed acyclic graphs. In *Proceedings of the Workshop on Efficient and experimental Algorithms (WEA)*, volume 3059 of *Lecture Notes in Computer Science*, pages 383–398. Springer-Verlag, May 2004.

[PKH03] David J. Pearce, Paul H. J. Kelly, and Chris Hankin. Online cycle detection and difference propagation for pointer analysis. In *Proceedings of the IEEE workshop on Source Code Analysis and Manipulation (SCAM)*, pages 3–12. IEEE Computer Society Press, September 2003.

[PKH04a] David J. Pearce, Paul H. J. Kelly, and Chris Hankin. Efficient field-sensitive pointer analysis for C. In *Proceedings of the ACM workshop on Program Analysis for Software Tools and Engineering (PASTE)*, pages 37–42. ACM Press, June 2004.

[PKH04b] David J. Pearce, Paul H. J. Kelly, and Chris Hankin. Online cycle detection and difference propagation: Applications to pointer analysis. *Software Quality Journal*, 12(4):309–335, 2004.

[PKL80] David A. Padua, David J. Kuck, and Duncan H. Lawrie. High-speed multiprocessors and compilation techniques. *IEEE Transactions on Computers*, C-29(9):763–776, September 1980.

[PT01] Boris Pittel and Ronald Tungol. A phase transition phenomenon in a random directed acyclic graph. *RSA: Random Structures & Algorithms*, 18(2):164–184, 2001.

[PvL88] Han La Poutré and Jan van Leeuwen. Maintenance of transitive closure and transitive reduction of graphs. In *Proceedings of the Workshop on Graph-Theoretic Concepts in Computer Science (WG)*, volume 314 of *Lecture Notes in Computer Science*, pages 106–120. Springer-Verlag, June 1988.

[PW86] David A. Padua and Michael J. Wolfe. Advanced compiler optimizations for supercomputers. *Communications of the ACM*, 29(12):1184–1201, 1986.

[Ram94] Ganesan Ramalingam. The undecidability of aliasing. *ACM Transactions on Programming Languages And Systems (TOPLAS)*, 16(5):1467–1471, 1994.

[Ram96] Ganesan Ramalingam. *Bounded incremental computation*, volume 1089 of *Lecture Notes in Computer Science. Ph.D. thesis.* Springer-Verlag, 1996.

[RC00] Atanas Rountev and Satish Chandra. Off-line variable substitution for scaling points-to analysis. In *Proceedings of the ACM conference on Programming Language Design and Implementation (PLDI)*, pages 47–56. ACM Press, June 2000.

[Rei97] Steven P. Reiss. Cacti: a front end for program visualization. In *Proceedings of the IEEE symposium on Information Visualization (InfoVis)*, pages 46–50. IEEE Computer Society Press, October 1997.

[Rep82] Thomas Reps. Optimal-time incremental semantic analysis for syntax-directed editors. In *Proceedings of the ACM Symposium on Principles of Programming Languages (POPL)*, pages 169–176. ACM Press, January 1982.

[Rey69] John C. Reynolds. Automatic computation of data set definitions. In *Proceedings of the Information Processing congress (IFIP)*, volume 1, pages 456–461. North-Holland, August 1969.

[RLS+01] Barbara G. Ryder, William A. Landi, Philip A. Stocks, Sean Zhang, and Rita Altucher. A schema for interprocedural modification side-effect analysis with pointer aliasing. *ACM Transactions on Programming Language Systems (TOPLAS)*, 23(2):105–186, 2001.

[RMR01] Atanas Rountev, Ana Milanova, and Barbara G. Ryder. Points-to analysis for Java using annotated constraints. In *Proceedings of the ACM conference on Object Oriented Programming Systems, Languages and Applications (OOPSLA)*, pages 43–55. ACM Press, October 2001.

[RMT86] Thomas Reps, Carla Marceau, and Tim Teitelbaum. Remote attribute updating for language-based editors. In *Proceedings of the ACM Symposium on the Principles of Programming Languages (POPL)*, pages 1–13. ACM press, January 1986.

[RP86] Barbara G. Ryder and Marvin C. Paull. Elimination algorithms for data flow analysis. *ACM Computing Surveys*, 18(3):277–316, September 1986.

[RP88] Barbara G. Ryder and Marvin C. Paull. Incremental data-flow analysis algorithms. *ACM Transactions on Programming Languages and Systems (TOPLAS)*, 10(1):1–50, January 1988.

[RR94] Ganesan Ramalingam and Thomas Reps. On competitive on-line algorithms for the dynamic priority-ordering problem. *Information Processing Letters*, 51(3):155–161, 1994.

[RR96] Ganesan Ramalingam and Thomas Reps. On the computational complexity of dynamic graph problems. *Theoretical Computer Science*, 158(1–2):233–277, 1996.

[RS88] Kosaraju S. Rao and Gregory Sullivan. Detecting cycles in dynamic graphs in polynomial time. In *Proceedings of the ACM Symposium on the Theory of Computing (STOC)*, pages 398–406. ACM Press, May 1988.

[RT96] Thomas Reps and Todd Turnidge. Program specialization via program slicing. In *Selected Papers from the International Seminar on Partial Evaluation*, volume 1110 of *Lecture Notes in Computer Science*, pages 409–429. Springer-Verlag, February 1996.

[Ruf95] Erik Ruf. Context-insensitive alias analysis reconsidered. In *Proceedings of the ACM conference on Programming Language Design and Implementation (PLDI)*, pages 13–22. ACM Press, June 1995.

[RY89] Thomas Reps and Wuu Yang. The semantics of program slicing and program integration. In *Proceedings of the Joint Conference on Theory and Practice of Software Development, Volume 2*, volume 352 of *Lecture Notes in Computer Science*, pages 360–374. Springer-Verlag, March 1989.

[RZ02] Liam Roditty and Uri Zwick. Improved dynamic reachability algorithms for directed graphs. In *Proceedings of the IEEE Foundations Of Computer Science (FOCS)*, pages 679–689. IEEE Computer Society Press, November 2002.

[Sch95] Erik Schön. On the computation of fixpoints in static program analysis with an application to AKL. Technical Report R95-06, Swedish Institute of Computer Science, November 1995.

[SFA00] Zhendong Su, Manuel Fähndrich, and Alexander Aiken. Projection merging: Reducing redundancies in inclusion constraint graphs. In *Proceedings of the symposium on Principles of Programming Languages (POPL)*, pages 81–95. ACM Press, January 2000.

[SH97a] Marc Shapiro and Susan Horwitz. The effects of the precision of pointer analysis. In *Proceedings of the Static Analysis Symposium (SAS)*, volume 1302 of *Lecture Notes in Computer Science*, pages 16–31. Springer-Verlag, September 1997.

[SH97b] Marc Shapiro and Susan Horwitz. Fast and accurate flow-insensitive points-to analysis. In *Proceedings of the Symposium on Principles of Programming Languages (POPL)*, pages 1–14. ACM Press, January 1997.

[Shm83] Oded Shmueli. Dynamic cycle detection. *Information Processing Letters*, 17(4):185–188, November 1983.

[Sim90] Klaus Simon. Finding a minimal transitive reduction in a strongly connected digraph within linear time. In *Proceedings of the Workshop on Graph-theoretic concepts in computer science (WG)*, volume 484 of *Lecture Notes in Computer Science*, pages 245–259. Springer-Verlag, June 1990.

[SLL02] Jeremy Siek, Lie-Quan Lee, and Andrew Lumsdaine. *The Boost Graph Library: User Guide and Reference Manual*. Addison-Wesley, 2002.

[SMH98] Byoungro So, Sungdo Moon, and Mary W. Hall. Measuring the effectiveness of automatic parallelization in SUIF. In *Proceedings of the ACM/IEEE Supercomputing Conference (SC)*, pages 212–219. ACM Press, November 1998.

[SRLZ98] Philip A. Stocks, Barbara G. Ryder, William A. Landi, and Sean Zhang. Comparing flow and context sensitivity on the modification-side-effects problem. In *Proceedings of ACM International Symposium on Software Testing and Analysis (ISSTA)*, pages 21–31. ACM Press, March 1998.

[SS00] Mirko Streckenbach and Gregor Snelting. Points-to for Java: A general framework and an empirical comparison. Technical report, University Passau, November 2000.

[Ste95] Bjarne Steensgaard. Points-to analysis in almost linear time. Technical Report MSR-TR-95-08, Microsoft Research, 1995.

[Ste96a] Bjarne Steensgaard. Points-to analysis by type inference of programs with structures and unions. In *Proceedings of the conference on Compiler Construction (CC)*, volume 1060 of *Lecture Notes in Computer Science*, pages 136–150. Springer-Verlag, April 1996.

[Ste96b] Bjarne Steensgaard. Points-to analysis in almost linear time. In *Proceedings of the ACM Symposium on Principles of Programming Languages (POPL)*, pages 32–41. ACM Press, January 1996.

[SUI] The SUIF 2 research compiler, Stanford University, http://suif.stanford.edu.

[SYM00] Tarja Systä, Ping Yu, and Hausi Müller. Analyzing Java software by combining metrics and program visualization. In *Proceedings of the IEEE conference on Software Maintenance and Reengineering (CSMR)*, pages 199–208. IEEE Computer Society, February 2000.

[Tar72] Robert E. Tarjan. Depth-first search and linear graph algorithms. *SIAM Journal on Computing*, 1(2):146–160, 1972.

[The96] The Vis Group. VIS: a system for verification and synthesis. In *Proceedings of the conference on Computer Aided Verification (CAV)*, volume 1102 of *Lecture Notes in Computer Science*, pages 428–432. Springer-Verlag, August 1996.

[Wad87] Philip Wadler. Strictness analysis on non-flat domains (by abstract interpretation). In Samson Abramsky and Chris Hankin, editors, *Abstract Interpretation of Declarative Languages*, chapter 12, pages 266–275. Ellis-Horwood, 1987.

[WFBA00] David Wagner, Jeffrey S. Foster, Eric A. Brewer, and Alexander Aiken. A first step towards automated detection of buffer overrun vulnerabilities. In *Proceedings of the Network and Distributed System Security Symposium (NDSS)*, pages 3–17. The Internet Society, February 2000.

[WH87] Philip Wadler and R. J. M. Hughes. Projections for Strictness Analysis. In *Proceedings of the conference on Functional Programming Languages and Computer Architecture (FPCA)*, volume 274 of *Lecture Notes in Computer Science*, pages 385–407. Springer-Verlag, September 1987.

[Wil97] Robert P. Wilson. *Efficient context-sensitive pointer analysis for C programs*. PhD thesis, Stanford University, California, United States, 1997.

[Wir93] Mats Wirn. Bounded incremental parsing. In *Proceedings of the Twente Workshop on Language Technology (TWLT)*, pages 145–156, University of Twente, Enschede, The Netherlands, June 1993. University of Twente.

[WL95] Robert P. Wilson and Monica S. Lam. Efficient context-sensitive pointer analysis for C programs. In *Proceedings of the ACM conference on Programming Language Design and Implementation (PLDI)*, pages 1–12. ACM Press, June 1995.

[WL02] John Whaley and Monica S. Lam. An efficient inclusion-based points-to analysis for strictly-typed languages. In *Proceedings of the Symposium on Static Analysis (SAS)*, volume 2477 of *Lecture Notes in Computer Science*, pages 180–195. Springer-Verlag, September 2002.

[WL04] John Whaley and Monica S. Lam. Cloning-based context-sensitive pointer alias analysis using Binary Decision Diagrams. In *Proceedings of the ACM conference on Programming Language Design and Implementation (PLDI)*, pages 131–144. ACM Press, June 2004.

[Wol82] Michael J. Wolfe. *Optimizing Supercompilers for Supercomputers*. PhD thesis, Deptartment of Computer Science, University of Illinois at Urbana-Champaign, United States, October 1982.

[Wol89] Michael Wolfe. *Optimizing supercompilers for supercomputers*. The MIT Press, Cambridge, MA, 1989.

[Yeh83] Dashing Yeh. On incremental evaluation of ordered attributed grammars. *BIT*, 23:308–320, 1983.

[YHR99] Suan Hsi Yong, Susan Horwitz, and Thomas Reps. Pointer analysis for programs with structures and casting. In *Proceedings of the ACM conference on Programming Language Design and Implementation (PLDI)*, pages 91–103. ACM Press, June 1999.

[ZC04] Jianwen Zhu and Silvian Calman. Symbolic pointer analysis revisited. In *Proceedings of the ACM conference on Programming Language Design and Implementation (PLDI)*, pages 145–157. ACM Press, June 2004.

[Zha98] Xiang-Xiang Sean Zhang. *Practical Pointer Aliasing Analysis*. PhD thesis, Rutgers Univsersity, New Jersey, United States, 1998.

[Zhu02] Jianwen Zhu. Symbolic pointer analysis. In *Proceedings of the IEEE/ACM international conference on Computer-Aided Design (ICCAD)*, pages 150–157. ACM Press, August 2002.

[ZM03] Jianjun Zhou and Martin Müller. Depth-first discovery algorithm for incremental topological sorting of directed acyclic graphs. *Information Processing Letters*, 88(4):195–200, 2003.